DEVELOPING STRATEGIES TO RE-ACTIVATE EPIGENETICALLY SILENCED TUMOR SUPPRESSOR GENES IN ACUTE MYELOID LEUKEMIA

A Thesis Submitted to the College of
Graduate Studies and Research
In Partial Fulfillment of the Requirements
For the Degree of Masters of Science
In the Department of Biochemistry
University of Saskatchewan
Saskatoon

By

Carolina Gonzalez Zuluaga

Permission to Use

In presenting this thesis in partial fulfilment of the requirements for a Postgraduate degree from the University of Saskatchewan, I agree that the Libraries of this University may make it freely available for inspection. I further agree that permission for copying of this thesis in any manner, in whole or in part, for scholarly purposes may be granted by the professor or professors who supervised my thesis work or, in their absence, by the Head of the Department or the Dean of the College in which my thesis work was done. It is understood that any copying or publication or use of this thesis or parts thereof for financial gain shall not be allowed without my written permission. It is also understood that due recognition shall be given to me and to the University of Saskatchewan in any scholarly use which may be made of any material in my thesis.

Requests for permission to copy or to make other use of material in this thesis in whole or part should be addressed to:

Head of the Department of Biochemistry
University of Saskatchewan
Saskatoon, Saskatchewan S7N 5E5

ABSTRACT

Epigenetic mechanisms are essential for normal cell development. Alteration in those normal processes leads to malignant cell transformation and with this to cancer development. Use of inhibitors that alter the epigenetics of DNA methylation and histone post translational modifications has lead to the exploration of the epigenetic mechanism involved in silencing of tumor suppressor genes in cancer, including acute myeloid leukemia (AML). Moreover, combinations of inhibitors that target various epigenetic enzymes have being recognized to be more effective in the re-activation of tumor suppressor genes than individual drug treatments. Here, we reported that p15, p21 and E-cadherin genes are more effectively re-expressed using a combination of DNA methyltransferase and histone methyltransferase inhibitors in AML cell lines. Re-expression of hypermethylated p15 and E-cadherin genes required reduced levels of promoter histone 3 lysine 9 (H3K9) methylation rather than inhibition of DNA methylation itself. Moreover, induction of p21 expression was associated with changes in promoter histone 3 lysine 9 methylation (H3K9Me) by achieving inhibition of the histone methyltransferase, SUV39H1, activity. Altogether, our results highlight the potential of combining epigenetic drugs in the re-activation of epigenetically silenced tumor suppressor genes and the need for evaluating histone methyltransferases as therapeutic targets for treatment of acute myeloid malignancies.

ACKNOWLEDGEMENTS

I want to give many thanks to my supervisor Dr. Ron Geyer, without his patience, guidance and directions the achievement of this project could not be finished. Acknowledgements, to Dr. Roesler for giving me continued encouragement and guidance. To my entire committee member Dr. Khandelwal, Dr. Wilson and Dr. Roesler for the guidance and continue feedback in this research project. To Margaret Ross for her infinite help and patience in assisting me with everything related to the graduate program.

I would like to especially thank Asha and Erika for their continued help and guidance in many of my experiments. Also, I want to thank all the members of Dr. Geyer Lab, Wendy Bernhard, Khris Barreto, Landon, Wayne Hill and specially to Alberto Aparicio, Theodora Zlateva and Bharathi Vellalore for their friendship and support during my graduate studies.

I also wish to thank Jennifer Nyarko for being a friend and support during this time as well as Family Gomez and all my friends in Saskatoon.

Special thanks to my Family and my fiancé and friend Juan for their encouragement, support and love throughout these years.

Finally, I want to dedicate this achievement to the memory of my mother and Elaine, two great women whose encouragement taught me that for more difficult that a situation would be you always need to keep your head high and have the strength to continue in life.

Thank you all.

TABLE OF CONTENTS

LIST OF TABLES

LIST OF FIGURES

LIST OF ABBREVIATIONS

ABL	Albenson kinase gene
AML	Acute myeloid leukemia
AML1	Acute myeloid leukemia gene 1
ANK	Ankyrin
BAALC	Brain and acute leukemia, cytoplasmic gene
BCR	Breakpoint cluster region gene
BIX	BIX-01294
CBF	Core binding factor
CDK	Cyclin dependent kinase
CDKI	Cyclin dependent kinase inhibitor
CDH	Cadherin
cDNA	Complementary DNA
CEBPA	CCAAT/ enhancer binding protein alpha
ChIP	Chromatin immunoprecipitation
CML	Chronic myeloid leukemia
DAC	5-Aza-2'-deoxycytidine
DCK	Deoxycytidine kinases
DMSO	Dimethyl sulfoxide
DNMT	DNA methyltransferase
ES	Embryonic stem cells
ETO	Eight-twenty-one gene
FAB	French-American-British classification
FLT-3	FMS-like tyrosine kinase 3
GAPDH	Glyceraldehyde-3-phosphate dehydrogenase
GM-CSF	Granulocyte macrophage colony stimulating factor
H2A	Histone 2A
H2B	Histone 2B
H3	Histone 3
H4	Histone 4

H3K9	Histone 3 lysine 9
H3K9Me	Histone 3 lysine 9 methylation
H3K9Me2	Histone 3 lysine 9 di-methylation
H3K9Me3	Histone 3 lysine 9 tri-methylation
HDAC	Histone deacetylase
HMT	Histone methyltransferase
HP1	Heterochromatin protein 1
HPRT	Hypoxanthine-guanine phosphoribosyltransferase
IL-3	Interleukin 3
ITD	Internal tandem duplications
MDS	Myeloid dysplastic syndrome
MDR	Multidrug resistance gene
MSP	Methylation specific PCR
MTT	3-(4,5-dimethylthiazol-2-yl)-2,5-diphenyltetrazolium bromide
Myc	Myelocytomatosis factor
MYH11	Myosin heavy chain 11
MOZ	Monocytic leukemia zinc finger protein
NPM1	Nucleophosmin mutation
PCR	Polymerase chain reaction
PCNA	Proliferating cell nuclear antigen
PML	Promyelocytic leukemia gene
PMSF	Phenylmethylsulfonyl fluoride
RARA	Retionic acid receptor alpha
RAS	Small GTPases proteins
Rb	Retinoblastoma
RT-PCR	Reverse transcriptase polymerase chain reaction
SAM	S-adenosylmethionin
SET	Suv3-9 Suppressor of Variegation, Enhancer of Zeste, Trithorax
TGF-β	Transforming growth factor beta
TSA	Trichostatin A

1. INTRODUCTION

Cancer has been classically recognized as a genetic disease. However, since the discovery of epigenetics, the cancer paradigm has changed and now it is recognized as a genetic and epigenetic disease.

Epigenetics involve the study of heritable changes on gene expression without any alteration in the DNA sequence. Thus, epigenetic mechanisms are essential for the maintenance of gene expression patterns in a cell and for normal cellular development. The major hallmark of epigenetics is that epigenetic changes are reversible, which suggests therapies could be developed to reverse and restore epigenetic aberrations that occur in cancer (Sharma *et al*., 2010).

Major breakthroughs in the discovery of epigenetic drugs have contributed to our understanding of epigenetic silencing of tumor suppressor genes in cancer (Cameron *et al.,* 1999; Bachman *et al.,* 2003; Ekmekci *et al.,* 2004; Baylin, 2005). For example, combinations of epigenetic drugs, such as DNA methyltransferase (DNMT) and Histone deacetylase (HDAC) inhibitors have been found to be more effective in reactivating silenced tumor suppressor genes and in reducing tumor formation compared to individual drug treatments (Cameron *et al.,* 1999; Zhu and Otterson, 2003). Hence, studies involving combinations of epigenetic-enzyme inhibitors might help to elucidate the epigenetic components involved in aberrant gene silencing and might contribute to the use of more effective treatments in cancer therapy.

The objective of this thesis was to investigate mechanisms involved in the epigenetic silencing of tumor suppressor genes in acute myeloid leukemia (AML) and to evaluate epigenetic drug combinations that allow re-expression of tumor suppressor genes. The following literature review will provide the current knowledge related to the molecular basis of cancer, AML, chromatin structure, general concepts of epigenetics, and a brief description of DNMT and HMT inhibitors and their potential use in epigenetic therapy. Emphasis will be placed on the regulation of epigenetic events in cancer and some important tumor suppressor genes in AML.

2. REVIEW OF THE LITERATURE

2.1. Molecular basis of cancer

2.1.1. Multistep molecular carcinogenesis

Classically, cancer has been recognized as a heterogeneous disease that is caused by progressive genetic abnormalities driven by mutational events that evoke a normal cell to become a cancer cell through a process called carcinogenesis (Hanahan *et al*., 2000). More recently, it has been recognized that cancer is also driven by epigenetic changes that do not affect the DNA sequence but cause alterations on gene activity by mechanisms that involve DNA methylation and histone modifications (Jones *et al*., 2007; Sharma *et al*., 2010). Carcinogenesis does not occur from a single event; rather it is due to the accumulation of sequential molecular changes that lead to the inactivation of tumor suppressor genes and the activation of oncogenes, which alter cell phenotypes and bring about tumor formation. Tumor cells are diverse and heterogenous but they all share common features of deregulated cell proliferation and apoptosis (Evan *et al*., 2001).

In 1990, Fearon proposed a genetic, multi-step model for colorectal cancer, suggesting that as a cell moves through the various stages of malignancy, hyperplasia, metaplasia, neoplasia, and metastasis that various genetic "hits" are acquired to affect multiple genes in several pathways (Fearon and Vogelstein, 1990). Similarly, in 1996 Knudson's proposed the 'two-hit' model in which a dominantly inherited predisposition to cancer entails a germline mutation, while tumorigenesis requires a second, somatic mutation. In contrast, non-hereditary cancer of the same type requires the same two hits but both are somatic (Knudson, 1996).

In leukemia, attempts to elucidate genetic and molecular steps that drive a variety of leukemic transformations have been investigated over the past three decades (Chen *et al*., 2010). For example, chronic myeloid leukemia (CML) is recognized to be caused in 95% of cases by the chromosomal translocation t (9; 22), which produces the fusion between the breakpoint cluster region gene and the Albenson kinase gene (BCR-ABL). Acute myeloid leukemia (AML) is recognized as heterogeneous disease that is caused by a variety of recurring chromosomal aberrations and genetic mutations (Melo *et al*., 2007; McCormack *et al*., 2008). However, these malignancies evolve into other types of leukemic forms and causes of these

transformations are still poorly understood. Due to the heterogeneity and complexity of leukemias, a multistep carcinogenesis model has not yet been established. Identifying molecular, genetic, and epigenetic irregularities involved in each type of cancer is essential for understanding the biological mechanisms, for predicting cancer development, and for identifying appropriate therapeutic approaches.

2.2. Chromatin organization and regulation

2.2.1. Chromatin structure

Chromatin structure defines the state in which genetic information is organized within a cell. The fundamental unit of chromatin is the nucleosome, which is composed of 147 base pairs of DNA wrapped around an octamer of core histone proteins, consisting of two copies of each histone protein: H2A, H2B, H3 and H4. Each of these core histones contains two major domains; a structured globular domain that mediates DNA-histone and histone-histone interactions and an amino domain or tail that is outside the core and serves as a substrate for histone modifying enzymes, which introduce post-translational modification such as acetylation, methylation, phosphorylation, ubiquitylation, and sumoylation (Kouzarides, 2007).

Chromatin is compacted into a higher order structure forming a 30 nm condensed fiber by repetitive folding of adjacent nucleosomes. Chromatin condensation is dynamic and structurally heterogenous and it is present principally in two different forms, heterochromatin and euchromatin. Heterochromatin is compact and associated with transcriptionally inert DNA regions. Heterochromatin is principally found at the chromosome centromere and telomeric regions (Martin *et* al., 2005). Euchromatin is characterized by uncondensed chromatin, which is accessible for gene activation (Cosgrove and Wolberger, 2005; Bernstein, 2007). Dynamic changes in chromatin structure greatly influence abilities of genes to be activated or silenced. These changes are principally driven by enzymatic modifications, such as DNA methylation and histone protein modification and they are broadly defined as epigenetic changes (Bernstein, 2007).

2.3. Epigenetics

The term epigenetics was first defined by Waddington in the 1940s, as 'the causal interaction between genes and their products, which bring phenotypes into being' (Waddington, 1942). Regardless of its many definitions, epigenetics is currently defined as the study of heritable changes in gene expression that occur without any changes in the genomic DNA sequence (Jones and Baylin, 2002). Epigenetic modifications are transmitted from one generation of cells to the next and heritable gene expression patterns are mediated by particular combinations of DNA methylation and posttranslational histone modifications (Sharma *et al*., 2010). These modifications regulate genome functioning and alter the structural dynamic of the chromatin, causing inactivation or activation of specific genes. Alteration in these processes results in dysregulation of gene expression profiles, causing permanent silencing of tumor suppressor genes and activation of oncogenes that lead to cancer development. However, events that lead to initiation and progression of these changes are still not completely understood (Feinberg, 2007; Jones *et al*., 2007; Sharma *et al*., 2010).

2.3.1. DNA methylation

DNA methylation is the only type of chemical modification that takes place on the DNA molecule without altering the DNA sequence itself (Espada and Esteller, 2010). In mammals, DNA methylation occurs through the addition of a methyl group at the C-5 position of cytosine in CpG dinucleotides, which is catalyzed by DNA methyltransferases (DNMTs) (Figure 2.1). CpG islands correspond to a genomic sequence that has high content of CG dinucleotides and typically occurs near the transcription start site of genes (Gardiner-Garden and Frommer, 1986). Approximately 60% of human gene-promoters are associated with CpG-rich regions. Even though only a relatively small fraction of these sequences become methylated, changes in methylation are necessary during cell development and differentiation as well as to maintain the stability of the cell (Bernstein, 2007). However, hypermethylation of CpG islands can stably repress genes and cause misregulation that are involved in cancer development (Mund *et al*., 2006; Jones *et al*., 2007).

DNA methylation mainly mediates gene silencing by either blocking transcription factors from accessing DNA binding sites or providing sites for methyl-binding proteins, which can

mediate gene repression through interactions with histone related enzymes, such as histone deacetylases (HDACs) and histone methyltransferases (HMTs) (Sharma *et al*., 2010).

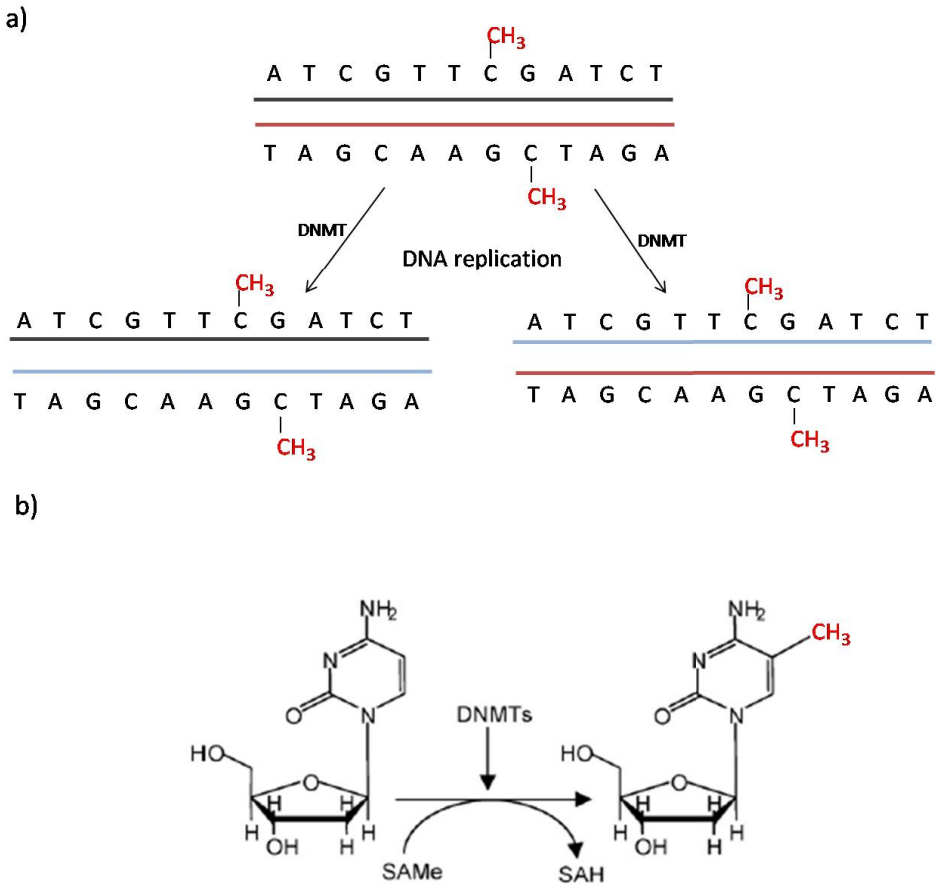

Figure 2.1. Chemical basis of DNA methylation. DNA methylation in mammalian genome occurs almost exclusively in cytosine residues contained in CpG dinucleotides and it essentially takes place to preserve genome DNA methylation (a) and to alter gene expression patterns through *de novo* methylation (b). (a) The pattern of symmetrically methylated CpG dinucleotides is copied and maintained during DNA replication in a process catalyzed by DNA methyltransferases. (b) DNA methyltransferases use S-adenosyl-L-methionine (SAMe) as the source of methyl groups, producing S-adenosyl-homocysteine (SAH). DNA methyltransferases catalyze the addition of methyl groups to the 5'-position of the pyrimidine ring of cytosine. (This figure was adapted and modified from Espada and Esteller, 2010).

2.3.1.1. CpG island hypermethylation

A cancer epigenome is marked by a global DNA hypomethylation and site-specific CpG island promoter hypermethylation (Esteller, 2007). Site specific DNA hypermethylation was initially associated with tumorogenesis when loss of function of the tumor suppressor gene Rb was discovered to be caused by promoter CpG hypermethylation (Greger *et al*., 1989). Following this discovery, various other tumor suppressor genes, including p16 (Gonzalez-Zuleta *et al*., 1995), p15 (Herman *et al*., 1997) MLH1 (Kane *et al*., 1997), and E-cadherin (Graff, 1995; Corn *et al*., 2000; Melki *et al*., 2000) were shown to undergo tumor-specific repression by promoter hypermethylation in a variety of cancers.

DNA hypermethylation also indirectly silences other genes by repressing transcription associated-factors and DNA repair genes, which interferes with the normal cellular processes (Sharma *et al*., 2010). Although, silencing of tumor suppressor genes by DNA hypermethylation is well established in cancer, it is not clear how genes are targeted to be silenced by this modification. Currently, DNA methylation markers are being investigated as prognostic factors, diagnostic tools, and treatment response predictors in a variety of cancers including leukemia, and demethylating agents are being used in cancer therapy (Esteller, 2007).

2.3.1.2. DNA methyltransferases

In mammals, DNA methylation is a process modulated by three DNA methyltransferase (DNMT) enzymes, DNMT1, DNMT2, and DNMT3, which includes DNMT3a and DNMT3b members. These DNMTs catalyze two important methylation patterns: methylation maintenance and *de novo* methylation (Zhu and Otterson, 2003).

DNMT1 is the largest methyltransferase with a molecular mass of 184 kDa (Smith *et al*., 1992) and it is the principal isoform responsible for methylation maintenance. In proliferating cells, DNMT1 has a high affinity for hemi-methylated DNA and it is found to be associated with the replication stage of the cell cycle; ensuring preservation of the pre-existing methylation pattern in the new synthesized cell during DNA replication (Leonhardt *et al*., 1992; Li *et al*., 1993). In human cells, a reduction in catalytic activity of DNMT1 results in a massive 5-methyl cytosine (5mC) demethylation, nuclear disorganization, genomic instability, and loss of cell viability (Espada and Esteller, 2010). Abnormalities in DNMT1 are found in a variety of cancer (Rhee *et al.,* 2000; Lee *et al.,* 2001; Peng *et al.,*2005, but loss in DNMT1 activity, in contrast to

normal cells, is required for activation of hypermethylated tumor suppressor genes that suppress tumor progression in malignant cells (Chen *et* al., 2007). DNMT1 has also been reported to interact with histone methyltransferase enzymes such as G9a and SUV39H1 to stably silence genes (Cedar and Bergman, 2009; Sharma *et al*., 2010).

DNMT2 is much smaller than DNMT1 with a predicted molecular weight of 45 kDa. Although DNMT2 contains the conserved methyltransferase motif, which is characteristic of DNMTs, this enzyme has very low DNA methyltransferase activity in comparison with DNMT1 and DNMT3. In addition, it has been reported that depletion of the DNMT2 gene in mice does not show phenotype changes and thus the function of DNMT2 still remains unknown (Okano *et al*., 1998; Herman *et al*., 2003).

DNMT3a and DMT3b isoforms have a molecular size between 100-130 kDa and they carry out *de novo* DNA methylation using unmethylated DNA as a substrate. However, several reports have shown that DNMT1 as well as DNMT3a and DNMT3b have both *de novo* and maintenance methylation *in vivo*, cooperating to establish global DNA methylation patterns in the cell (Kim *et al*., 2002). These enzymes are mainly expressed in embryonic and non-differentiated cells and they are critical for embryonic development (Okano *et al.,* 1999). DNMT3L is also a member of the DNMT3 family but unlike DNMT3a/3b it lacks DNA methyltransferase activity (Ooi *et al*., 2007). The function of this enzyme is to recruit DNMTs to DNA by binding to histone H3 in the nucleosomes. DNMT3a and DNMT3b are associated with SET domain proteins such as histone methyltransferases G9a, SUV39H1, and SUV39H2, which are required for heterochromatinization and histone lysine methylation (Cedar and Bergman 2009).

2.3.1.3. DNA methyltransferase inhibitors

Since the discovery of the association between promoter hypermethylation of tumor suppressor genes and the development of cancer, DNA demethylating agents (in reference to DNMT inhibitors, which lead to the loss of methyl groups from DNA) have emerged as therapeutic reagents for reversing this process. The most extensively studied DNMT inhibitors are 5-aza-cyditine and 5-aza-2'-deoxycytidine (DAC) (Figure 2.2). These chemotherapeutic agents are nucleoside analogues that incorporate into the DNA to inhibit the activity of DNMT enzymes (Zhu and Otterson, 2003; Hellebrekers *et al*., 2007). However, a major disadvantage

of these aza-nucleosides is their instability in aqueous solution. This limitation has prompted the development of more stable nucleosides analogues, such as 5-fluoro-2'deoxycytidine and zebularine, enabling oral administration of the drugs. Even though zebularine is more stable and less toxic, it requires higher concentrations to cause an effect in comparison with DAC (Cheng *et al.,* 2004). Non-nucleoside analogue DNMT inhibitors have also been discovered as well as natural products derived from teas (Hellebrekers *et al*., 2007). Most DNMT inhibitors are not specific for a particular DNMT enzyme, which may result in unfavourable effects and toxicities. Consequently, new compounds specific for DNMT types are being developed, such as MG98, which is an oligonucleotide antisense inhibitor of DNMT1 (Hellebrekers *et al*., 2007).

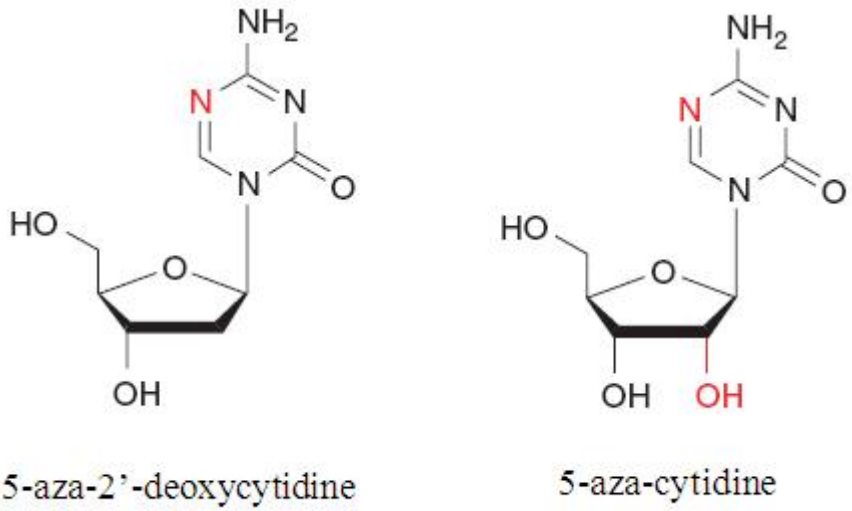

Figure 2.2. Chemical structures of DNMT inhibitors. 5-aza-2'-deoxycytidine (DAC) and 5-aza-cytidine. The difference between these compounds is that the ribose at position 3 of the cytosine ring in 5-aza-cytidine is replaced with deoxyribose in DAC.

2.3.1.4. 5-Aza-2'-deoxycytidine (DAC)

The remarkable discovery that treatment of cells with the cytotoxic agents, 5-azacytidine and DAC, inhibits DNA methylation, induces expression of genes, and causes differentiation of cancer cells, led to the use of these drugs in cancer therapy. DAC is a derivate of 5-azacytidine and a more potent demethylating agent (Jain *et al*., 2009). This compound is also a cytidine analogue that is incorporated into the DNA in place of the natural base cytosine during DNA replication. Once incorporated into the DNA, this compound irreversibly binds to DNMT1, leading to a rapid loss of DNMT1 activity and therefore to the demethylation of DNA (Figure 2.3) (Chen *et al*., 2004; Hellebrekers *et al*., 2007). Accumulated evidence from studies on hypermethylated silenced genes has demonstrated that DAC induced the re-expression of tumor suppressor genes in cancer cells if methylation is the primary reason for gene silencing (Jones and Baylin *et al*., 2002; Daskalakis *et al*., 2002, Chen *et al*, 2004). In addition, DAC can also induce expression of apoptotic genes and DNA damage response genes, such p53 (Chen *et al*., 2004).

The Food and Drug Administration has recently approved the use of 5-azacytidine and DAC for treatment of myelodysplastic syndromes (MDS) and promising results have emerged from the treatment of hematological malignancies, such as AML and CML (Plickmark *et* al., 2007; Jain *et al*., 2009). Although, DAC provides an effective treatment of these cancers, toxicity on normal cells have been a concern due to the incorporation of this compound into DNA. However, since this drug only acts in dividing cells and tumor cells are rapidly dividing in comparison with normal cells, it is thought that treatment with this drug may have a minimal effect on normal cell populations, making this compound a good candidate in cancer therapy (Sharma *et al*., 2010).

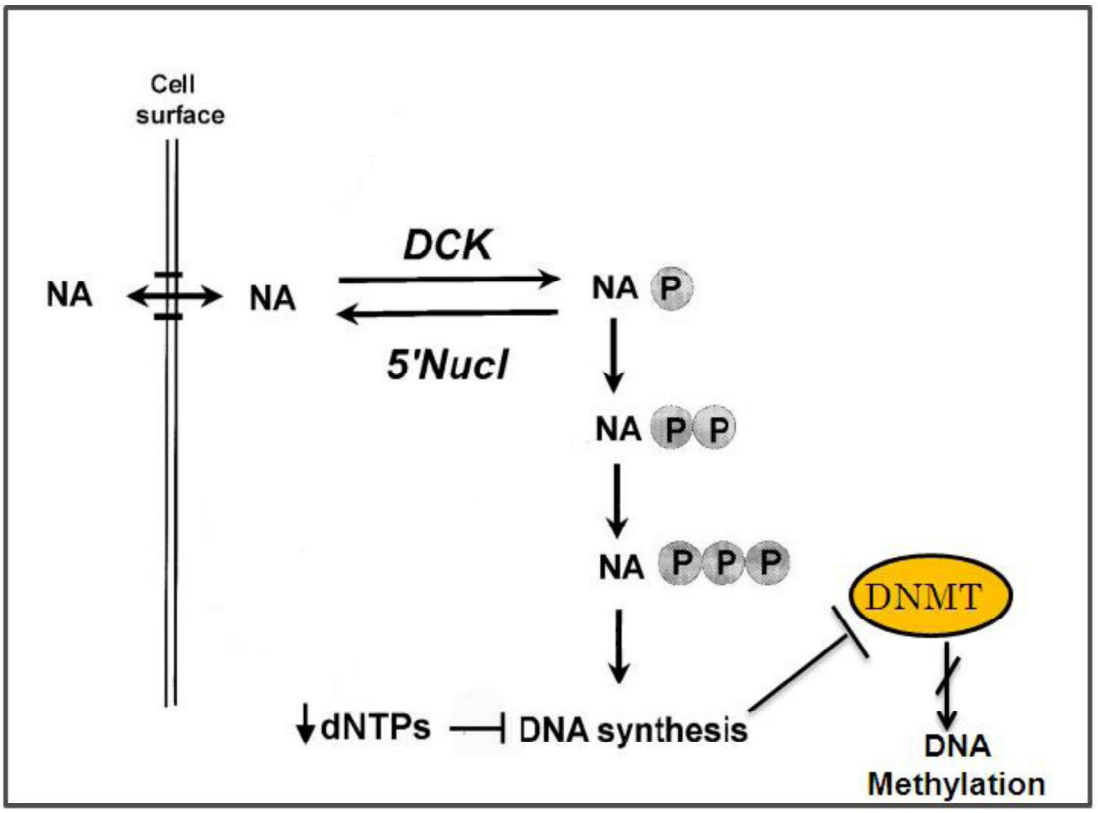

Figure 2.3. Nucleoside analogue (NA) incorporation into the DNA of proliferating cells. Nucleoside analogues enter the cell via specific nucleoside transporters. Once inside the cell, nucleoside analogues are phosphorylated by deoxycytidine kinases (*DCK)* to produce active 5'-triphosphate derivatives. Nucleoside analogues are incorporated into newly synthesized DNA, where they covalently interact with DNMTs, inhibiting DNA methylation. (Adapted from Galmarini *et al*., 2001; Ewald *et al*., 2008).

2.3.2. Histone methylation

Post-translational modifications that occur on histone tails have been recognized to play important roles in regulation of chromatin structure (Esteller 2007; Hublitz *et al*., 2009). Histone methylation is catalyzed by histone methyltransferases (HMTs) and it usually occurs on the Arginine (R) and Lysine (K) residues. Histone methylation, in contrast to other modifications, does not alter the charge of the histone tail but influences the basicity and hydrophobicity of histones and their affinity to other proteins, such as transcription factors for chromatin regulation (Esteller, 2007; Hublitz *et al*., 2009).

The Histone methyltransferase enzymes can be subdivided into three classes; SET domain (Suv3-9 Suppressor of Variegation, Enhancer of Zeste, Trithorax) lysine methyltransferases, non-SET domain lysine methyltransferases, and arginine methyltransferases (Kouzarides, 2007; Albert *et al.*, 2010; Spannhoff *et al*., 2009).

Lysine methyltransferases are highly specific. They usually modify one specific lysine residue on a single histone, which can be linked either to activation or repression of transcription. Lysine methylation is predominantly found within tails of histone 3 and histone 4 (H3 and H4); however the core globular domain of histones can also undergo methylation, for example at lysine 79 of H3 (Martin *et al*., 2005; Kouzarides, 2007; Albert *et al*., 2010). Lysine residues can be mono-, di-, or tri-methylated and more than twenty lysine methyltransferase enzymes have been identified in humans. However, misregulation of many of these methyltransferases has been linked to cancer (Table 2.1) (Martin *et al*., 2005; Albert *et al*., 2010).

Table 2.1. Lysine methyltransferases and their link to cancer. Enzymes that fall into the same family are grouped.

Enzyme	Lysine residues	Links to cancer
SUV39H1/2	H3K9	Increased mRNA levels in colon cancer patients (Kang *et al*., 2007) B-cell lymphoma in knockout mice (Peters *et al*., 2001)
G9a	H3K9	Contributes to H3K9 dimethylation involved in tumor suppressor gene silencing (McGarvey *et al*., 2006)
EU-HMTase1	H3K9	Overexpressed in gland tumors (Aniello *et al*., 2006)
SETDB1/ESET	H3K9	Association with DNMTs in promoter silencing in tumors (Li *et al*., 2006)
MLL1	H3K4	Mutations/rearrangements involved in leukemogenesis (Chen *et al*., 2010)
MLL3	H3K4	Intragenic mutations in colorectal cancer (Sjoblom *et al*., 2006)
SMYD2	H3K4	Overexpressed in hepatocellular carcinoma (Skawran *et al*., 2008) Suppression of p53 transcriptional activity (Huang *et al*., 2007)
SMYD3	H3K4	Overexpressed in colorectal and hepatocellular carcinoma (Hamamoto *et al*., 2004) Overexpression enhanced breast cancer cell growth (Hamamoto *et al*., 2006)
DOT1L	H3K79	Involved in leukemogenesis (Chen *et al*., 2010)
SET8/PR-SET7	H4K20	Suppresses p53 dependent transcription (Shi *et al*., 2007)
SUV20H1/2	H4K20	Decrease of H4K20 tri-methylation is associated to lymphoma cancer and Knock-downed SUV20H1/2 mice (Fraga *et al*., 2005)
EZH2	H3K27	Associated with aggressive tumor growth in several tumor types, including lymphomas and melanomas (Bachmann *et al*., 2006) Marker for precancerous state and aggressive breast cancer (Ding *et al*., 2006; (Collet *et al*., 2006) Promotes proliferation and invasiveness of prostate cancer cells (Bryan *et al*., 2007) Biomarker for poor prostate cancer prognosis (Cooper *et al*., 2007)

2.3.2.1. Histone 3 lysine 9 methylation (H3K9Me)

Lysine methylation is an abundant epigenetic modification found in all eukaryotes and it is associated with different states of chromatin (Kouzarides, 2007). In histone 3 (H3), mono- (Me) and di-methylation (Me2) of lysine 9 (K9) is associated with activation of transcription, whereas tri-methylation (Me3) is commonly involved in transcriptional silencing. Despite H3K9 di-methylation being related with transcriptional activation, it can also be associated with gene repression in euchromatin and heterochromatin regions, which suggest that H3K9 methylation might have different functions depending on whether it occurs in coding regions or in gene-promoters (Rice *et al*., 2003; Martin and Zhang, 2005; Kouzarides, 2007). In mammals, several lysine methyltransferases target different levels of H3K9 methylation, such as SUV39H1/2, G9a, GLP, and RIZ (Martin *et al*., 2005; Hublitz *et al*., 2009).

McManus and colleagues reported a dynamic role for H3K9 methylation in controlling the cell cycle. They revealed that mono- and di-methylation levels of H3K9 remain unaltered during cell cycle progression, while H3K9 tri-methylation levels increased for maintenance of chromosomal segregation in the transition from late G2 into mitosis. They also observed that H3K9 tri-methylation mark is rapidly lost after completion of mitosis and it returns to basal levels by early G1. Importantly, this study demonstrated that absence of pericentromeric H3K9 tri-methylation correlates with an increase in abnormal mitosis, premature chromatid separation, genomic instability, and cancer predisposition (McManus *et al*., 2006). Thus, perturbations of H3K9 methylation patterns and enzymes associated with these modifications leads to misregulation of the cell cycle control and then to the aberrant silencing of tumor suppressor genes that control proliferation in various forms of cancer (Sharma *et al*., 2010).

2.3.2.2. Histone methyltransferase SUV39H1

SUV39H1 was the first histone methylation enzyme discovered in humans and it is responsible for tri-methylation of lysine 9 at histone 3 (H3K9). This enzyme belongs to the SET domain lysine methyltransferases class. The SET domain of SUV39H1 carries out the H3K9 methyltransferase activity using monomethylated H3K9 as a substrate to finally induce tri-methylation at the same residue (Aagaard *et al*., 1999; Rea *et al.*, 2000; Peters *et al*., 2003).

The role of SUV39H1 and its associated H3K9 methyltransferase activity in heterochromatin function was first indicated by the association with the heterochromatin protein

HP1 (Aagaard *et al*., 1999; Rea *et al.*, 2000). Subsequent studies showed that SUV39H1-mediated H3K9 methylation provides a binding site for chromodomain transcriptional repressor HP1 proteins, which in turn recruit other transcriptional repression machinery, such as DNA methyltransferases and histone deacetylases (HDACs) to achieve gene silencing (Wang *et al.*, 2000). Moreover, evidence supports that SUV39H1 and SUV39H2 recruit DNMT3a and DNMT3b in order to methylate CpG sites in the satellite sequence (Cedar and Bergman, 2009). For example, a loss of H3K9 methylation in *SUV39H1* knockout embryonic stem (ES) cells decreases DNMT3b-dependent CpG methylation at major centromere satellites. This data suggests that DNA methylation may be a secondary event in gene silencing (Lehnertz *et al*., 2003). In addition, alteration of *SUV39H1* expression has been related to cancer development and silencing of tumor suppressor genes, such as p16, p15, and E-cadherin (Bachman *et al*, 2003; Albert *et al*., 2010; Lakshmikuttyamma *et al*., 2010)

2.3.2.3. Histone methyltransferase G9a

G9a belongs to the SET domain lysine methyltransferase class and in contrast to SUV39H1; G9a regulates H3K9 mono- and di-methylation in euchromatin regions and has a major function in transcriptional control. The dominant role of this enzyme in euchromatin regions is supported by the observation that the H3K9 methylation pattern is severely eliminated in *G9a*-deficient mice and cells (Tachibana *et al*., 2002, 2005).

G9a, apart from having the SET catalytic domain, also contains an ankyrin (ANK) domain, which has been recently recognized to be associated with DNMT3a and DNMT3b and is involved in directing *de novo* DNA methylation (Cedar and Bergman, 2009). Accordingly, Epztejn-Litman and Dong reported that H3K9 methylation is eliminated upon inactivation of G9a SET domain without affecting DNA methylation; instead it was recognized that the ankyrin domain physically interacts with DNMT3a and DNMT3b to establish DNA methylation (Epztejn-Litman *et al*., 2008; Dong *et al*., 2008). This data indicates that *de novo* DNA methylation is not dependent on G9a-mediated histone modification *per se*; however, G9a is required for recruiting DNMT3a and DNMT3b for stable gene silencing (Epztejn-Litman *et al*., 2008; Dong *et al*., 2008). Conversely, it was reported that G9a directly interacts with DNMT1 to establish a coordinated mechanism for DNA and histone methylation during cell replication and that this interaction perhaps depends on G9a methyltransferase activity (Esteve

et al., 2006). Increased levels of G9a have been linked to gain in promoter H3K9 dimethylation in tumor suppressor genes, consequently leading to their silencing in various types of cancer (McGarvay *et al*., 2006; Kondo *et al*., 2008).

2.3.3. Histone methyltransferase inhibitors

Since the discovery that epigenetic aberrations can be reverted in cancer cells, a number of DNA methyltransferase (DNMT) and histone deacetylase (HDAC) inhibitors have been introduced, extensively studied, and clinically tested for use in cancer therapy (Hellebrekers *et al*., 2007). More recently, histone methyltransferase (HMTs) inhibitors have been found to enhance anti-cancer therapy due to their ability to block repressive histone lysine methylation marks, such as H3K9 di- and tri-methylation. To date, two lysine methyltransferase inhibitors have been identified: chaetocin and BIX-01294.

2.3.3.1. Chaetocin

Chaetocin, a fungal mycotoxin isolated from the fermentation broth of *Chaetomium minutum*, belongs to a class of molecules called 3-6-epidithiodiketopiperazines (Figure 2.4). Functionally, chaetocin was found to inhibit the *Drosophila melanogaster* histone methyltransferase SU(VAR)3-9 and its human ortholog, the H3K9 trimethylase SUV39H1 (Greiner *et al*., 2005). Although chaetocin is effective in inhibiting SUV39H1 activity, its role in reactivation of silenced genes by promoter H3K9 demethylation is limited. Attempts to elucidate this role have been investigated. Recently, it was reported that treatment of cancer cells with chaetocin results in activation of tumor suppressor genes and a drastic decrease in promoter H3K9 di- and tri-methylation (Cherrier *et al*., 2009; Lakshmikuttyamma *et al*., 2010). Interestingly, chaetocin reactivates genes that have been silenced by promoter hypermethylathion in leukemia cells, which suggests that inhibition of SUV39H1 activity perhaps is required to abolish DNMTs interaction and therefore the recruitment of other repressive marks crucial for aberrant gene silencing (Lakshmikuttyamma *et al*., 2010). In addition to its demethylating function, chaetocin seems to be a selective drug for myeloma therapy, affecting myeloma cancer cells without toxicity on normal bone marrow and B-cells (Isham *et al*., 2007), which makes this compound a promising target for treatment of myeloid malignancies, including leukemia.

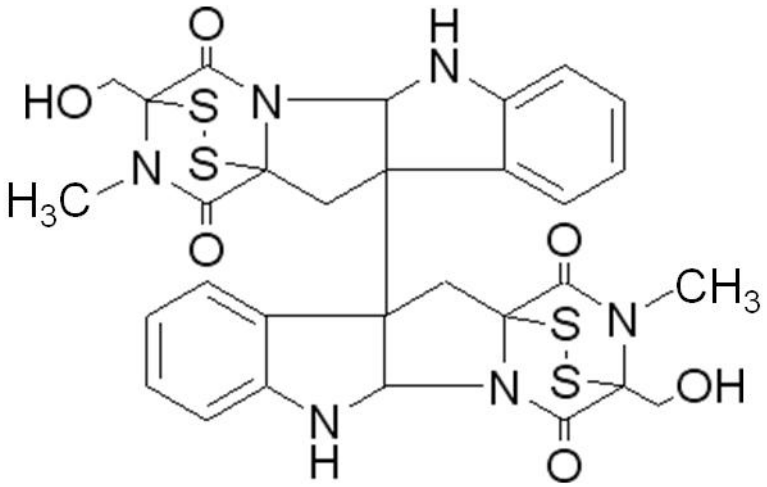

Figure 2.4. Chemical structure of chaetocin.

2.3.3.2. BIX-01294

BIX-01294 (BIX) is a diazepi-quinazolin-amine derivative that selectively impairs the histone methyltransferase activity of G9a and the generation of H3K9 di-methylation (Figure 2.5). BIX does not compete with the cofactor S-adenosylmethionine (SAM) and does not inhibit SUV39H1 activity (Kubicek *et al*., 2007; Chang *et al*., 2009).

It has been reported that G9a induces inactivation of post-implantation genes by the accumulation of H3K9 di-methylation marks during embryogenesis. In mouse ES cells and embryonic fibroblast cells, treatment with BIX results in a significant reduction of di-methyl H3K9 in proximal-promoters, thereby allowing the transient reversal of this mark and the activation of G9a target genes (Kubicek *et al*., 2007). BIX has not been tested for its ability to reactivate tumor suppressor genes in cancer. The evaluation of BIX treatment in cancer cells might be of crucial importance for activation of tumor suppressor genes that contain H3K9 di-methylation as a repressive mark and more importantly BIX could be used to potential reverse misregulated G9a activity that leads a faulty cell development in cancer stem cells (Wen *et al*., 2009).

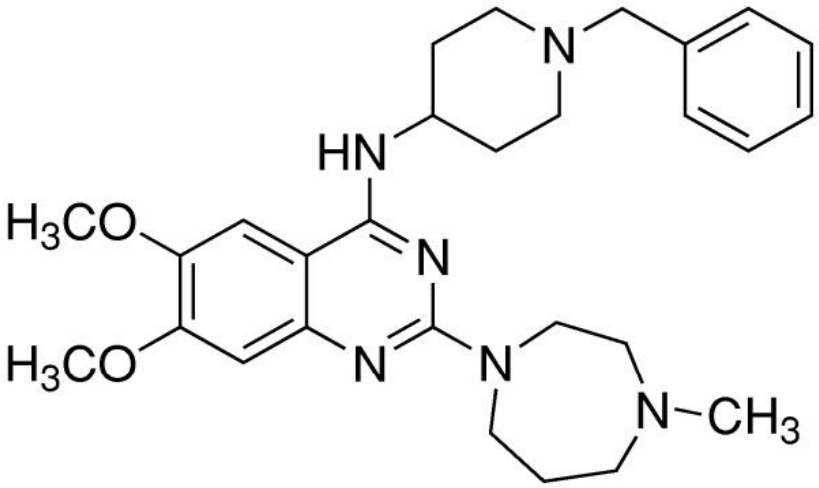

Figure 2.5. Chemical structure of BIX-01294.

2.3.4. Regulation of epigenetic events in cancer

Knowing the order in which epigenetic changes occur might have important implications for understanding normal cell development and tumorigenesis. Previously it was recognized that DNA hypermethylathion was the major epigenetic deregulation linked to cancer. Cancer cells are subject to abnormal DNA methylation within promoters of tumor suppressor genes and this event is responsible for inhibiting their function and inducing cell proliferation (Jones and Baylin, 2002). However, these observations have been restricted to re-activation of silenced genes by promoter demethylation using the demethylating agent 5-aza-2´-deoxycytidine (DAC) (Jones and Baylin, 2002; Herman and Baylin, 2003). Conversely, it was shown that DAC also induces expression of non-hypermethylated genes. Tumor suppressor genes that have been reactivated by DAC still maintain heterochromatic marks, such as histone H3K9 and H3K27 methylation, in their promoters. Thus, DAC treatment does not return reactive genes to a fully euchromatin state (Zhu and Otterson, 2003; McGarvey *et al*., 2006). In this regards, transcriptional silencing of cancer-associated genes depends not only upon DNA methylation, but it is also associated with multiple promoter chromatin modifications, including histone deacetylation, histone methylation of H3 at lysine 9, and loss of the transcriptional activating mark H3K4 di- and tri-methylation (Coombes *et al*., 2003; Scott *et al*., 2006; Sharma *et* al., 2010). Despite the fact that the exact sequence of events is not known, the current study of

epigenetic inhibitors has opened the possibility to investigate dynamic alterations and interactions of epigenetic modified marks that are linked to silenced-promoter of tumor suppressor genes.

Several reports have shown that aberrant gene silencing is associated with a concomitant loss of histone acetylation. Trichostatin A (TSA) and other HDAC inhibitors have been associated with the reactivation of silenced genes; however there is evidence suggesting that they cannot reactivate the expression of hypermethylated tumor suppressor genes (Herman *et al*., 1997; Cameron *et al*., 1999; Suzuki *et al*., 2002; Hellebrekers *et al*., 2007). Combinatorial therapy with histone deacetylase and DNA methyltransferase inhibitors enhances re-expression of several genes silenced by promoter hypermethylation to levels higher than when they are induced with DNMT inhibitors alone (Zhu and Otterson, 2003; Hellebrekers *et* al., 2007). Nonetheless, HDAC inhibitors are unable to block the re-silencing of genes after treatment with DNMT inhibitors. This data then indicates that DNA methylation is a dominant event over histone deacetylation (Egger *et al*., 2007). In this view, histone methylation seems to play an important role in hypermethylated gene silencing. For example, alterations in H3K9 and H3K27 methylation patterns are associated with aberrant gene silencing in various forms of cancer and more importantly DNA regions that have been hypermethylated are often pre-marked with tri-methyl H3K27 mark in cancer ES cells (Ohm *et al*., 2007; Schlesinger, *et al*., 2007). H3K9 methylation can be rapidly reversed by treatment with DAC, suggesting a direct relationship between DNA and histone methylation in gene inactivation (Nguyen *et al*., 2002; Coombes *et al*., 2003).

Currently, histone methyltransferase inhibitors have being targeted in epigenetic therapy for re-activation of tumor suppressor in cancer, due to its ability to interact between each other and form repressor silencing complexes that inactivate gene expression (Fritsch, *et al*., 2010). So far, it has been reported that treatment with chaetocin, the specific inhibitor of H3K9 trimethylase SUV39H1, induces the expression of hypermethylated p15 and E-cadherin genes without any changes in promoter methylation (Lakshmikuttyamma *et al*., 2010). Moreover, treatment with chaetocin induces re-expression of the non-hypermethylated gene p21 by reducing levels of trimethyl H3K9 and by blocking the interaction between SUV39H1 and the repressor CTIP2 protein (Cherrier *et al*., 2009). This suggests that histone methylation itself

may be a dominant event that leads to transcriptional gene silencing or it cooperatively interact with DNMTs to initiate aberrant promoter methylation.

Altogether, these findings reinforce the potential of histone methyltransferase inhibitors in re-expressing tumor suppressor genes. As well it highlights the need for further development of combinatorial treatments that reverse aberrant gene silencing in cancer.

2.4. Acute myeloid leukemia

Acute myeloid leukemia (AML) is a heterogeneous clonal disorder of hematopoietic progenitor cells, which is characterized by the rapid proliferation of abnormal cells that are accumulated in the bone marrow and interfere with the production of normal blood cells (Figure 2.6). AML is the most common type of leukemia in adults with an equal frequency in males and females, and like other cancers, its incidence increases with age (Estey and Dohner 2006; Deschler *et al.*, 2006).

Although the etiology of leukemia is unknown, recurrent genetic and chromosomal alterations are associated with leukemia etiology, and they are recognized to be crucial to the disease pathogenesis (Chen *et al*., 2010). The genotypic diversity of AML depends on numerous chromosomal translocations that result in the generation of oncogenic fusion proteins, such as AML1-ETO (generated by a translocation between 8 and 21, t (8; 21)), PML-RARA, t (15; 17), CBF-MYH11, t (16; 16), and MOZ-CBP, t (8; 16), etc), as well as point mutations involved in specific genes (MDR, FLT-3 ITD, C/EBPα, BAALC, NPM). These genetic alterations confer proliferative and survival advantage to hematopoietic progenitors with a minimal capacity to differentiate (Frankfurt *et al*., 2007; Chen *et al*., 2010). Besides those genetic factors, aberrant epigenetic regulation of genes in AML is being recognized as becoming increasingly important to the pathogenesis of AML (Plass *et al*., 2008). Promoter hypermethylation of several tumor suppressor genes with well-established functions in cell cycle control, apoptosis, or DNA repair are associated with the development of the disease (Agrawal *et al*., 2007; Melki *et al*., 1999; Melki *et al.*, 2000; Ekmekci *et al*., 2004; Shimamoto *et al*., 2005).

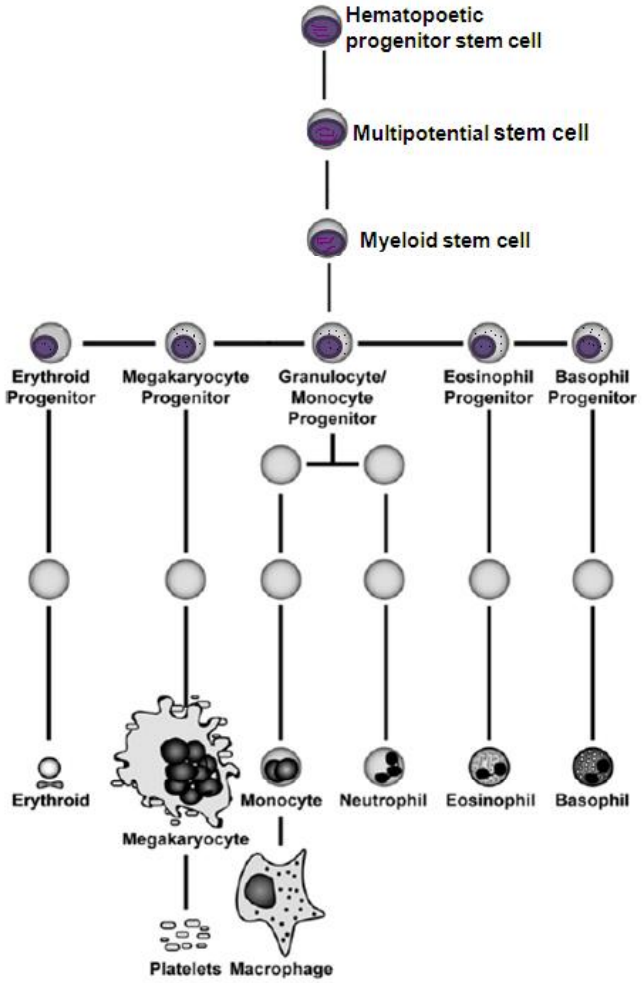

Figure 2.6. Myeloid cell differentiation. Illustrated are the differentiation pathways of blood cell development. The bone marrow makes progenitor stem cells that develop into mature blood cells over time. Progenitor stem cells may become a myeloid stem cell or lymphoid stem cells. The myeloid stem cell differentiates into one of the five types of mature blood cells: erythroid, platelets, macrophage, neutrophil, eosinophil, and basophil. Acute myeloid leukemia (AML) is originated when a disorder of the hematopoetic progenitor stem cell occurs, causing the accumulation of abnormal cells that cannot be differentiated into the variety of normal blood cells (mature blood cells).

2.5. Tumor suppressor genes in acute myeloid leukemia

Tumor suppressor genes encode proteins that are involved in receiving or processing of growth inhibitory signals and therefore they are very important in preventing malignant transformation. Like almost all genes, tumor suppressor genes are present in two copies per cell. Knudson's 'two hit' hypothesis explains the loss-function of these genes in cancer development, meaning that both alleles of a gene have to be inactivated in order to promote unregulated cell proliferation (Knudson, 1996; Krug *et al*., 2002). However, it was proposed that the function of some tumor suppressor genes can be disrupted solely by alteration of one allele, resulting in a dominant negative mode of action that compromise the normal function of its counterpart in the same cell (Blagosklonny, 2000). Genetic disruption and epigenetic inactivation of several tumor suppressor genes has been associated with AML development (Krug *et al*., 2002; Chen *et al*., 2010). Particularly, genes that are involved in cell cycle control, such as cyclin dependent kinases (CDK) inhibitors p15 and p21 have been recognized to be silenced by aberrant epigenetic modifications in AML (Herman, 1997; Scott *et al*, 2006; Lakshmikuttyamma *et al*., 2010). In addition, the E-cadherin gene, a potential suppressor of metastasis, is also epigenetically silenced in AML (Corn *et al*., 2000; Melki *et al.*, 2000).

2.5.1. p15 $^{(INK4b)}$ gene

p15 belongs to the INK4 family that consist of a group of small (15-19 KDa) ankyrin repeat proteins. $p15^{INK4b}$, $p16^{INK4a}$, $p18^{INK4c}$, and $p19^{INK4d}$ function as inhibitors of CDK4 and CDK6 (Sharpless, 2005). $P16^{INK4a}$ (p16) and $p15^{INK4b}$ (p15) proteins bind directly to CDK4 and CDK6 blocking their association with regulatory D cyclins and enabling other cyclin-dependent kinase inhibitors, such as p21CIP1 and p27KIP1 to associate with and inhibit the assembly of cyclin E/A-CDK2 complexes. The lack of cyclin E/A-CDK2 complexes in turn inhibits phosphorylation of retinoblastoma (Rb) family members causing inactivation of proteins involved in DNA synthesis and thus arresting the cell cycle progression in G1-phase (Figure 2.7) (Massagué, 2004; Sharpless, 2005; Gil and Peters, 2006). p15, p16, and *ARF* share the same locus *INK4a/ARF/INK4b*, but they play independent roles in tumor suppression (Gil and Peters, 2006). *INK4b* gene expression can be activated by the regulation of proteins such as the transforming growth factor beta (TGFβ) and small GTPases (RAS) and it can be repressed by myelocytomatosis (MYC) factor, which usually leads to the unregulation of other several genes

involved in cell proliferation (Hannon and Bench, 1994; Warner *et al*., 1999; Seosane *et al*., 2001).

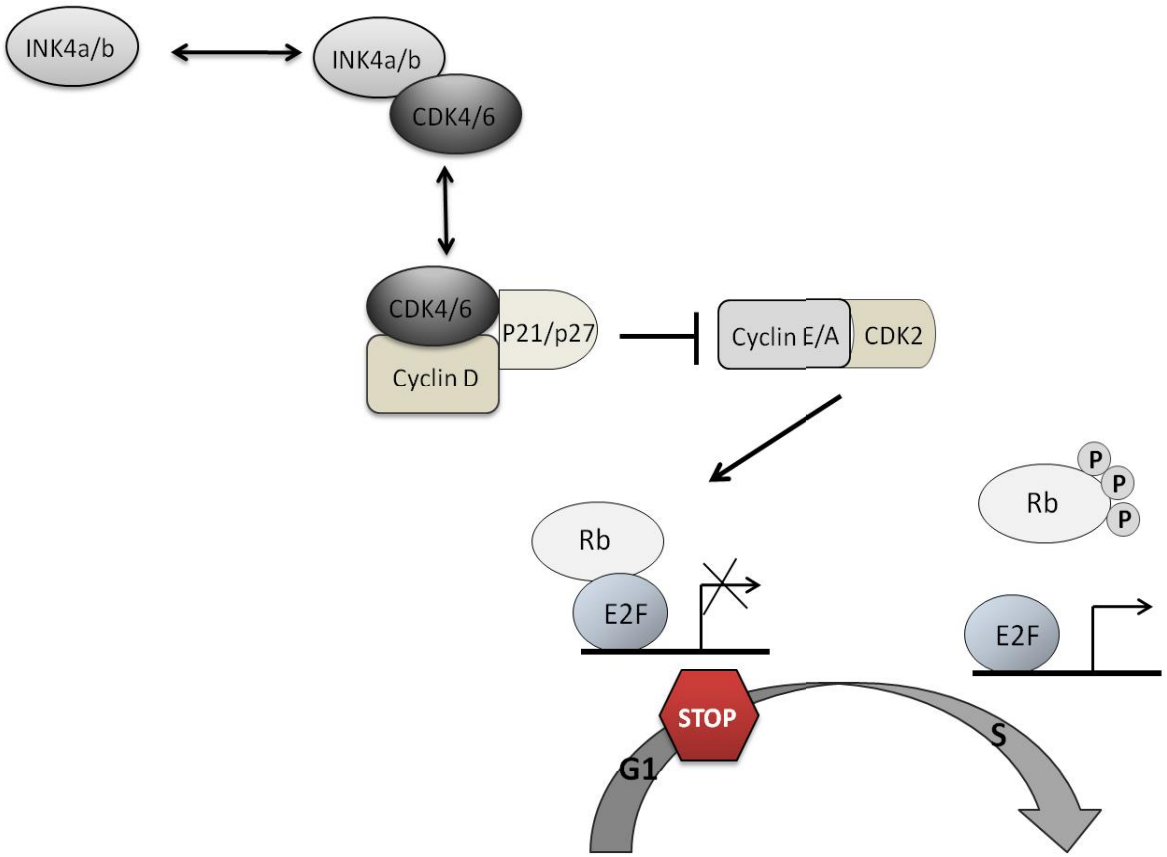

Figure 2.7. Schematic representation of check points control during G1-S progression. By binding directly to CDK4 and CDK6, INK4a/b proteins block the assembly of catalytically active cyclin D-CDK complexes and enable the cyclin-dependent kinase inhibitors p21CIP1 and p27KIP1 to associate with and inhibit cyclin E/A-CDK2. This in turn inhibits phosphorylation of retinoblastoma (Rb) family members, blocking the release and activation of E2F-dependent genes and the activation of proteins involved in DNA synthesis. The net result is the promotion of cell cycle arrest in G1-phase during G1-S progression (Adapted from Malumbres and Barbacid, 2009).

The *INK4* genes are commonly silenced by mutations and epigenetic modifications in diverse types of cancers (Okamoto *et al*., 1994; Gil and Peters, 2006; Kim and Sharpless, 2006; Malumbres and Barbacid, 2009). Point mutations and intragenic alterations in the locus target *INK4a* rather than *ARF* or *INK4b* (Sharpless, 2005). However, most alterations occur by epigenetic inactivation of *p16* and *p15* genes due to hypermethylation of their promoters or by deletions in the 9p21 chromosome region (Krug *et al*., 2002). *p15* is frequently silenced by promoter hypermethylation in myeloid dysplastic syndrome (MDS) and AMLs (Herman *et al*., 1997; Chim *et al*., 2001; Christiansen *et al*., 2003). Hypermethylation of p15 occurs in the majority of patients with AML and it has been strongly associated with disease progression (Woong *et al*., 2000; Krug *et al*., 2002). Therapeutic DNA demethylating agents, such as DAC have been used for the re-activation of hypermethylated genes in AML cell lines (Jain *et al*., 2009). Interestingly, it was recently showed that *p15* is not only re-expressed by promoter demethylation, but blocking histone H3K9 methylation with histone methyltransferases inhibitors also induced *p15* expression in AML cell lines (Lakshmikuttyamma *et al*., 2010). This suggest that use of combinatorial therapies might efficiently leads to the re-expression of silenced tumor suppressor genes rather than the use of epigenetic inhibitors alone.

2.5.2. p21 $^{(WAF1/CIP1)}$ gene

p21 gene encodes a small 165 amino acid protein that belongs to the CIP and KIP family of CDK inhibitors that includes p21CIP/WaFI (p21), p27KIP1 (p27), and p57KIP2 (p57) (Sherr and Roberts, 1995). The p21 protein contains two functional domains, an amino-terminal CDK interaction region that is sufficient for CDK inhibition, and a carboxy-terminal region that binds proliferating cell nuclear antigen (PCNA), a processivity factor associated with DNA polymerase-δ, and several other proteins involved in DNA synthesis (Chen *et al*., 1995).

p21 inhibits cell cycle progression primarily by blocking CDK2 activity, which is required not only for the phosphorylation of Rb family proteins, which releases and activates E2F-dependent gene expression, but also for the activation of proteins directly involved in DNA synthesis (Massagué, 2004; Malumbres and Barbacid, 2005). Thus, suppression of p21 activity is essential for checkpoint control in G1/S progression within the cell cycle (Figure 2.7) (Malumbres and Barbacid, 2005). Moreover, by inhibiting cell cycle progression, p21 also allows DNA repair processes to occur by binding to proliferating cell nuclear antigen (PCNA),

which interferes with PCNA-dependent DNA polymerase activity, inhibiting DNA replication (Chen *et al*., 1995; Luo *et al*., 1995; Moldovan *et al*, 2007). The ability of p21 to promote cell cycle arrest and DNA repair responses can be dependent or independent of the tumor suppressor protein p53 activity. However, other evidence indicates that p21 mediates its various biological activities independent of the classical p53 tumor suppressor pathways (Abbas and Dutta 2009).

p21 expression can be regulated by a variety of transcriptions factors, such as p53, Sp1, or C/EBP for a positive regulation and MYC and inactivation of p53 for a negative regulatory effect (Gartel and Tyner, 1999; Abbas and Dutta, 2009). p21 deregulation has been reported in various forms of cancer (Shiohara *et al*., 1994; Poole *et al*., 2004). Accordingly, several studies have shown that p21 deficiency increased frequency and development of spontaneous tumors in mice (Martin-caballero *et al*., 2001). Moreover, evidence suggests that p21 is crucial for maintaining stem cell potential by restricting their self-renewal capacity in various tissues (Cheng *et al*., 2000; Kippin *et al*., 2005).

Epigenetic silencing of p21 has been reported in human cancer and DNA methylation and histone deacetylation are crucial for this silencing (Suzuki *et al*., 2002; Lagger *et al*., 2003; Scott *et al*., 2006). p21 is unmethylated in most types of cancers; however some lung cancer cell lines show hypermethylation within the CpG islands of the p21 gene-promoter (Zhu and Otterson, 2003; Ying *et al*., 2004; Scott *et al*., 2006). Treatment with demethylating agents induces re-expression of p21 by mechanisms that are dependent or independent of promoter demethylation and by HDAC inhibition (Zhu *et al*., 2004; Scott *et al*., 2006). Scott and colleagues reported that p21 gene is epigenetically silenced in AML by a mechanism that does not involve promoter hypermethylation, due to the lack of p21 promoter methylation in AML cell lines. Moreover, they also showed that treatment with DAC and TSA cause p21 re-expression by release of HDAC1 (Scott *et al*., 2006). In AML cell lines, similar studies have not been performed to determine the effect of histone methylation on p21 gene re-expression.

2.5.3. E-cadherin gene

E-cadherin gene encodes a glycoprotein that is involved in calcium dependent cell-cell adhesion. E-cadherin is one of the most important molecules in cell adhesion in epithelial tissues and is also considered a potential invasion/metastasis suppressor. Loss of E-cadherin

function contributes to the progression of several types of cancers such as gastric, breast, colorectal, thyroid, and ovarian cancer and recently it has been recognized as potential invasion/metastasis suppressor in leukemia (Hirohashi, 1998; Melki *et al*., 2000). The inactivation of the E-cadherin gene occurs in undifferentiated solid tumors by both genetic and epigenetic mechanisms (Yoshiura *et al*., 1995). In addition, it has been shown that E-cadherin gene expression is reduced or absent in leukemia due to the promoter hypermethylation (Melki *et al*., 2000). Dysfunction of this gene in AML is important to pathogenesis and therefore it could have clinical importance in the treatment of AML (Shimamoto *et al*., 2005). Recently, it was reported that E-cadherin silencing can be reverted either by promoter demethylation or by inhibition of promoter H3K9 tri-methylation in AML cell lines (Lakshmikuttyamma *et al*., 2010).

3. EXPERIMENTAL OBJECTIVES

The efficient reactivation of epigenetically silenced genes requires the development of combinatorial epigenetic therapies that reverse aberrant chromatin modifications and lead to transcriptional activation of tumor suppressor genes in cancer. The objective of this study was to investigate epigenetic mechanisms involved in the re-expression of three tumor suppressor genes: p15, p21 and E-cadherin in AML using the DNMTinhibitor, 5-Aza-2'-deoxycytidine (DAC), and the HMT inhibitors, BIX-01294 (BIX), and chaetocin.

To achieve this goal, the following aims were undertaken:

1. Evaluate the p15, p21, and E-cadherin promoter methylation status using methylation specific PCR and DNA pyrosequencing.

2. Determine the effect of DAC, BIX, and chaetocin on acute myeloid leukemia cell proliferation using MTT assay (3-(4,5-dimethylthiazol-2-yl)-2,5-diphenyltetrazolium bromide).

3. Evaluate the effect of individual treatments of DAC, BIX, and chaetocin on p15, p21, and E-cadherin gene expression using real time PCR.

4. Develop combinatorial treatments of DAC, BIX, and chaetocin that lead to re-expression of p15, p21, and E-cadherin genes in acute myeloid leukemia.

5. Determine changes in DNA methylation and histone 3 lysine 9 di- and tri-methylation associated with p15, p21 and E-cadherin promoters using chromatin immunoprecipitation assays.

4. MATERIALS AND METHODS

4.1 Reagents and suppliers

The reagents and commercially available kits used in this study are listed in Table 4.1. and 4.2., respectively. All reagents used for experiments were molecular biology or reagent grade.

Table 4.1. List of reagents and suppliers used in this study

Reagent	Supplier Name
100 bp DNA ladder	Fermentas
5-aza-2'deoxycytidine	Sigma-Aldrich
Acetic acid	EMD Chemicals
Agarose	Invitrogen Life Technologies
Aprotinin	Sigma-Aldrich
BIX-01294	Sigma-Aldrich
Boric acid	EMD Chemicals
Chaetocin	Sigma-Aldrich
dATP	Fermentas
dCTP	Fermentas
dGTP	Fermentas
DMSO	Sigma-Aldrich
dTTP	Fermentas
Ethanol	EMD Chemicals
Ethidium bromide	Invitrogen Life Technologies
Fetal bovine serum	Invitrogen Life Technologies
Formaldehyde	BDH
GM-CFS	R&D Systems
GlycoBlue coprecipitant	Ambion
HCl	EMD Chemicals
HotStar*Taq* Polymerase	Qiagen
IL-3	R&D Systems
IMDM	Invitrogen Life Technologies
Isopropanol	EMD Chemicals
Loading dye 6X solution	Fermentas
Methanol	BDH
$MgCl_2$	Qiagen
MTT reagent	Sigma-Aldrich

NaOH	BDH
Nuclease free water	Qiagen
PCR buffer 10X	Qiagen
Penecillin/Sterptomycin 100X mix	Invitrogen Life Technologies
Pepstatin A	Sigma-Aldrich
Phenol:chloroform:isoamyl alcohol	Ambion
PMSF	Sigma-Aldrich
Power SYBR green PCR master mix 10X	Applied Biosystems
Propidium iodide	Sigma-Aldrich
Proteinase K	Qiagen
RNAse	Worthington
RNasin	Promega
RPMI	Invitrogen Life Technologies
Salmon sperm DNA/protein A Agarose	Millipore
SDS	Promega
Sodium azide	Sigma
Sodium bicarbonate	BDH
Sodium borate	EMD Chemicals
Trypan blue	Invitrogen Life Technologies

Table 4.2. Comercially available kits used in this study

Kits	Company
DNeasy Blood and Tissue Kit	Qiagen
EZ DNA Methylation Kit	Cedarlane
iScript cDNA Synthesis Kit	Bio-Rad
RNeasy MinElute Cleanup Kit	Qiagen

4.2 Oligonucleotides

Table 4.3 lists primers and their optimal annealing temperature. PCR, Real-time PCR, and methylated PCR primers were purchased from Integrated DNA technologies (IDT). Pyrosequencing DNA primers were purchased from EpigenDex and IDT.

Table 4.3. Sequences and optimal annealing temperatures of primers used in this study

Name	Sequence	Annealing temperature
E-cadherin-PCR-F	5'-CCTGGGACTCCACCTACAGA-3'	55°C
E-cadherin-PCR-R	5'-GGATGACACAGCGTGAGAGA-3'	
E-cadherin-qRT-F	5'-AAGAAGCTGGCTGACATGTACGGA-3'	60°C
E-cadherin-qRT-R	5'-CCACCAGCAACGTGATTTCTGCAT-3'	
E-cadherin-ChIP-F	5'-AGAGGGTCACCGCGTCTATG-3'	61°C
E-cadherin-ChIP-R	5'-CTCACAGGTGCTTTGCAGTT-3'	
E-cadherin-MSP-M-F	5'-TTAGGTTAGAGGGTTATCGCGT-3'	57°C
E-cadherin-MSP-M-R	5'-TAACTAAAAATTCACCTACCGAC-3'	
E-cadherin-MSP-U-F	5'-TAATTTTAGGTTAGAGGGTTATTGT-3'	55°C
E-cadherin-MSP-U-R	5'-CACAACCAATCAACAACACA-3'	
GAPDH- PCR-F	5'-AAGTGAAGGTCGGAGTCAAC-3'	59°C
GAPDH-PCR-R	5'-ATGACAAGCTTCCCGTTCTC-3'	
HPRT-qRT-F	5'-TGGCGTCGTGATTAGTGATG-3'	60°C
HPRT-qRT-R	5'-GCACACAGAGGGCTACAATG-3'	
p15-PCR-F	5'-ATGCGCGAGGAGAACAAGGG-3'	63°C
p15-PCR-R	5'-GTACCCTGCAACGTCGCGGT-3'	
p15-qRT-F	5'-AAGCTGAGCCCAGGTCTCCAT-3'	58°C
p15-qRT-R	5'-CCACCGTTGGCCGTAAAC-3'	
p15-ChIP-F	5'- GCAGGCTTCCCCGCCCTCGTGACGC-3'	60°C
p15-ChIP-R	5'- ATTACCCTCCCGTCGTCCTTCTGC-3'	
p15-MSP-M-F	5'-GCGTTCGTATTTTGCGGTT-3'	60°C
p15-MSP-M-R	5'-CGTACAATAACCGAACGACCGA-3'	
p15-MSP-U-F	5'-TGTGATGTGTTTGTATTTTGTGGTT-3'	60°C
p15-MSP-U-R	5'-CCATACAATAACCAAACAACCAA-3'	
p21-PCR-F	5'-ATGTCAGAACCGGCTGGGGA-3'	61°C
p21-PCR-R	5'-AGCCTGCTCCCCTGAGCGAG-3'	
p21-qRT-F	5'-CTGGAGACTCTCAGGGTCGAA-3'	58°C
p21-qRT-R	5'-GGCGTTTGGAGTGGTAGAAATCT-3'	

p21-ChIP-F	5'-GTGGCTCTGATTGGCTTTCTG-3'	59°C
p21-ChIP-R	5'-CTGAAAACAGGCAGCCCAAG-3'	
p21-MSP-M-F	5'-TTTCGGGGAGGGCGGTTTCGGGCGGCGCGG-3'	67°C
p21-MSP-M-R	5'-CGATACCTCGACGAATCCGC-3'	
p21-MSP-U-F	5'-GGTGGTGTGGTGGGTTGAGT-3'	62°C
p21-MSP-U-R	5'-ACAAATCCACACCCAACTCC-3'	

4.3 Antibodies

Antibodies used in this thesis are listed in Table 4.4.

Table 4.4. Antibodies used in chromatin immunoprecipitation Assays

Antibody	Supplier Name	Catalog Number
Anti-Histone H3	Millipore	06-755
Normal mouse IgG	Millipore	12-371
Normal rabbit IgG	Millipore	12-370
MsmAb Histone H3 dimethyl K9	Abcam	Ab1220
RbpAb Histone H3 trimethyl K9	Abcam	Ab8898

4.4 Cell lines and culture conditions

Human AML cell lines, Kasumi, KG-1a, and AML193 were purchased from DSMZ (Braunschweig, Germany). AML-193 cells were cultured in Iscove's modified Dulbecco's medium (IMDM) with 20% (v/v) fetal bovine serum (FBS, Invitrogen) supplemented with 2 ng/mL human granulocyte macrophage colony stimulating factor (GM-CSF) and 3 units/mL human Interleukin-3 (IL-3) (R&D Systems). KG-1a cells were cultured in IMDM with 20% (v/v) FBS and Kasumi cells were maintained in RPMI with 10% (v/v) FBS. All cultures contained 1% (v/v) penicillin/streptomycin (Gibco) and were maintained at 37°C and 5% CO_2. Culture media was obtained from Invitrogen.

4.5. Drug treatments

For cell proliferation assays, cells were treated with different doses of DAC, BIX-01294, and chaetocin either alone or in combination for 72 hours. DMSO or an equivalent volume of 50:50 acetic acid/water was used as vehicle control. For gene expression analysis using drugs alone, a dose response assay of DAC, BIX-01294, and chaetocin was performed in AML cell lines for 72 hours. For gene expression analysis using drugs in combination, AML-193 cells were treated with 1 μM or 8 μM DAC, 4 μM BIX-01294 and 100 nM chaetocin. Kasumi and KG-1a cells were treated with 4 μM DAC, 4 μM BIX-01294, and 100 nM chaetocin for 72 hours. Concentration of drugs in combination is described in the appropriate figure(s).

4.6. Molecular techniques

4.6.1. DNA extraction from AML cells

Genomic DNA was isolated using the DNeasy Blood and Tissue Kit (Qiagen) according to manufacturer's instructions using 5 x 10^6 cells. Concentration and purity of DNA was determined by standard A_{260}/A_{280} spectrophotometric reading. DNA samples were stored at -20°C until needed.

4.6.2. RNA extraction from AML cells

Total RNA was isolated using TRIzol (Invitrogen). Cells were lysed and harvested to a concentration of 1 mL trizol for each 5-10 x 10^6 cells. 4-bromo-2-chlorophenol (BCP) (200 μL) was subsequent added to each harvested sample and mixed thoroughly by vortexing. Samples were incubated at room temperature for 3 minutes and centrifuged at 12,000 x g for 20 minutes. The top, aqueous layer was transferred to a MinElute Cleanup column (Qiagen) and isolated RNA was then cleaned using the RNeasy MinElute Cleanup Kit (Qiagen) as described in manufacturer's instruction. RNA pellets were dissolved in 20 μL of nuclease-free water (Qiagen) and concentration and purity was determined by standard A_{260}/A_{280} spectrophotometric reading. RNA samples were stored at -80°C until needed.

4.6.3. Reverse transcriptase polymerase chain reaction (RT-PCR)

Complementary DNA (cDNA) was synthesized from 1 µg total RNA using the iScript cDNA Synthesis kit (Bio-Rad). Briefly, 1 µg of total RNA was added to a mix containing 4 µL 5X iScript Reaction Mix and 1 µL iScript Reverse Transcriptase in a final volume of 20 µL. cDNA was synthesized by incubating the reaction at 25°C for 5 minutes, 42°C for 30 minutes, and 85°C for 5 minutes. Samples were used for PCR and Real-Time PCR or stored at -20°C until needed.

PCR was performed in 50 µL reaction mixture containing 1.0 µL of cDNA, 1X buffer (Qiagen), 0.2 mM of each dNTP (Fermentas), 0.2 µM of each primers, and 1.5 U of HotStar *Taq* Polymerase (Qiagen). Reactions were run at 95°C for 15 minutes followed by 35 amplification cycles (95°C for 1 minute, annealing Temperature 1 minutes and 72°C for 1 minute) and final incubation at 72°C for 10 minutes. Primer sequences and annealing temperatures are presented in Table 4.3.

4.6.4. Agarose gel electrophoresis

For visualization of DNA, samples were mixed with loading dye 6X solution (Fermentas) and resolved in 2% (w/v) agarose gel containing 0.5 µg/mL ethidium bromide and run at 150 V for 30 to 40 minutes using 1X of sodium borate buffer. Visualization and photography was done by using the UV light transilluminator GeL Doc (BioRad).

4.6.5. Real-time PCR

Amplification of cDNA was performed in a 10 µL reaction containing 5 µL Power SYBR green PCR master mix (Applied Biosystems), 0.45 µM of each primer and 0.2 µg cDNA using a StepOnePlus Real-Time PCR system (Applied Biosystems). Amplification consisted of 1 cycle at 95°C for 10 minutes and 40 cycles at 95°C and annealing temperature for 50 seconds. Hypoxanthine-guanine phosphoribosyltransferase was used as housekeeping gene to normalize mRNA expression. Data was analyzed using the ΔΔCT method (Livak method) as described in the StepOnePlus Analysis manual and by Livak and Schmittgen, 2001.

4.7. DNA methylation analysis

4.7.1. Sodium bisulfite modification

Genomic DNA was treated with sodium bisulfite reagent, which converts unmethylated cytosine to uracil (Figure 4.1), and eventually thymidine following PCR. This procedure allowed us to distinguish between methylated and unmethylated cytosine and was performed using the EZ DNA methylation kit (Cedarlane). In this procedure, 2 µg of genomic DNA was modified per sample as describe in the manufacturer's instructions. Samples were used to perform methylation specific PCR and pyrosequencing analysis or were stored at -20°C.

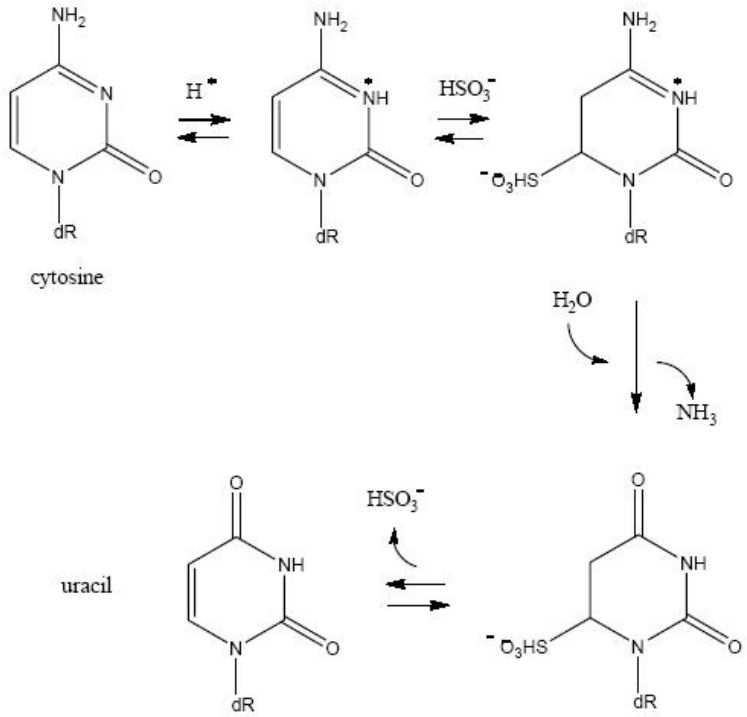

Figure 4.1. Schematic representation of the chemical conversion of cytosine to uracyl. The bisulfite mediated deamination of cytosine proceeds by three steps in an acid-catalized reaction. The first step is a reversible addition of HSO_3^- to cytosine. Second step, is the liberation of NH_3 by hydrolysis and third step is the release of HSO_3^- to regenerate the 5,6-doble bond, forming uracyl (Hayatsu, 2008). dR, deoxyribose.

4.7.2. Methylation specific PCR (MSP)

DNA methylation within the CpG islands of the p15, p21, and E-cadherin promoters was determined using methylation-specific PCR after sodium bisulfite treatment of genomic DNA as mentioned above. PCR was performed in a 50 μL final volume reaction containing 1 μL of modified DNA, 1X PCR buffer (Qiagen), 2.5 mM $MgCl_2$, 0.4 mM of each dNTP, 0.2 μM of each primer set (methylated or unmethylated set) and 1 U of HotStar *Taq* Polymerase (Qiagen). PCR reaction was performed at 95°C for 15 minutes followed by 35 amplification cycles (95°C 1minute, annealing temperature for 1 minute, and 72°C for 1.5 minutes) and a final elongation step at 72°C for 10 minutes. Methylation specific PCR primers were described previously by Scott, *et al* 2007 and Lakshmikuttyamma *et al*., 2010. Primer sequences and annealing temperatures are listed in Table 4.3. Modified DNA from HeLa and HL-60 cells were used as unmethylated MSP positive control for E-cadherin and p15 genes, respectively.

4.7.3 Pyrosequencing

Sodium bisulfite treated genomic DNA was PCR-amplified using the MSP PCR method as described above. PCR products were then sequenced to determine levels of CpG island methylation within the p15, p21 and E-cadherin gene promoters using pyrosequencing analaysis. Pyrosequence was performed by EpigenDX (USA).

Briefly, pyrosequencing employs a cascade enzyme system (Polymerase, Sulfurylase, Luciferase and Apyrase enzymes) that generates light for every incorporated nucleotide that form a pair with the complementary base in the DNA strand. The intensity of light (measured as peak heights) is proportional to the number of nucleotide molecules incorporated (for example if two sequential TT are incorporated it will be shown as a higher peak than a single T and same for double or single G, C or A). By pyrosequencing, unmethylated cytosine is measured as the relative content of T (see sodium bisulfite conversion above) at the CpG site and methylated cytosine, is measured as the relative content of C at the CpG site (appearing as TC at each CpG site).

The degree of methylation is calculated by the QCpG software, where it compares the generated pyrogram (pyrosequencing- chromatogram) to the theoretical histogram (Figure 4.2)

and then calculates the percentage methylation (%C) from the ratio of C/T as follows (EpigenDX, 2010):

$$\% C = \frac{C \text{ peak height} \times 100}{C \text{ peak height} + T \text{ peak height}}$$

4.8. Cell cycle

Cell cycle analysis was performed using the propidium iodide staining method. AML cells were treated with DAC, BIX-01294, or chaetocin for 72 hours and 1.5 x 10^6 cells were harvested and washed in ice cold 1X PBA (1X PBS, 0.1% (w/v) bovine serum albumin, 0.02% (w/v) sodium azide). Cells were fixed in ice cold ethanol and incubated overnight at 4°C for pellet precipitation. Cell pellets were reconstituted in Triton-PBA [0.1% (v/v) Triton X-100 and 1X PBA] for 5 minutes, pelleted by centrifugation, and resuspended in 500 units/mL RNAse working solution (Worthington) at 37°C for 30 minutes. Following by cell staining in propidium iodide working solution (0.05 mg/mL PI in PBA; Sigma) at room temperature in the dark for 15 minutes and filtered through 35µm nylon mesh. Samples were run in a Flow cytometer (Coulter Epics XL) and analyzed using the FloJo software (Tree Star, Inc).

4.9. MTT spectrophotometric assay

Cell proliferation and cytotoxicity was measured by MTT assay. Cells were plated in triplicate at 2 x 10^5 cells per well in a 96 well plate and treated with a vehicle control and different doses of DAC, BIX, and chaetocin for 72 hours. After treatment 1/10 culture volume of 5 mg/mL MTT reagent (3-(4,5-dimethylthiazol-2-yl)-2,5-diphenyltetrazolium bromide) (Sigma-Aldrich) was added and incubated for 4 hours at 37°C to allow formation of formazan crystals. The resulting crystal were solubilized by adding 100 µL of solubilization solution (10% (v/v) SDS and 0.01 M HCl) to each well and incubating at 37°C overnight. Spectrophotometric absorbance reading was taken at 570 nm with 650 nm background subtraction using a Spectcramax 340 PC plate reader (Molecular Devices).

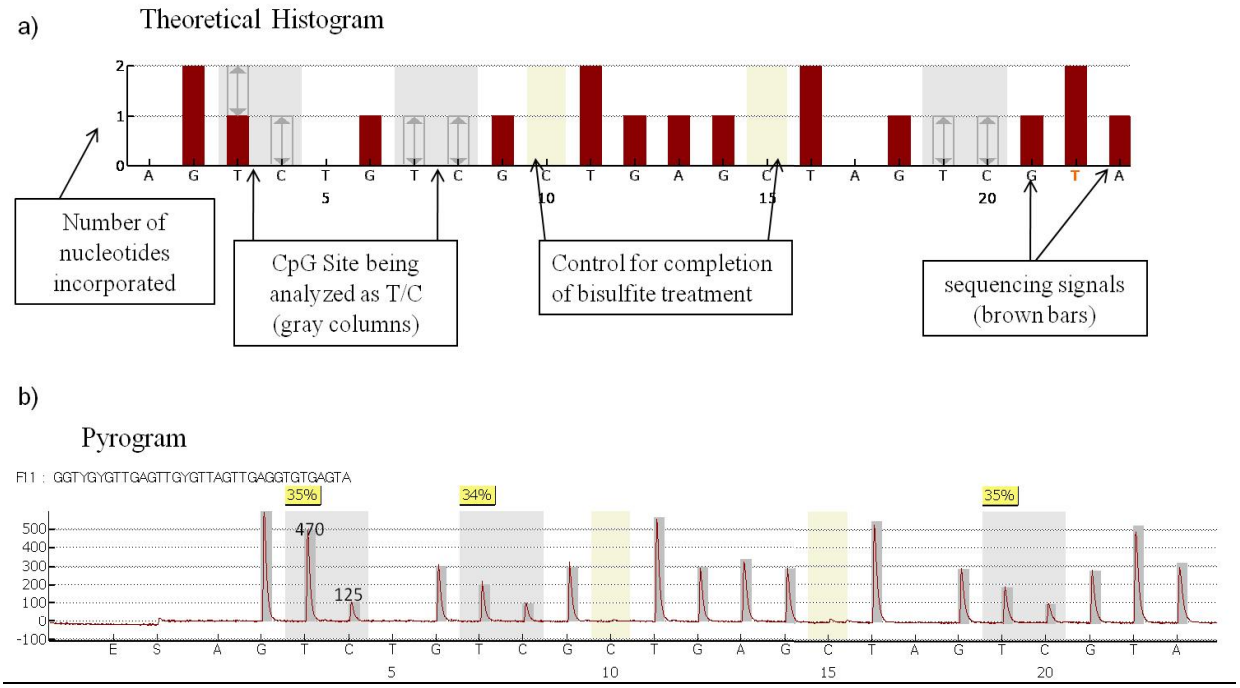

Figure 4.2. Pyrosequencing analysis of CpG methylation. An example of pyrosequencing analysis at 3 CpG sites (gray columns) showing a theoretical histogram (a) and the pyrogram generated (b). The theoretical histogram (a) indicates the number of nucleotides incorporated in the Y-axis at each nucleotide dispensation in the X-axis (the sequence around the analyzed C/T plus some control bases). In the histogram, the dark brown bars represent the nucleotide positions conserved between alleles and arrow empty bars portray the number of nucleotides incorporated. The pyrogram (b) represents the sequential nucleotide dispensations (X-axis) plotted against the resultant measured light intensity (Y-axis). The sequence analyzed is shown above the pyrogram under FI1 name, where Y represents the potential methylated cytosine in the CpG. In the pyrogram, E and S (X-axis) denote the addition of the enzyme and substrate, respectively. The A dispensation at position 1, T at position 5, and A at position 17, represent negative controls (used as internal control for pyrosequencing reaction). In the template sequence [GGTYGYGTTGAGTTGYGTTA…], identical following nucleotides (underlying) result in higher peak heights, such as G at position 2 that contains signal for (GG), T at position 11, position 16, and position 22 for (TT). Each T (highlighted) proceeding a CpG site (denotes as Y) is counted as unmethylated cytosine (T) in the CpG. In both figures, light yellow columns indicate control regions for completion of bisulfite treatment represented as C at position 10 and 15. Percentage methylation is calculating by the QCpG software (C% = C peak/(Cpeak + T peak)). For example, in the first analyzed CpG (first gray column) C peak = 125 and T peak = (470/2) = 235. Then, C%= 35%.

4.10. Chromatin immunoprecipitation (ChIP) assay

ChIP assays were performed based on the Upstate ChIP assay protocol (Upstate biotechnology). Modifications to the protocol were made. Briefly, Cells were collected and resuspended in 10 mL growth medium containing 1% formaldehyde and incubated at room temperature for 10 minutes. The cross-link reaction was stopped by adding 1 mL of 1.25 M Glycine. Cells were washed with cold 1X PBS and lysed in 600 µL SDS lysis buffer (1% (v/v) SDS, 10 mM EDTA, 50 mM Tris at pH 8.0) supplemented with protease inhibitors (1 mM PMSF, 1 µg/mL aprotinin, 1 µg/mL pepstatin A). Genomic DNA was sheared to a size of 200-1000 bp using a Branson Sonifier 450 sonicator (output control of 1.5, 60% duty cycle). Sheared lysates were cleared by centrifugation and split into fractions, Input fraction, positive antibody fraction (5 µg specific antibody) and negative antibody fraction (5 µg IgG). Immunoprecipitation was performed at 4°C overnight.

Cross-linked protein/DNA samples were reversed by heating and genomic DNA was isolated by proteinase K digestion, phenol:chloroform extraction (Ambion), and ethanol precipitation with the assistance of 30 µg GlycoBlue coprecipitant (Ambion). DNA pellets were dissolved in 20 µL nuclease free water and used for Real-Time PCR or stored at -20°C.

4.11. Statistical analysis

Differences between control (untreated cells) and drug treatments (treated cells) were assessed using the 2-sided *t* test. The significance levels were set at $p < 0.05$ (*) and $p < 0.01$ (**).

5. RESULTS

5.1. p15, p21, and E-cadherin promoter silencing in AML cell lines

5.1.1. Analysis of p15, p21, and E-cadherin expression and promoter methylation in AML cell lines

In cancer, genes that encode for cyclin-dependent kinase inhibitors (CDKI) and cadherin proteins (CDH) are frequently deregulated, leading to inactivation of growth inhibitory signals, excessive proliferation of malignant cells, and metastasis (Corn *et al*., 2000; Melki *et al*, 2000; Malumbres and Barbacid, 2009). p15, p21, and E-cadherin genes have been reported to be epigenetically silenced in a variety of AML cell lines and patients and more importantly, it has been suggested that loss of function of these genes is correlated with promoter hypermethylation (Herman, 1997; Corn *et al*., 2000; Melki *et al*, 2000; Scott *et al*, 2006; Lakshmikuttyamma *et al*., 2010). In order to investigate the p15, p21, and E-cadherin gene expression and promoter methylation in AML, three model cell lines were studied: AML-193, KG-1a, and Kasumi. p15, p21, and E-cadherin expression were detected by reverse transcriptase PCR. Only positive control cell lines HL-60, THP-1, and HeLa expressed p15, p21, and E-cadherin genes, respectively (Figure 5.1).

Promoter methylation was analyzed using two techniques: methylation-specific PCR (MSP) and DNA pyrosequencing (explanation of analysis in Figure 4.2). Methylated and unmethylated cytosines levels within CpG islands were measured using DNA bisulfite modification in both assays. Bisulfite converts unmethylated cytosines to uracil and subsequently to thymidine after PCR amplification. MSP analysis of p15 and E-cadherin promoter regions detected only the presence of methylated alleles in AML-193, KG-1a, and Kasumi cell lines (Figure 5.3a and Figure 5.3b). MSP analysis of the p21 promoter region detected only unmethylated alleles in AML cell lines tested (Figure 5.3c). To confirm p15, p21, and E-cadherin MSP results and to quantify the degree of promoter methylation, DNA pyrosequencing was performed. Pyrosequencing results correlated with MSP data and revealed that cytosines present as CpGs within regions of p15 and E-cadherin promoters were heavily methylated in AML cell lines studied (Figure 5.4 and Figure 5.5). In contrast, the cytosines

present as CpGs in regions of the p21 promoter that were analyzed were completely unmethylated in AML-193 and Kasumi cell lines (Figure 5.6).

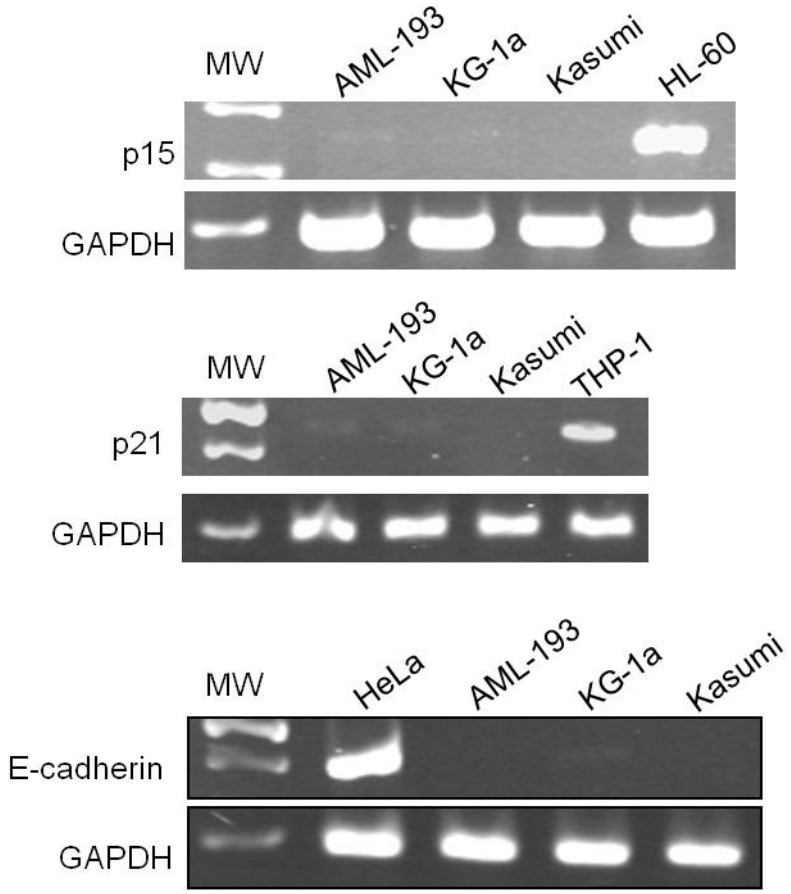

Figure 5.1. p15, p21, and E-cadherin expression in AML cell lines. p15, p21 and E-cadherin gene expression in AML cell lines was analyzed using reverse transcriptase PCR. GAPDH expression levels were used as cDNA input controls. HL-60, THP-1, and HeLa cell lines were used as positive control expression for p15, p21, and E-cadherin, respectively.

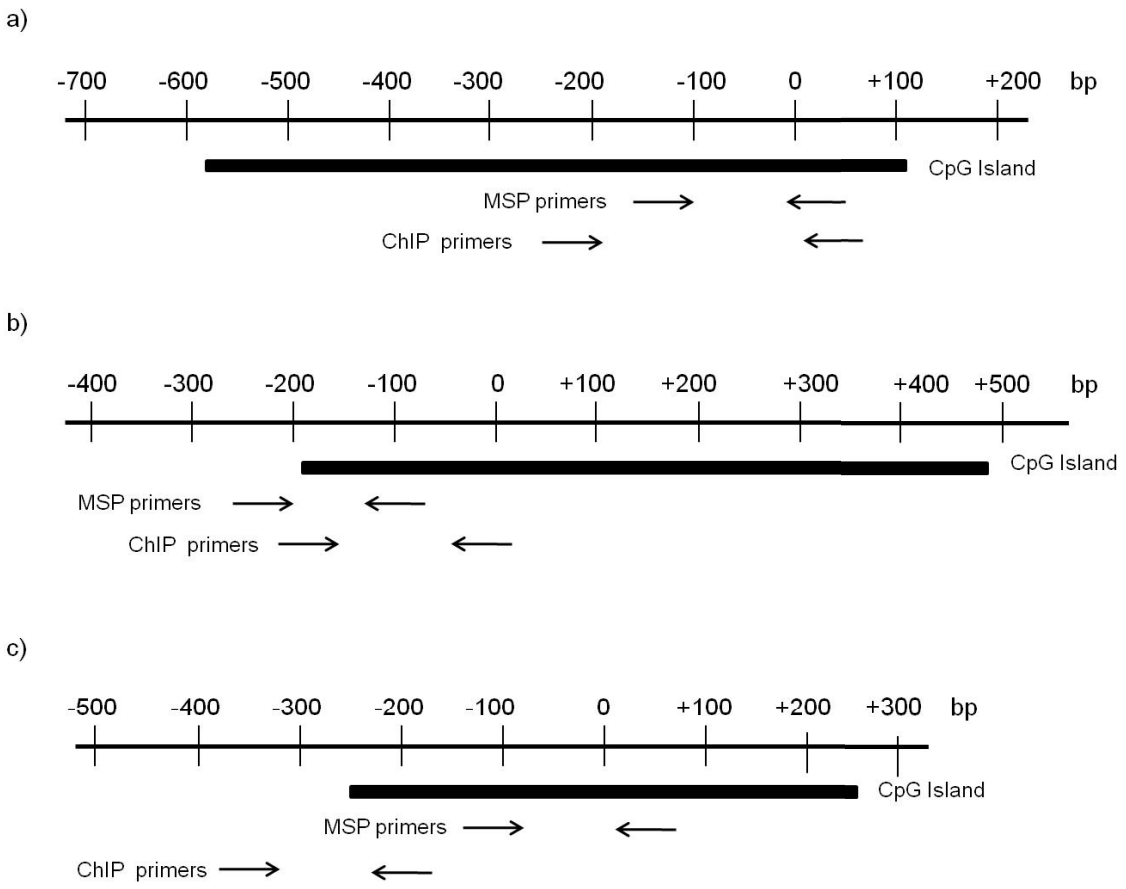

Figure 5.2. p15, p21, and E-cadherin MSP and ChIP PCR product location. Illustrated are the CpG island associated promoter region of the p15 (a) E-cadherin (b) and p21 (c) genes. CpG islands for p15 (chr9:21998658-21999471), p21 (chr6:36754223-36754715) and E-cadherin (chr16:67328536-67329145) were identified using UCSC genome browser (http://genome.ucsc.edu). PCR primer locations are indicated by arrows. The scale represents the distance from the transcription start site.

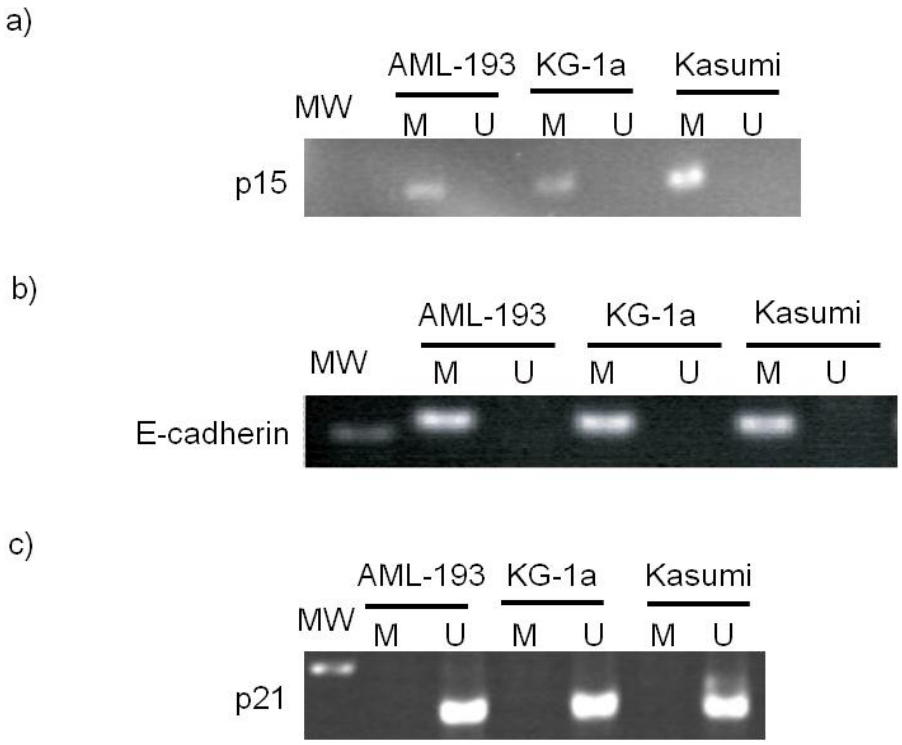

Figure 5.3. p15, E-cadherin, and p21 promoter methylation in AML cell lines**.** MSP analysis of p15 (a), E-cadherin (b), and p21 (c) promoter methylation. U and M indicate PCR amplicons generated using primers specific for unmethylated and methylated p15, p21, and E-cadherin promoter alleles, respectively.

AML-193
% Methylation: 90.3; SD: 13.7

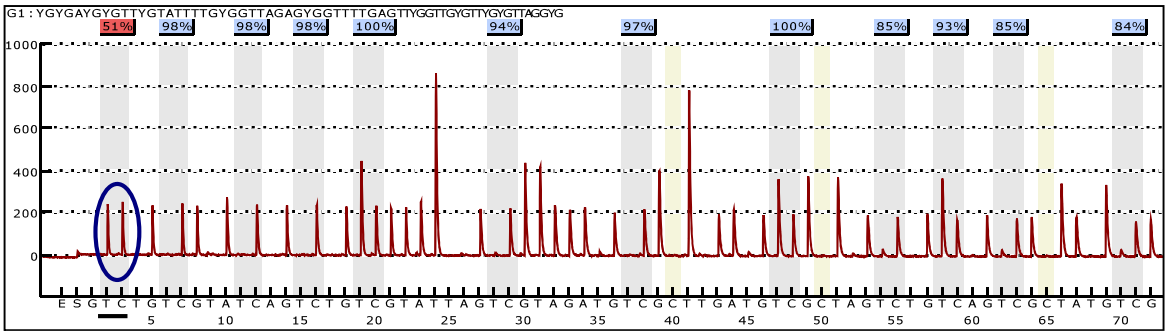

KG-1a
% Methylation: 92.3; SD: 13.1

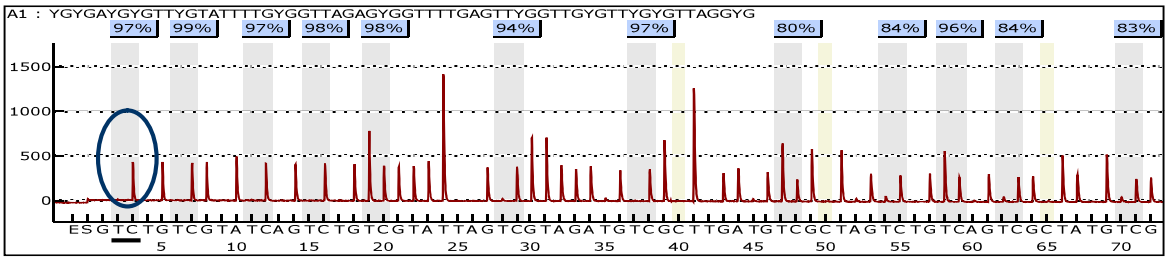

Kasumi
% Methylation: 88.5; SD: 13.7

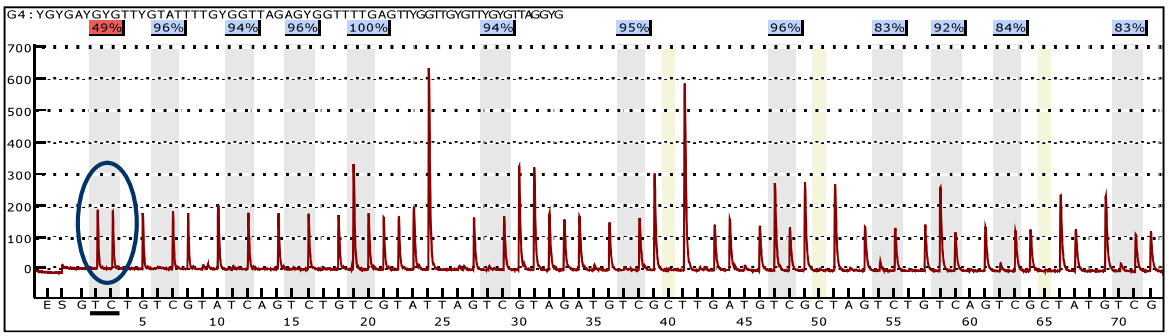

Figure 5.4. DNA pyrosequencing analysis of p15 promoter methylation in AML cell lines. Percentage methylation is the mean methylation of CpGs in the p15 promoter. SD, represents the standard deviation of the percentage mean methylation. The sequence analyzed is shown above each pyrogram, where Y represents the location of the cytosine in the CpG. In the pyrogram, the Y-axis represents the signal intensity (arbitrary units), which is proportional to the number of nucleotides incorporated (as peaks heights) and the X-axis is the dispensation order. The gray bars highlight the peaks resulting from sequential dispensations of C and T from which methylation is assessed. Pyrosequencing output then indicates the methylation percentage calculated from the ratio of the peaks heights of C and T (underlying TC and blue circles) in the analyzed CpG positions (first grey bar). Blue and red colours represent the confidence of the sequence pattern matches: greater than 90 percent and less than 70 percent, respectively.

AML-193
% Methylation: 96.9; SD: 3.4

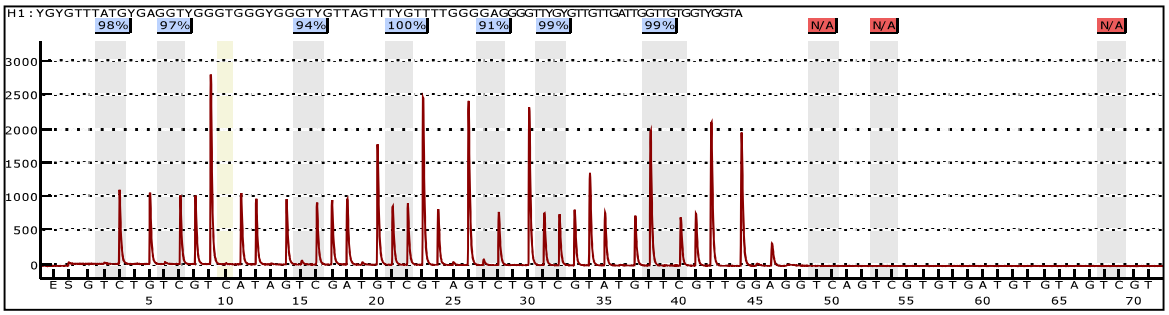

KG-1a
% Methylation: 82.1; SD: 12.3

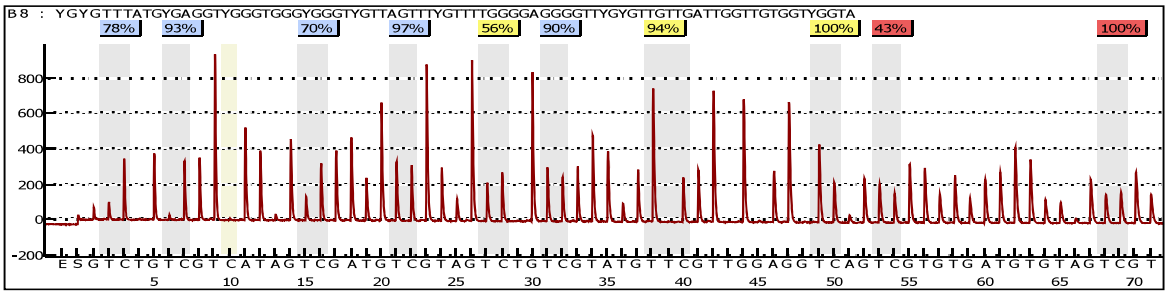

Kasumi
% Methylation: 96.5; SD: 3.3

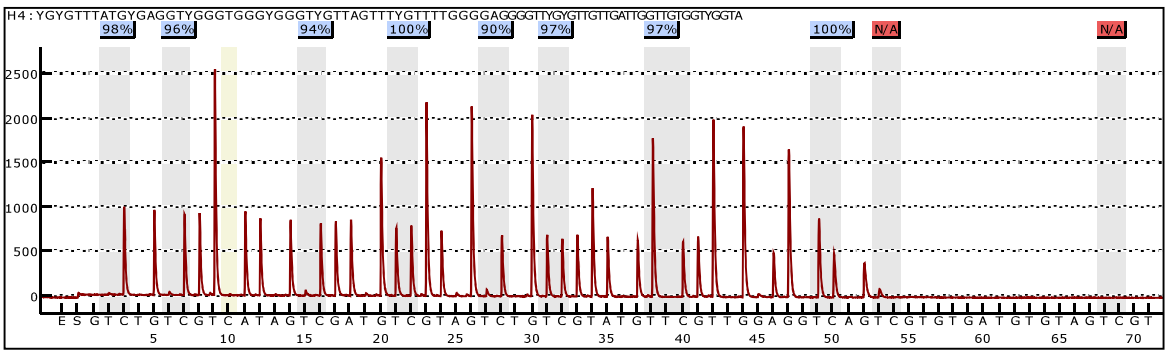

Figure 5.5. DNA pyrosequencing analysis of E-cadherin promoter methylation in AML cell lines. Percentage methylation is the mean methylation of CpGs in the E-cadherin promoter. SD, represents the standard deviation of the percentage mean methylation. The sequence analyzed is shown above each pyrogram, where Y represents the location of the cytosine in the CpG. In the pyrogram, the Y-axis represents the signal intensity (arbitrary units), which is proportional to the number of nucleotides incorporated (as peaks heights) and the X-axis is the dispensation order. The gray bars indicate the CpG positions, where the degree of methylation is assessed from the ratio of the peaks heights of C and T. Blue, yellow and red colours represent the confidence of the sequence pattern matches: greater than 90 percent, 70-89 percent and less than 70 percent, respectively.

AML-193

% Methylation: 2.9; SD: 1,2

a) Region1 (CpG No 8-21)

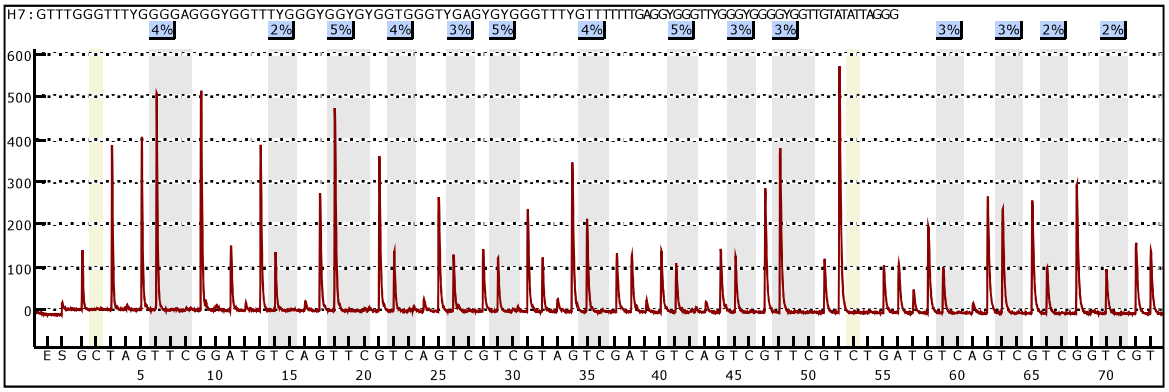

b) Region 2 (CpG No 22-24)

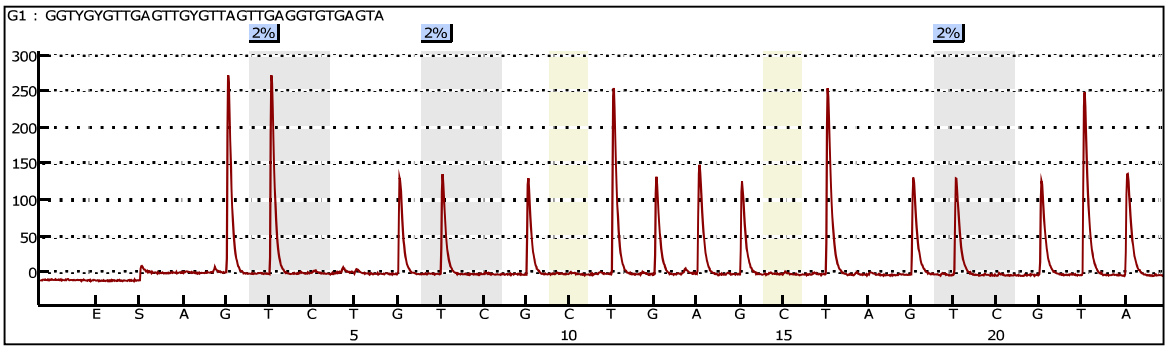

c) Region 3 (CpG No 25-31)

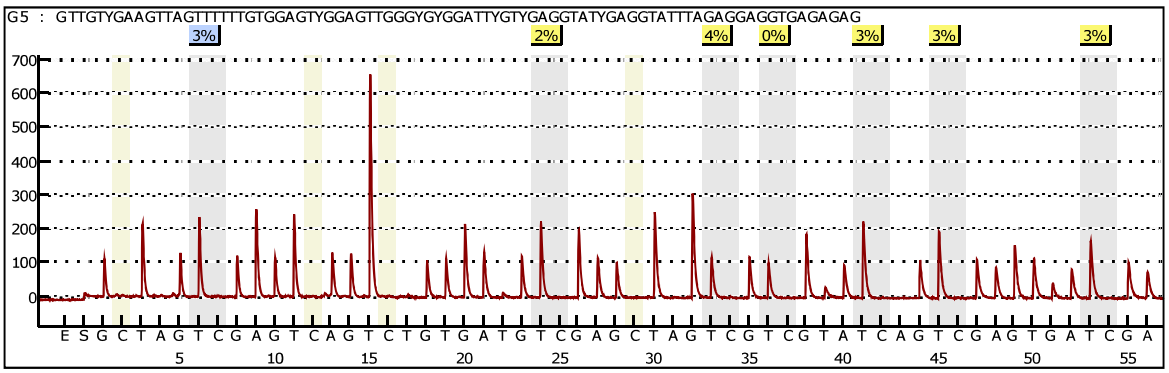

Kasumi- p-21
% Methylation: 2.8; SD: 1.5
d) Region1 (CpG No 8-21)

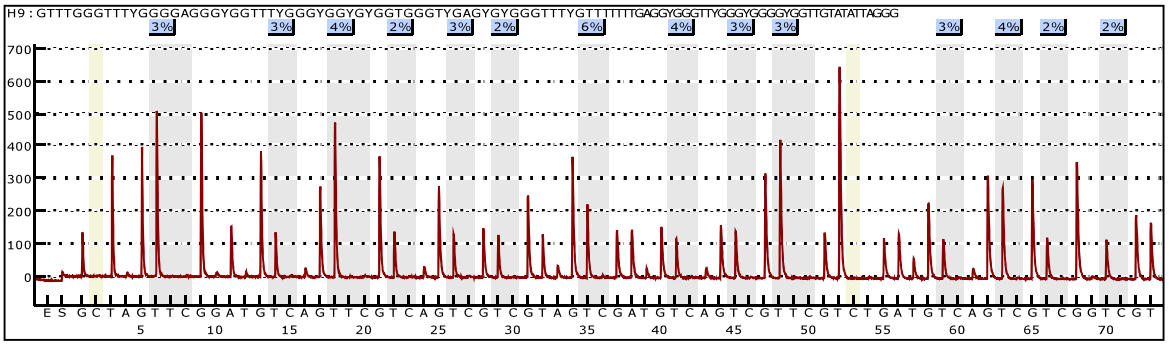

e) Region 2 (CpG No 22-24)

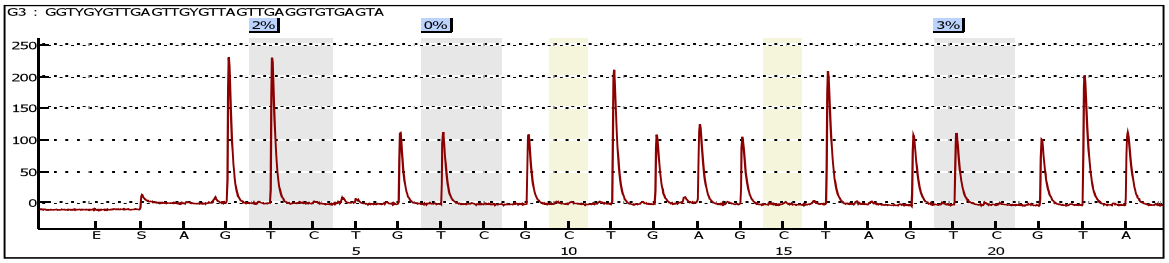

f) Region 3 (CpG No 25-31)

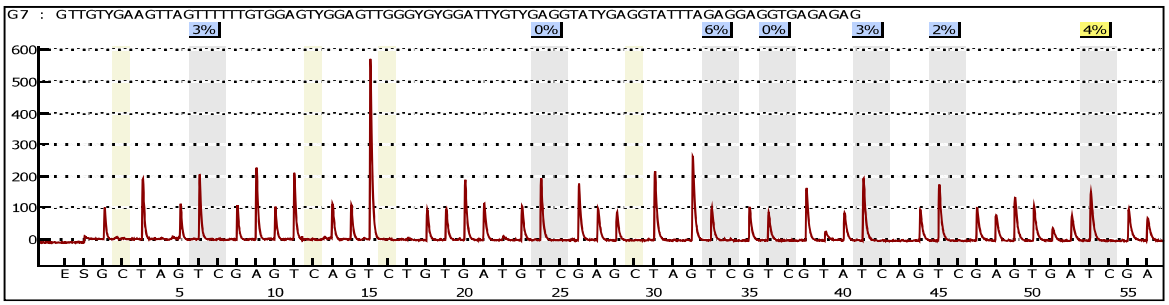

Figure 5.6. Continued**.** DNA pyrosequencing analysis of p21 promoter methylation in AML-193 and Kasumi cell lines. Percentage methylation is the mean methylation of CpGs in p21 promoter. SD, represents the standard deviation of the percentage mean methylation. (a), (b) and (c) indicate 3 different regions analyzed at the p21 promoter in AML-193 cells. (d), (e) and (f) indicate regions analyzed at the p21 promoter in Kasumi cells. The sequence analyzed is shown above each pyrogram, where Y represents the location of the cytosine in the CpG. In the pyrogram, the Y-axis represents the signal intensity (arbitrary units), which is proportional to the number of nucleotides incorporated (as peaks heights) and the X-axis is the dispensation order. The gray bars indicate the CpG positions, where the degree of methylation is assessed from the ratio of the peaks heights of C and T. Blue, yellow and red colours represent the confidence of the sequence pattern matches: greater than 90 percent, 70-89 percent and less than 70 percent, respectively.

5.2. The effect of DAC, BIX, and chaetocin on AML cell proliferation

To determine whether epigenetic inhibitors DAC, BIX, and chaetocin can induce re-expression of epigenetically silenced genes in AML, we first measured the effects of these drugs on AML cells proliferation using the MTT assay. The MTT assay colorimetrically quantifies the effect of these drugs on AML cell proliferation by measuring mitochondrial enzyme activity based on the reduction of MTT to formazan, which produces a colour change from yellow to purple. The mitochondrial enzymes that catalyze the reaction are only active when a cell is viable, allowing the correlation between viability and spectrophotometric readings (Carmichael *et al*., 1987).

Previous work in our lab established that DAC does not affect AML cell viability at doses up to 16 μM (Geyer *et al*., unpublished). Therefore, we evaluated the effect of BIX and chaetocin on AML-193, KG-1a, and Kasumi cell viability. AML-193, KG-1a, and Kasumi cell lines were treated for 72 hours with different doses of BIX and chaetocin and then analyzed using the MTT assay. Both BIX and chaetocin treatment reduce AML cell viability as shown in Figure 5.7. Chaetocin was the most toxic drug to AML-193, KG-1a, and Kasumi cell lines, causing a dramatic decrease on cell viability at doses above 100 nM, 20 nM, and 50 nM, respectively (Figure 5.7).

Since DAC has little effect on cell viability it was added to AML cells treated with BIX and chaetocin in order to analyze its ability to potentiate the anti-proliferative effects of BIX and chaetocin. The effect of chaetocin and BIX on AML cell proliferation was greater when DAC was used in combination with these two drugs (Figure 5.7). Furthermore, decreases in cell proliferation observed with BIX and chaetocin were consistent with changes in the cell cycle profile. BIX decreased the population of cells in the dividing phase (S phase) and G2/M and increased the population in G1 phase, which contains check points control for cell cycle arrest (Figure 5.8). Similarly, chaetocin induced changes on cell cycle, increasing the population in subG1 and decreasing the population of dividing cells (S - G2/M) (Figure 5.9).

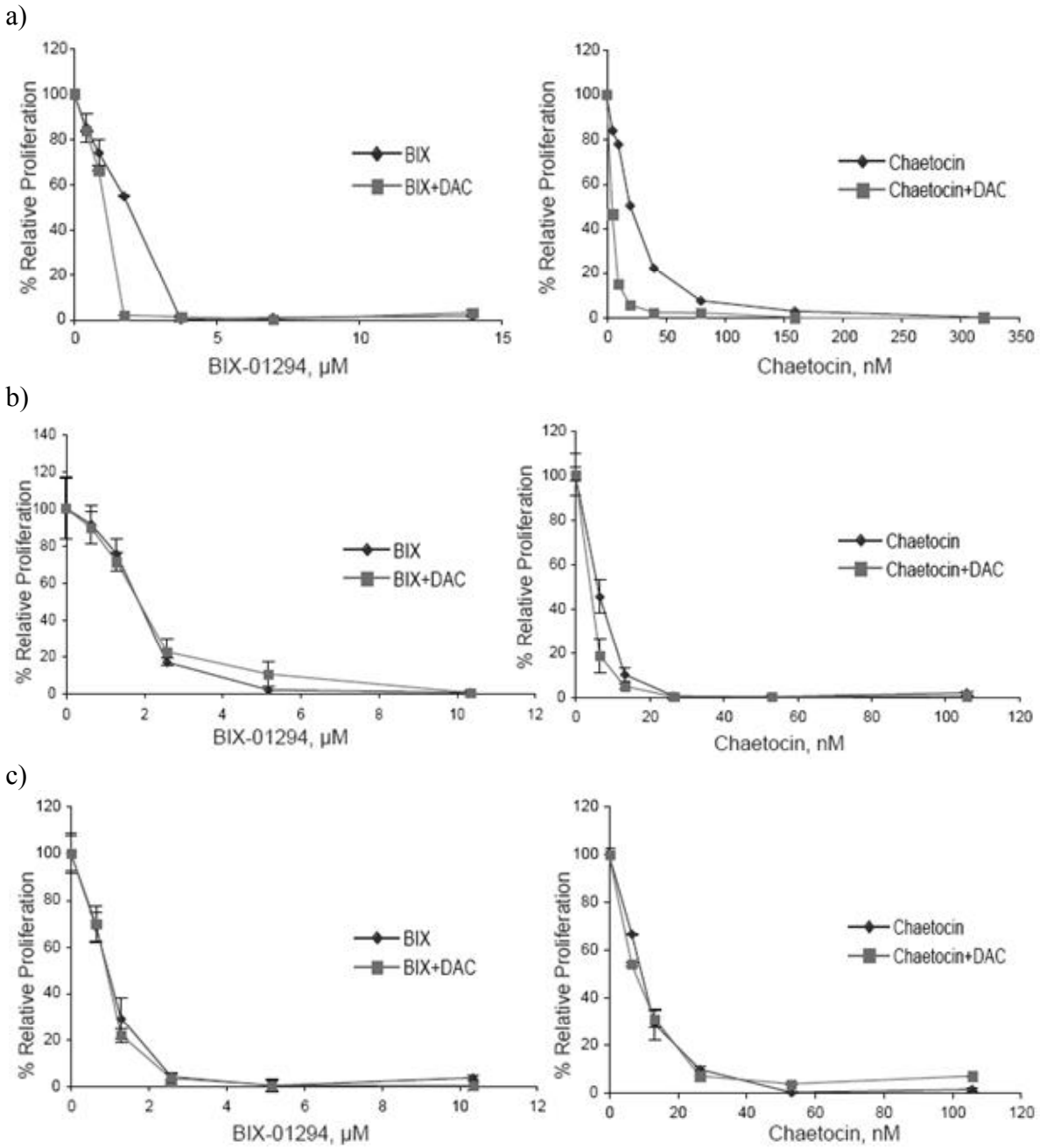

Figure 5.7. Proliferation of AML cell lines treated with BIX and chaetocin. AML-193 (a), KG-1a (b), and Kasumi (c) cell lines were treated for 72 hours with indicated concentrations of BIX-01294 (BIX) and chaetocin in presence (BIX+DAC and chaetocin+DAC) or absence (BIX-DAC and chaetocin-DAC) of DAC (1 μM). Samples were analyzed using the MTT assay. The data is represented as percentage (%) relative proliferation, which is based on the proliferation normalized to the untreated cells (100% proliferation). Error bars represent standard deviation from three independent experiments.

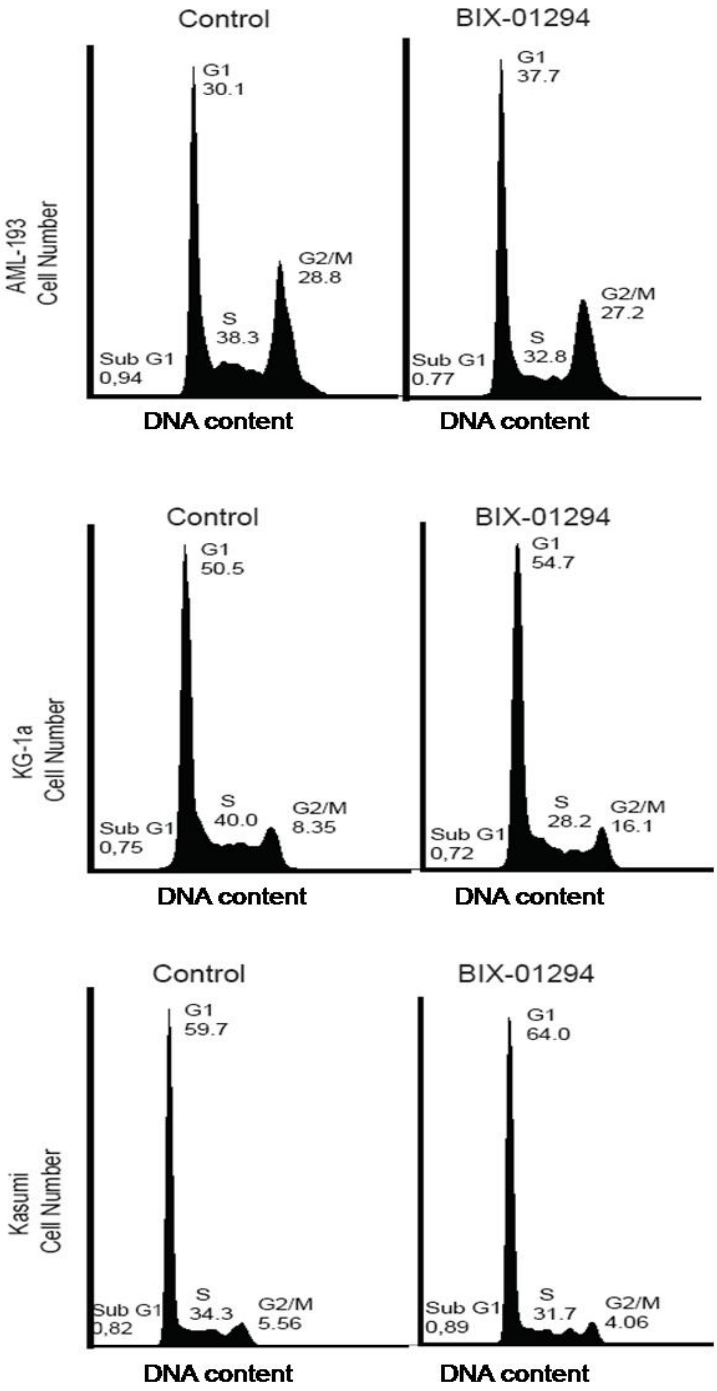

Figure 5.8. Effect of BIX-01294 on the cell cycle in AML cell lines. Cell cycle histograms represent the propidium iodide (PI) staining of DNA content in different phases of the cell cycle before and after treatment with BIX. AML-193, KG-1a, and Kasumi cells were treated for 72 hours with either BIX (4 μM) or vehicle control (DMSO). The percentage of cells in each phase of the cell cycle is shown on the histograms. At 4 μM dose, BIX increased the number of cells undergoing G1 phase but does not cause cell apoptosis.Cell cycle analysis was performed with the Watson algorithm using the FloJo software.

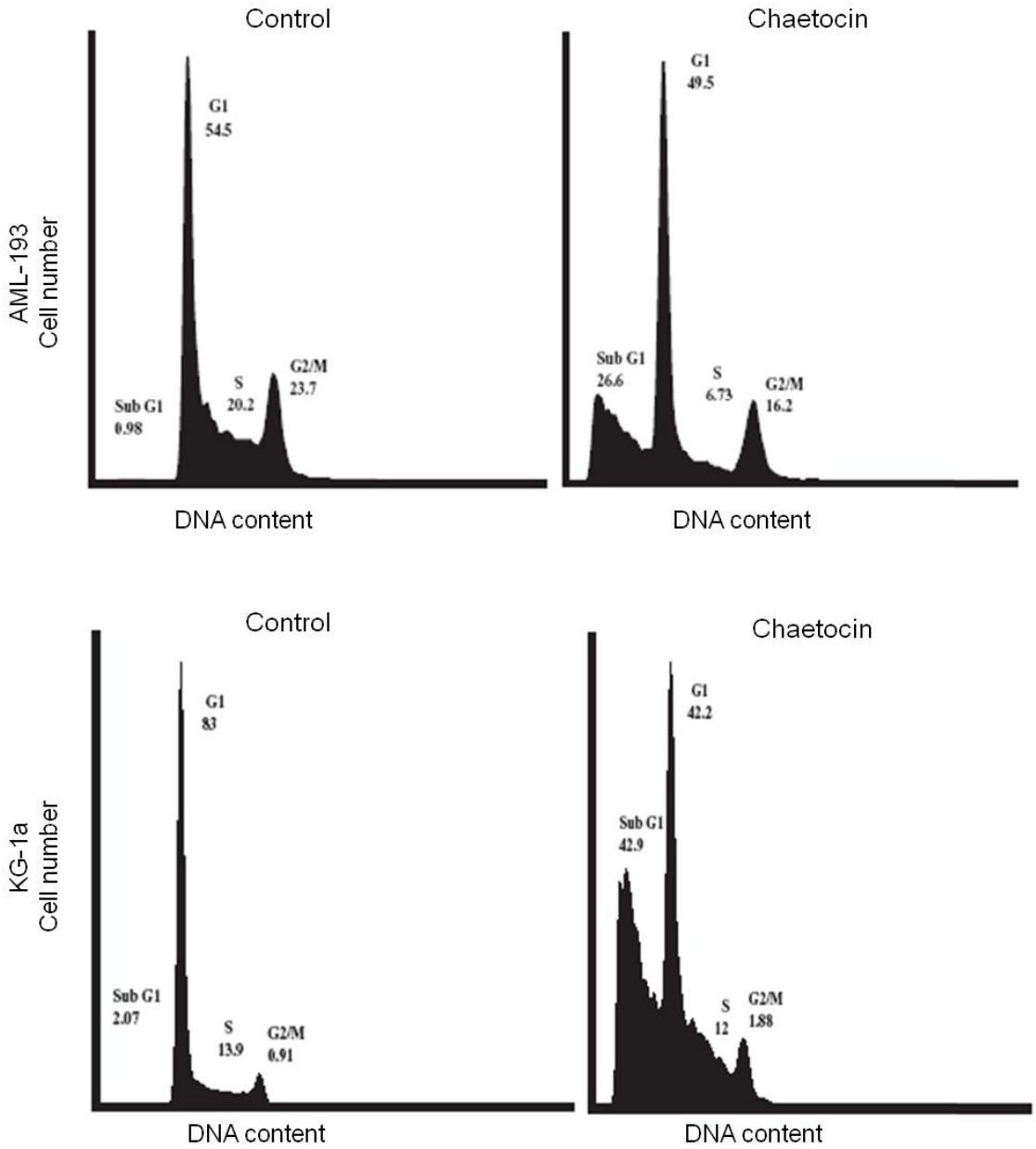

Figure 5.9. Effect of chaetocin on the cell cycle in AML cell lines. Cell cycle histograms represent the propidium iodide (PI) staining of DNA content in different phases of the cell cycle before and after treatment with chaetocin. AML-193 and KG-1a cells were treated for 72 hours with either chaetocin (100 nM) or vehicle control (DMSO). The percentage of cells in each phase of the cell cycle is shown on the histograms. At 100 nM dose, chaetocin increased the number of cells undergoing apoptosis. Cell cycle analysis was performed with the Watson algorithm using the FloJo software.

5.3. Effect of DAC on p15, p21, and E-cadherin gene expression

5.3.1. DAC-induced expression of p15, p21, and E-cadherin genes

DAC has been extensively used in cancer epigenetic therapy for inducing expression of genes that are silenced by promoter hypermethylation in various types of cancer (Hellebrekers *et al.*, 2007; Jain *et al*., 2009). Moreover, DAC has also been recognized to induce expression of genes without promoter methylation, which is the case of p21 gene in this study (Zhu and Otterson, 2003; McGarvey *et al*., 2006). In order to investigate epigenetic changes that lead to re-activation of tumor suppressor genes in AML, we evaluated the effect of DAC, BIX, and chaetocin on p15, p21, and E-cadherin gene re-expression in AML cell lines.

To optimize concentrations of DAC that leads to gene re-activation, AML-193, KG-1a, and Kasumi cell lines were treated with DAC in a dose response induction manner and p15, p21 and E-cadherin expression were analyzed by real time PCR. DAC significantly induced expression of p15 at doses higher than 1 μM in AML-193 and 4 μM in KG-1a and Kasumi cell lines (Figure 5.10a). Similarly, in KG-1a and Kasumi cells, E-cadherin expression was induced with 4 μM DAC, whereas 8 μM DAC was required to induce E-cadherin expression in the AML-193 cell line (Figure 5.10b). Despite the p21 promoter being unmethylated, DAC induced expression of p21 in all AML cell lines studied. Significant p21 expression was observed in AML-193, KG-1a, and Kasumi cell lines after treatment with 4 μM DAC (Figure 5.10c).

5.3.2. DAC-induced p15 and E-cadherin expression by reducing promoter methylation

Based on the ability of DAC to induce expression of hypermethylated p15 and E-cadherin genes in AML cell lines, we measured the effect of DAC on promoter demethylation using DNA pyrosequencing. Since treatment of KG-1a and Kasumi cells with 4 μM DAC significantly increased p15 and E-cadherin gene expression, we chose only Kasumi and AML-193 cell lines to analyze promoter demethylation. Treatment of AML-193 with 1 μM DAC and Kasumi with 4 μM DAC resulted in a decrease of p15 and E-cadherin promoter methylation across the region of the CpG island analyzed. The mean level of p15 and E-cadherin promoter methylation was reduced on the order of 30% in all AML cell lines studied (Figure 5.11, Figure 5.12, Figure 5.13, and Figure 5.14). In the unmethylated p21 promoter, pyrosequencing results revealed that the level of CpG island methylation did not change, which was in agreement with previous MSP and pyrosequencing results (Figure 5.15 and Figure 5.16).

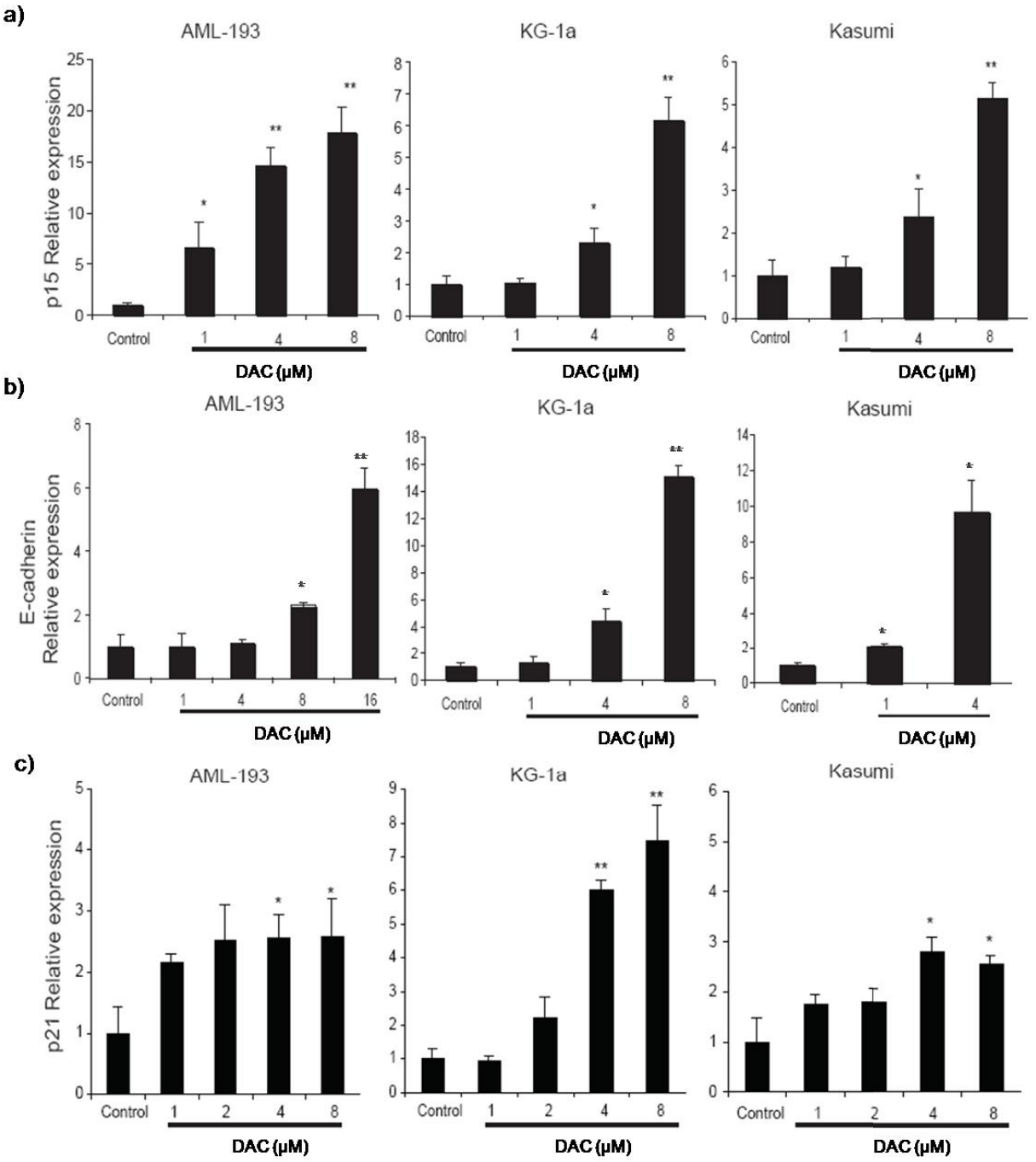

Figure 5.10. Real time PCR analysis of p15, p21, and E-cadherin expression in AML cell lines. AML-193, KG-1a, and Kasumi cell lines were treated with different doses of DAC for 72 hours. P15 (a), E-cadherin (b), and p21(c) expression was analyzed using HPRT as endogenous control gene. Error bars represents standard deviation of three independent experiments and (*) represents P-value < 0.05 and (**) represent P-value <0.01 between treated and untreated cells. Control represents the untreated cells.

a) Control
% Methylation: 95.1%; SD: 8.0

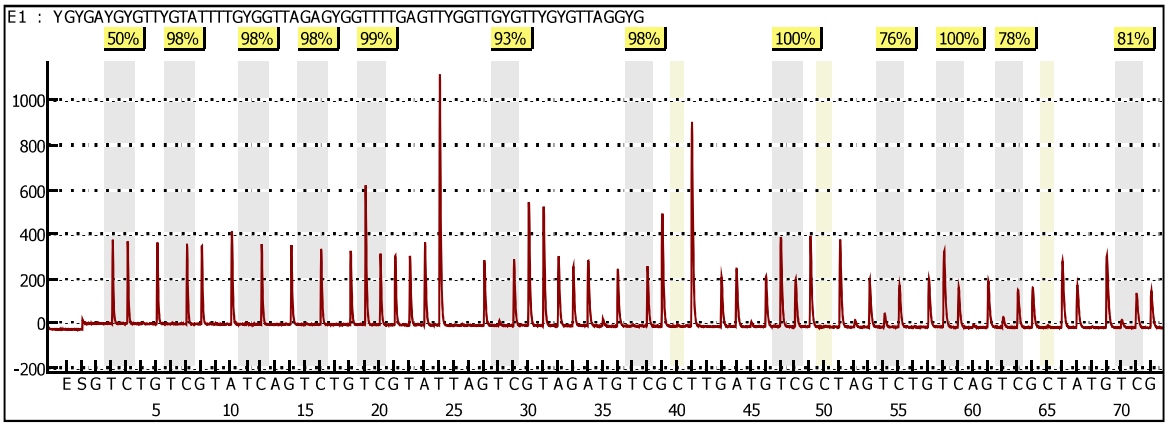

b) 1 µM DAC
% Methylation: 57.7%; SD: 6.2

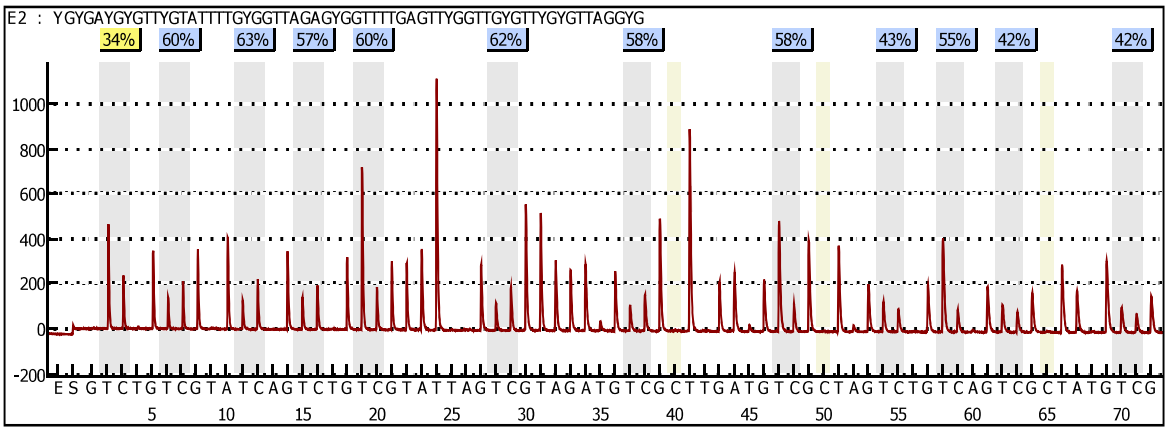

Figure 5.11. Effect of DAC on p15 promoter methylation in AML-193 cell line. Cells were untreated (a) or treated (b) for 72 hours with the indicated concentration of DAC. Percentage methylation is the mean methylation of CpGs in the p15 promoter. SD, represents the standard deviation of the percentage mean methylation. The sequence analyzed is shown above each pyrogram, where Y represents the location of the cytosine in the CpG. In the pyrogram, the Y-axis represents the signal intensity (arbitrary units), which is proportional to the number of nucleotides incorporated (as peaks heights) and the X-axis is the dispensation order. The gray bars indicate the CpG positions, where the degree of methylation is assessed from the ratio of the peaks heights of C and T. Blue and yellow colors represent the confidence of the sequence pattern matches: greater than 90% and between 70-89%, respectively.

a) Control
% Methylation: 95%; SD: 4.9

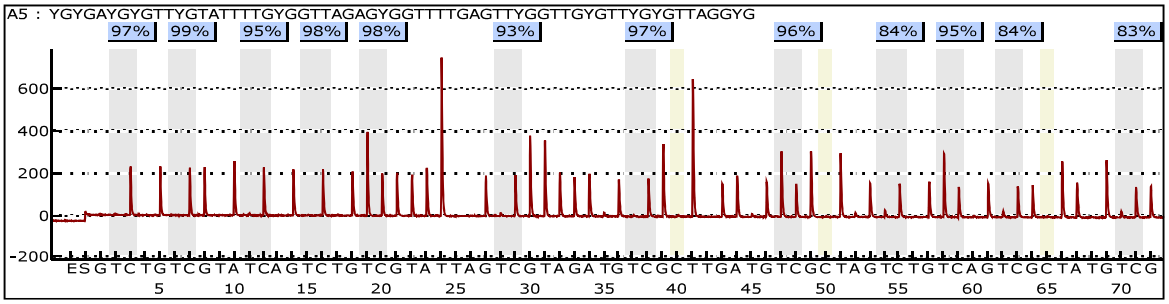

b) 4 µM DAC
% Methylation: 57.7%; SD: 6.2

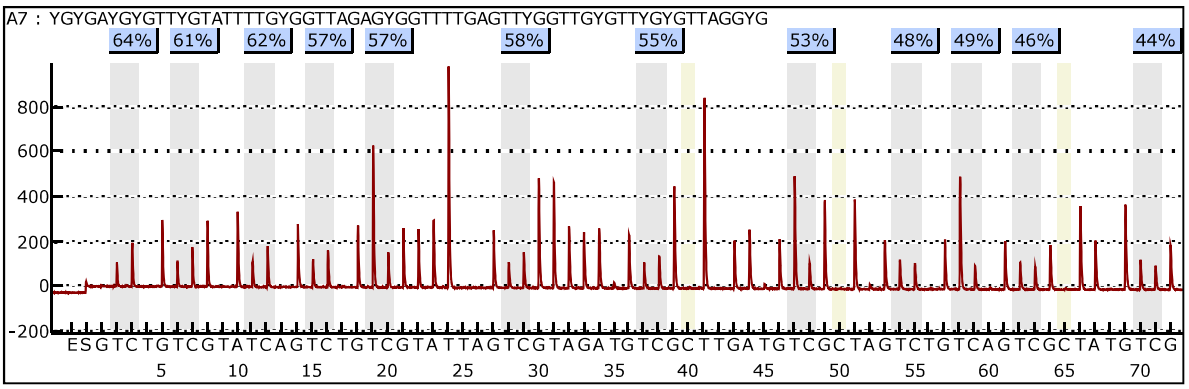

Figure 5.12. Effect of DAC on p15 promoter methylation in Kasumi cell line. Cells were untreated (a) or treated (b) for 72 hours with the indicated concentration of DAC. Percentage methylation is the mean methylation of CpGs in the p15 promoter. SD, represents the standard deviation of the percentage mean methylation. The sequence analyzed is shown above each pyrogram, where Y represents the location of the cytosine in the CpG. In the pyrogram, the Y-axis represents the signal intensity (arbitrary units), which is proportional to the number of nucleotides incorporated (as peaks heights) and the X-axis is the dispensation order. The gray bars indicate the CpG positions, where the degree of methylation is assessed from the ratio of the peaks heights of C and T. Blue color represents the confidence of the sequence pattern matches greater than 90 percent.

a) Control
% Methylation: 95.5; SD:4.7

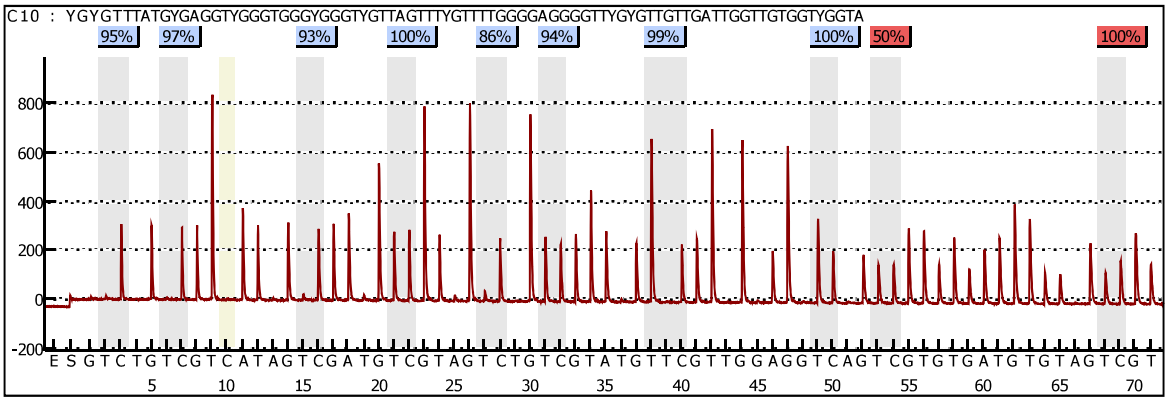

b) 8 µM DAC
% Methylation: 66.8; SD: 7.0

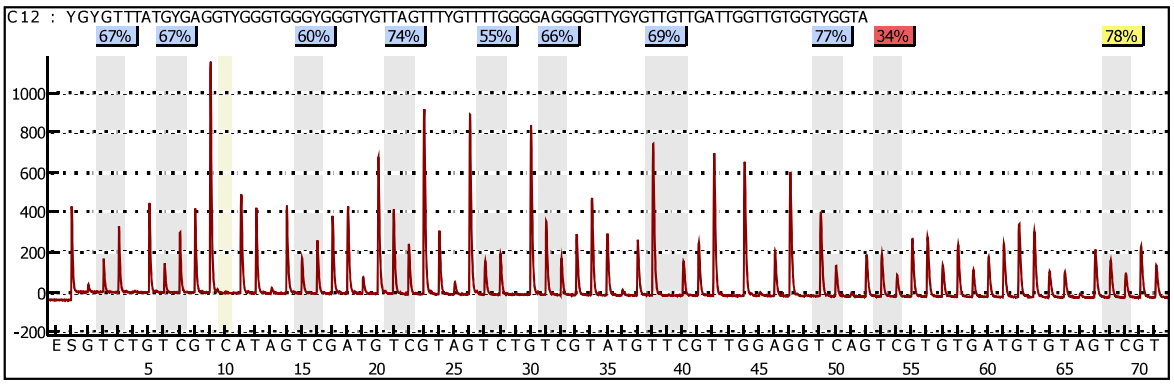

Figure 5.13. Effect of DAC on E-cadherin promoter methylation in the AML-193 cell line. Cells were untreated (a) or treated (b) for 72 hours with the indicated concentration of DAC. Percentage methylation is the mean methylation of CpGs in the E-cadherin promoter. SD, represents the standard deviation of the percentage mean methylation. The sequence analyzed is shown above each pyrogram, where Y represents the location of the cytosine in the CpG. In the pyrogram, the Y-axis represents the signal intensity (arbitrary units), which is proportional to the number of nucleotides incorporated (as peaks heights) and the X-axis is the dispensation order. The gray bars indicate the CpG positions, where the degree of methylation is assessed from the ratio of the peaks heights of C and T. Blue, yellow and red colours represent the confidence of the sequence pattern matches: greater than 90 percent, 70-89 percent and less than 70 percent, respectively.

a) Control
% Methylation: 90.1; SD: 9.0

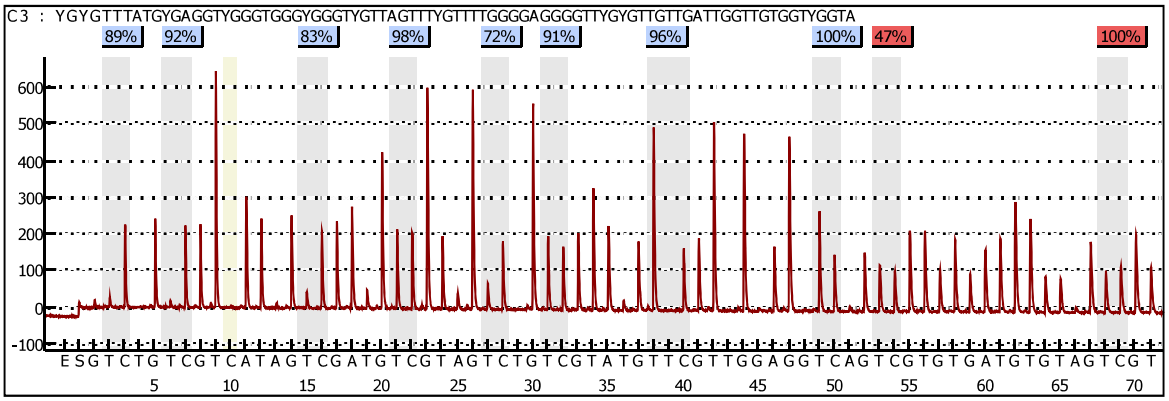

b) 4 µM DAC
% Methylation: 55.8; SD: 9.2

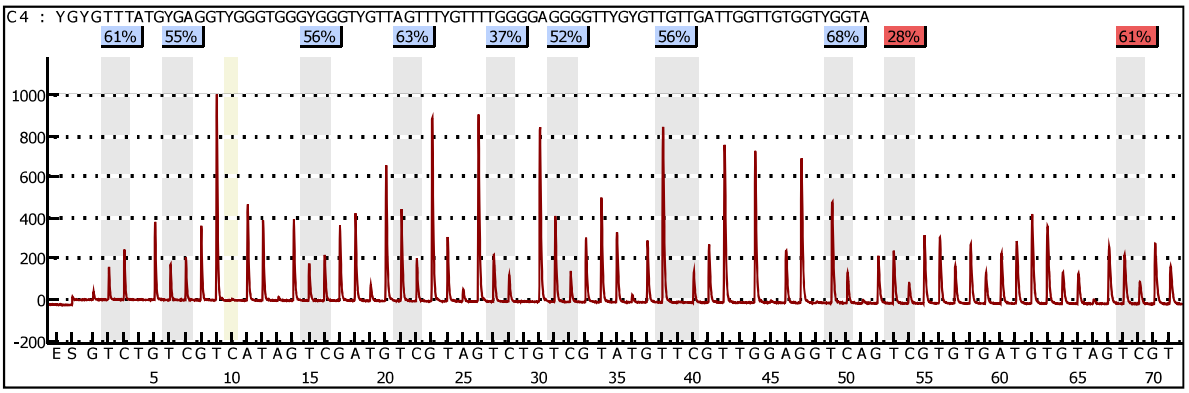

Figure 5.14. Effect of DAC on E-cadherin promoter methylation in Kasumi cell line. Cells were untreated (a) or treated (b) for 72 hours with the indicated concentration of DAC. Percentage methylation is the mean methylation of CpGs in the E-cadherin promoter. SD, represents the standard deviation of the percentage mean methylation. The sequence analyzed is shown above each pyrogram, where Y represents the location of the cytosine in the CpG. In the pyrogram, the Y-axis represents the signal intensity (arbitrary units), which is proportional to the number of nucleotides incorporated (as peaks heights) and the X-axis is the dispensation order. The gray bars indicate the CpG positions, where the degree of methylation is assessed from the ratio of the peaks heights of C and T. Blue, yellow and red colours represent the confidence of the sequence pattern matches: greater than 90 percent, 70-89 percent and less than 70 percent, respectively.

AML-193, Control

a) Region1 (CpG No 8-21)
% Methylation: 3.4; SD: 1.08

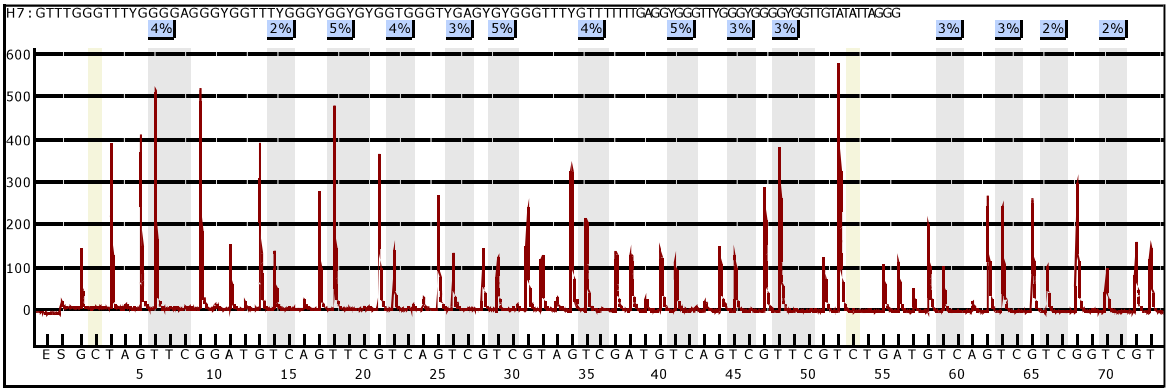

b) Region 2 (CpG No 22-24)
% Methylation: 1.9; SD: 0.34

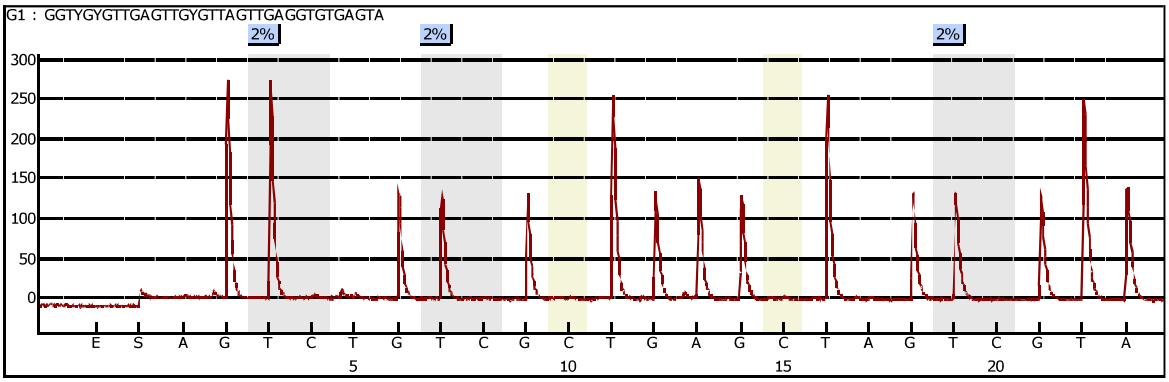

c) Region 3 (CpG No 25-31)
% Methylation: 1.7; SD: 1.26

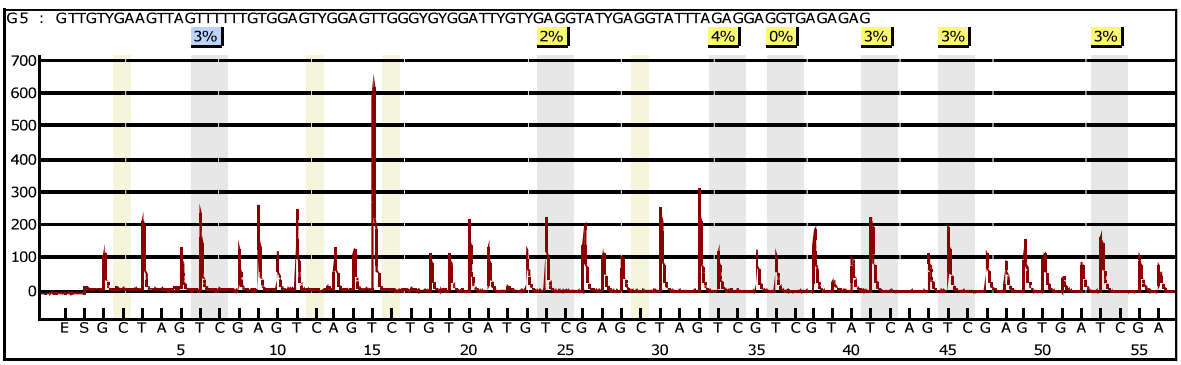

AML-193, 1 µM DAC

a) Region1 (CpG No 8-21)
% Methylation: 2.5; SD: 1.06

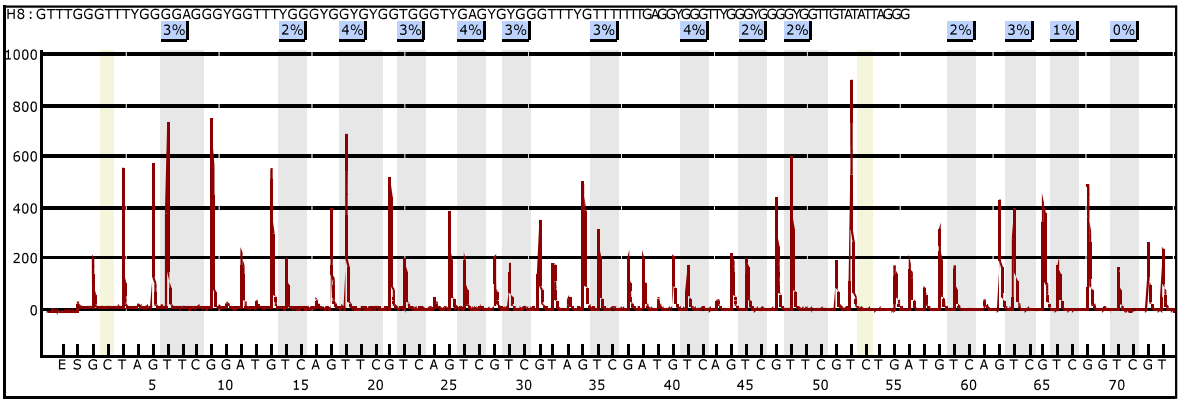

b) Region 2 (CpG No 22-24)
% Methylation: 2.5; SD: 0.91

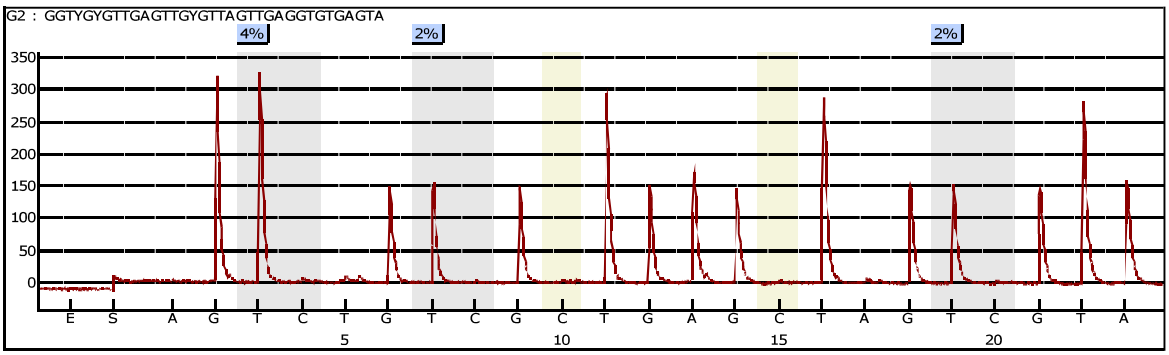

c) Region 3 (CpG No 25-31)
% Methylation: 2.4; SD: 0.87

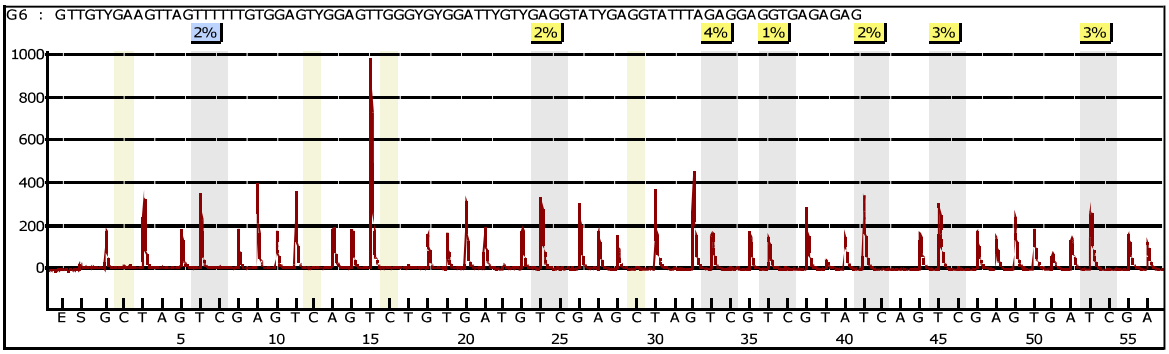

Figure 5.15. Effect of DAC on p21 promoter methylation in AML-193 cell line. AML-193 cells were untreated (Control) or treated (1μM DAC) for 72 hours with the indicated concentration of DAC. (a), (b) and (c) represent the analyzed CpG regions in the p21 promoter. Percentage methylation is the mean methylation of CpGs in the p21 promoter. SD, represents the standard deviation of the percentage mean methylation. The sequence analyzed is shown above each pyrogram, where Y represents the location of the cytosine in the CpG. In the pyrogram, the Y-axis represents the signal intensity (arbitrary units), which is proportional to the number of nucleotides incorporated (as peaks heights) and the X-axis is the dispensation order. The gray bars indicate the CpG positions, where the degree of methylation is assessed from the ratio of the peaks heights of C and T. Blue and yellow colours represent the confidence of the sequence pattern matches: greater than 90 percent and between 70-89 percent, respectively.

Kasumi, Control

a) Region 1 (CpG No 8-21)
% Methylation: 2.9; SD: 1.04

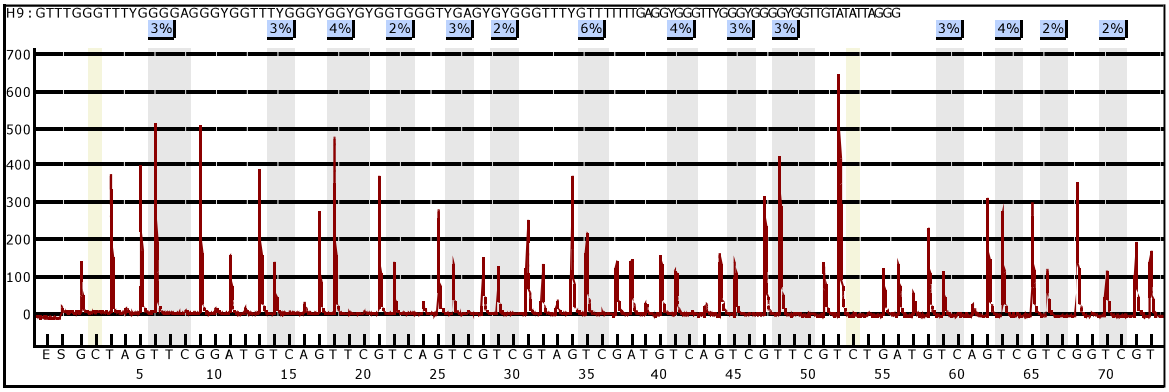

b) Region 2 (CpG No 22-24)
% Methylation: 1.6; SD: 1.53

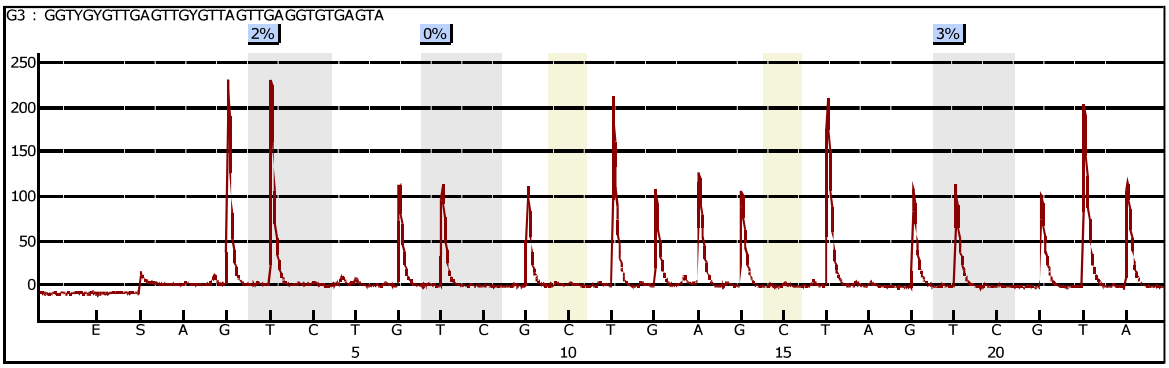

b) Region 3 (CpG No 25-31)
% Methylation: 2.6; SD: 2.03

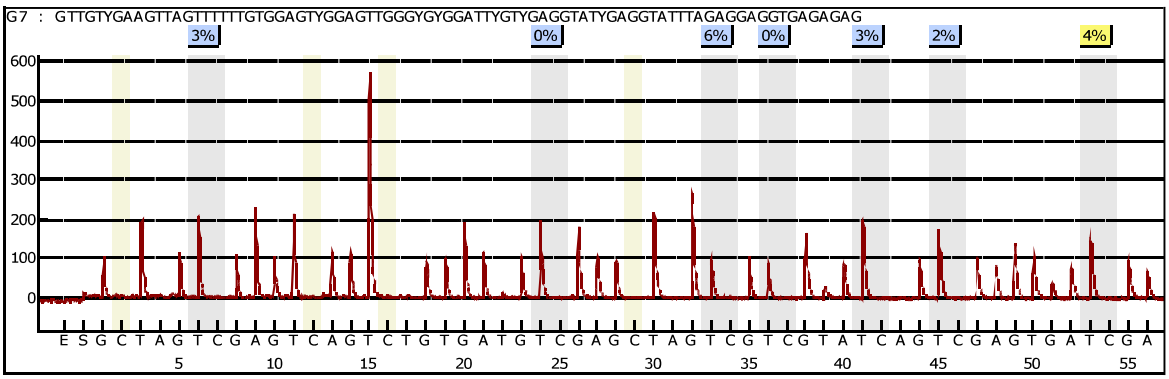

Kasumi, 4 μM DAC

a) Region 1 (CpG No 8-21)
% Methylation: 2.9; SD: 0.82

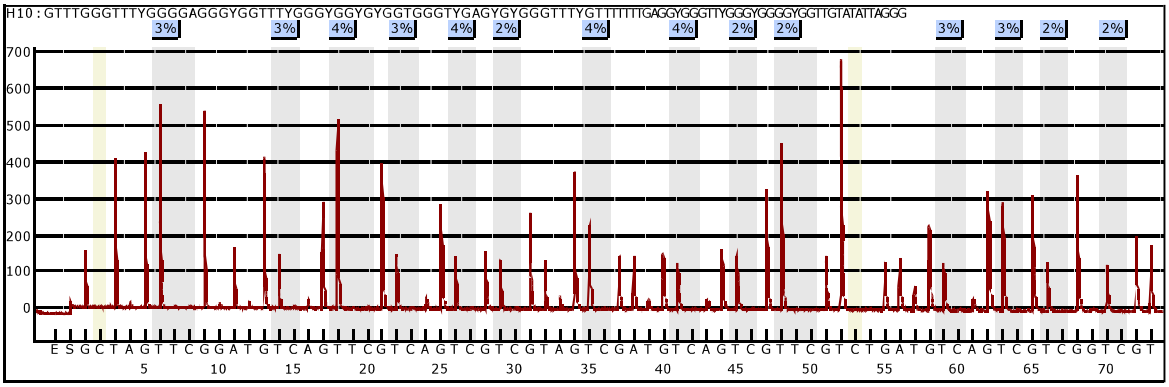

b) Region 2 (CpG No 22-24)
% Methylation: 3.9; SD: 1.14

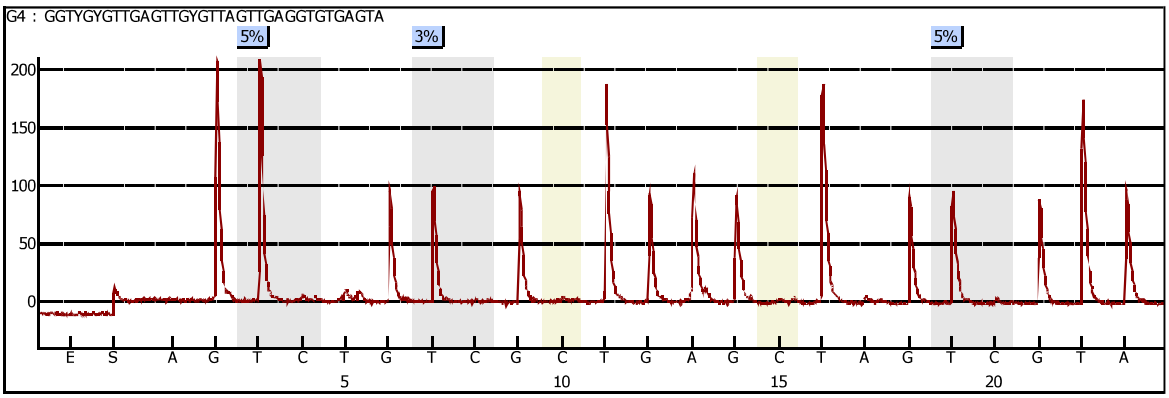

c) Region 3 (CpG No 25-31)
% Methylation: 2.8; SD: 1.47

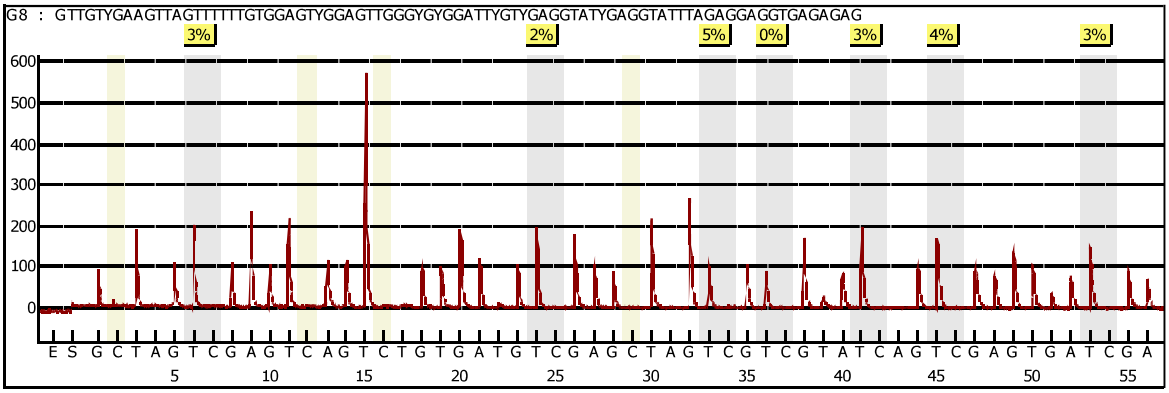

Figure 5.16. Effect of DAC on p21 promoter methylation in Kasumi cell line. Cells were untreated (Control) or treated (4μM DAC) for 72 hours with the indicated concentration of DAC. (a), (b) and (c) represent the analyzed CpG regions in the p21 promoter. Percentage methylation is the mean methylation of CpGs in the p21 promoter. SD, represents the standard deviation of the percentage mean methylation. The sequence analyzed is shown above each pyrogram, where Y represents the location of the cytosine in the CpG. In the pyrogram, the Y-axis represents the signal intensity (arbitrary units), which is proportional to the number of nucleotides incorporated (as peaks heights) and the X-axis is the dispensation order. The gray bars indicate the CpG positions, where the degree of methylation is assessed from the ratio of the peaks heights of C and T. Blue and yellow colours represent the confidence of the sequence pattern matches: greater than 90 percent and between 70-89 percent, respectively.

5.3.3. DAC-mediated induction of p15, p21, and E-cadherin correlated with changes in H3K9 methylation

DNA methylation has been recognized to cooperatively interact with histone methylation in silencing of gene expression (Esteve *et al*., 2006; Epztejn-Litman *et al*., 2008; Dong *et al*., 2008). Histone 3 Lysine 9 (H3K9) di- and tri-methylation are common repressive marks present in regulatory regions of transcriptional silenced genes (Kouzarides, 2007). Since previous studies reported that DAC treatment decreased H3K9 methylation in promoter regions of silenced genes (Fahrner *et al*., 2002; Nguyen *et al*., 2002; Coombes *et al*., 2003), we used chromatin immunoprecipitation (ChIP) assays to analyze the effect of DAC and other epigenetic drugs on p15, p21, and E-cadherin promoter H3K9 methylation (Table 5.1). AML-193 and Kasumi cells were treated with DAC for 72 hours and protein lysates were subjected to chromatin immunoprecipitation using antibodies for anti-dimethyl-H3K9 and anti-trimethyl-H3K9. DAC decreased both H3K9 di- and tri-methylation levels at p15 and E-cadherin promoters relative to the untreated control (Figure 5.17a and Figure 5.17b). H3K9 tri-methylation levels decreased to a greater extent than H3K9 di-methylation in response to DAC treatment in AML-193 and Kasumi cell lines (Figure 5.17a and Figure 5.17b). In contrast, at the p21 promoter DAC treatment increased levels of H3K9 di- and tri-methylation in both AML-193 and Kasumi cell lines (Figure 5.17a and Figure 5.17b). Levels of histone 3 (H3) were also measured to analyze the possibility of nucleosome depletion. However, we did not observe significant changes in H3 levels, indicating that variations in histone H3K9 di- and tri-methylation were not due to nucleosome depletion (Figure 5.17c).

Table 5.1. Chromatin immunoprecipitation assays of the effect of epigenetic drugs on H3K9 methylation in AML-193 cell line

		p15 gene		E-cadherin gene		p21 gene	
	Treatment	Fold difference	SD	Fold difference	SD	Fold difference	SD
H3K9Me2	Control	1.00	0.14	1.00	0.14	1.00	0.07
	DAC	0.65	0.16	0.78	0.06	1.67	0.21
	BIX	0.58	0.04	0.89	0.03	0.35	0.01
	Chaetocin	0.54	0.07	0.63	0.02	0.49	0.02
	BIX+DAC	2.57	0.25	0.74	0.04	0.89	0.04
	Chaetocin+DAC	0.28	0.07	0.59	0.02	0.31	0.02
	BIX+Chaetocin	0.86	0.05	1.17	0.10	0.97	0.06
H3K9Me3	Control	1.00	0.07	1.00	0.07	1.00	0.08
	DAC	0.25	0.06	0.66	0.08	2.49	0.54
	BIX	0.78	0.08	1.17	0.17	0.78	0.03
	Chaetocin	0.17	0.17	0.30	0.01	0.23	0.01
	BIX+DAC	2.04	0.14	1.44	0.30	1.05	0.07
	Chaetocin+DAC	0.25	0.06	0.58	0.10	1.51	0.21
	BIX+Chaetocin	2.00	0.16	2.36	0.37	1.75	0.08
H3	Control	1.00	0.13	1.00	0.08	1.00	0.07
	DAC	1.04	0.19	0.97	0.19	0.99	0.02
	BIX	0.96	0.06	1.00	0.16	1.13	0.03
	Chaetocin	1.08	0.12	1.03	0.19	1.00	0.04
	BIX+DAC	1.02	0.04	1.04	0.17	1.23	0.06
	Chaetocin+DAC	1.06	0.12	1.07	0.19	1.04	0.28
	BIX+Chaetocin	1.16	0.01	1.13	0.23	0.91	0.10

AML-193 cells were treated or untreated for 72 hours with the indicated concentration of drugs: DAC (1μM), BIX (4 μM), and chaetocin (100nM), either alone or as a combinatorial treatment. Untreated cells represent the Control treatment. Quantitative real time PCR was performed and ChIP results obtained by three independent replicate experiments are represented as fold difference between untreated (Control) and treated cells. H3K9Me2 and H3K9Me3 represent the di-methylation and tri-methylation levels at Histone 3 lysine 9. Background signal were measured with No Antibody (Ab) control and IgG Antibody control and then subtracted from signal obtained from the ChIP samples. Changes on H3-core histone were measured to assure no nucleosome depletion. SD, represents the standard deviation of three independent experiments.

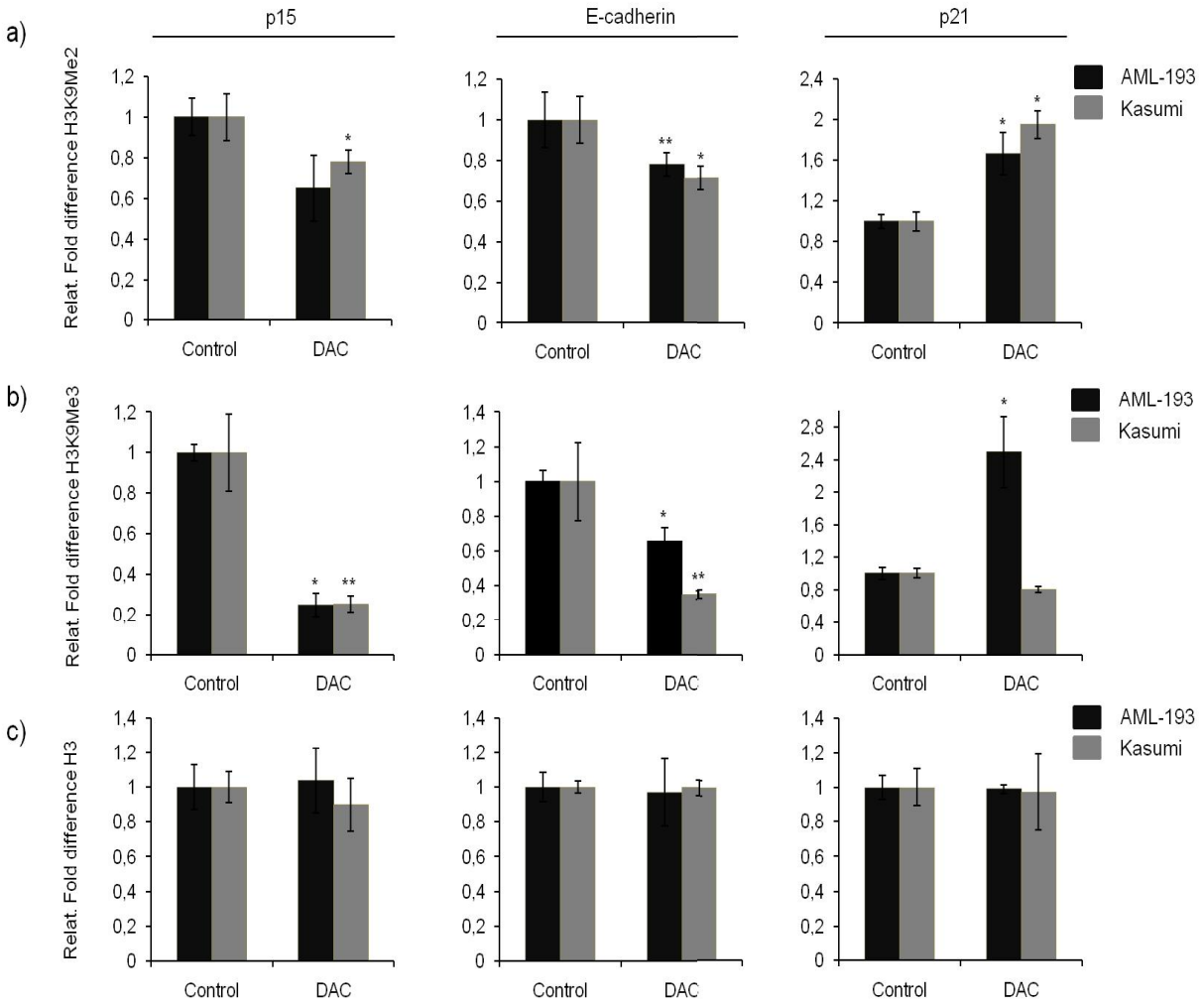

Figure 5.17. Chromatin immunoprecipitation analysis of the effect of DAC on H3K9 di- and tri-methylation and H3 associated with p15, E-cadherin, and p21 promoters in AML cell lines. (a) ChIP assay using dimethyl-H3K9 (H3K9Me2) antibodies. (b) ChIP assay using trimethyl-H3K9 (H3K9Me3) antibodies. (c) ChIP assay using H3 (H3) antibodies. AML-193 and Kasumi cells were treated for 72 hours with the following concentrations of DAC: AML-193: p15 and p21 (1 μM), E-cadherin (8 μM); Kasumi: p15, E-cadherin and p21 (4 μM). Histograms show the relative fold expression of PCR products (immunoprecipitated DNA) quantified using real time PCR. Error bars represent standard deviation from three independent experiments. ** Represents P-values < 0.05 and (**) represent P-value <0.01 between treated and untreated cells. Control represents the untreated cells.

5.4. Effect of BIX on p15, p21, and E-cadherin gene expression

5.4.1. BIX treatment did not re-activate expression of p15 and E-cadherin genes in AML cell lines

Like DNA methylation, histone methylation is an important epigenetic mark for regulation of gene expression (Kouzarides, 2007). Alterations in histone methylation, such as those observed at positions H3K9 and H3K27 have been associated with aberrant gene silencing in various form of cancer (Ohm *et al*., 2007; Schlesinger *et al*., 2007). Moreover, previous studies reported that epigenetically silenced genes that are re-activated by DAC treatment still present repressive H3K9 methylation marks in their promoter regions (Zhu and Otterson, 2003; McGarvey *et al*., 2006). To evaluate whether inhibition of histone methylatransferase activity leads to a changes in H3K9 methylation that might influence re-expression of epigenetically silenced genes, we used a specific G9a (dimethyl-H3K9) inhibitor BIX-01294 (BIX). This drug was first tested for its ability to re-express p15, p21, and E-cadherin genes in AML cell lines. Initially, expression of p15, p21, and E-cadherin was monitored in the presence of various concentrations of BIX. AML-193, KG-1a, and Kasumi cells were treated with BIX for 72 hours and relative expression was measured by real time PCR. BIX did not significantly induce the expression of p15 and E-cadherin at doses up to 4 μM in AML-193 and Kasumi cells and at doses up to 8 μM in the KG-1a cell line (Figure 5.18a and Figure 5.18b). In contrast, BIX induced a significant increase of p21 expression with an increase of 3.5-fold following treatment with 4 μM BIX in AML-193 cells. No increase in p21 expression however was observed in KG-1a and Kasumi cell lines (Figure 5.18 c).

5.4.2. BIX reduced H3K9 methylation levels at p15, p21, and E-cadherin promoters without inducing gene expression

Although BIX did not significantly induce expression of p15, p21, and E-cadherin in AML cell lines (with exception of p21 expression in AML-193 cells), we still determined whether BIX decreased H3K9 di- and tri-methylation at p15, p21, and E-cadherin promoters in AML-193 and Kasumi cell lines. Using ChIP assays with anti-dimethyl-H3K9 and anti-trimethyl-H3K9 antibodies, we tested the ability of BIX (4 μM) to cause changes in promoter H3K9 di and tri-methylation. BIX treatment significantly reduced H3K9 di-methylation levels at p15

promoter in AML-193 and Kasumi cell lines (Figure 5.19a). BIX had no effect on H3K9 tri-methylation at p15 and E-cadherin promoter in any of the cell lines tested (Figure 5.19a and Figure 5.19b). However, a decrease in H3K9 di-methylation levels at E-cadherin promoter was only observed in Kasumi cells (Figure 5.19a). In contrast, the p21 promoter region was associated with reduced levels of H3K9 di- and tri-methylation in AML-193 treated cells (Figure 5.19a and Figure 5.19b). No changes were observed in histone H3 levels, indicating that changes in H3K9 methylation were not due to nucleosome depletion (Figure 5.19c).

5.4.3. BIX did not induce changes in promoter methylation at p15 and E-cadherin promoters

Previous it has been shown that G9a directly interacts with DNMTs to establish a coordinated mechanism for DNA and histone methylation in silencing of genes during cell replication (Esteve *et al*., 2006). In order to evaluate whether BIX induced changes in promoter methylation, we analyzed the effect of BIX on p15 and E-cadherin promoter methylation in AML-193 and Kasumi cells. Treatment with BIX did not produce any change in the mean of p15 and E-cadherin promoter methylation state as determined by DNA pyrosequencing (Figure 5.20, Figure 5.21, Figure 5.22 and Figure 5.23).

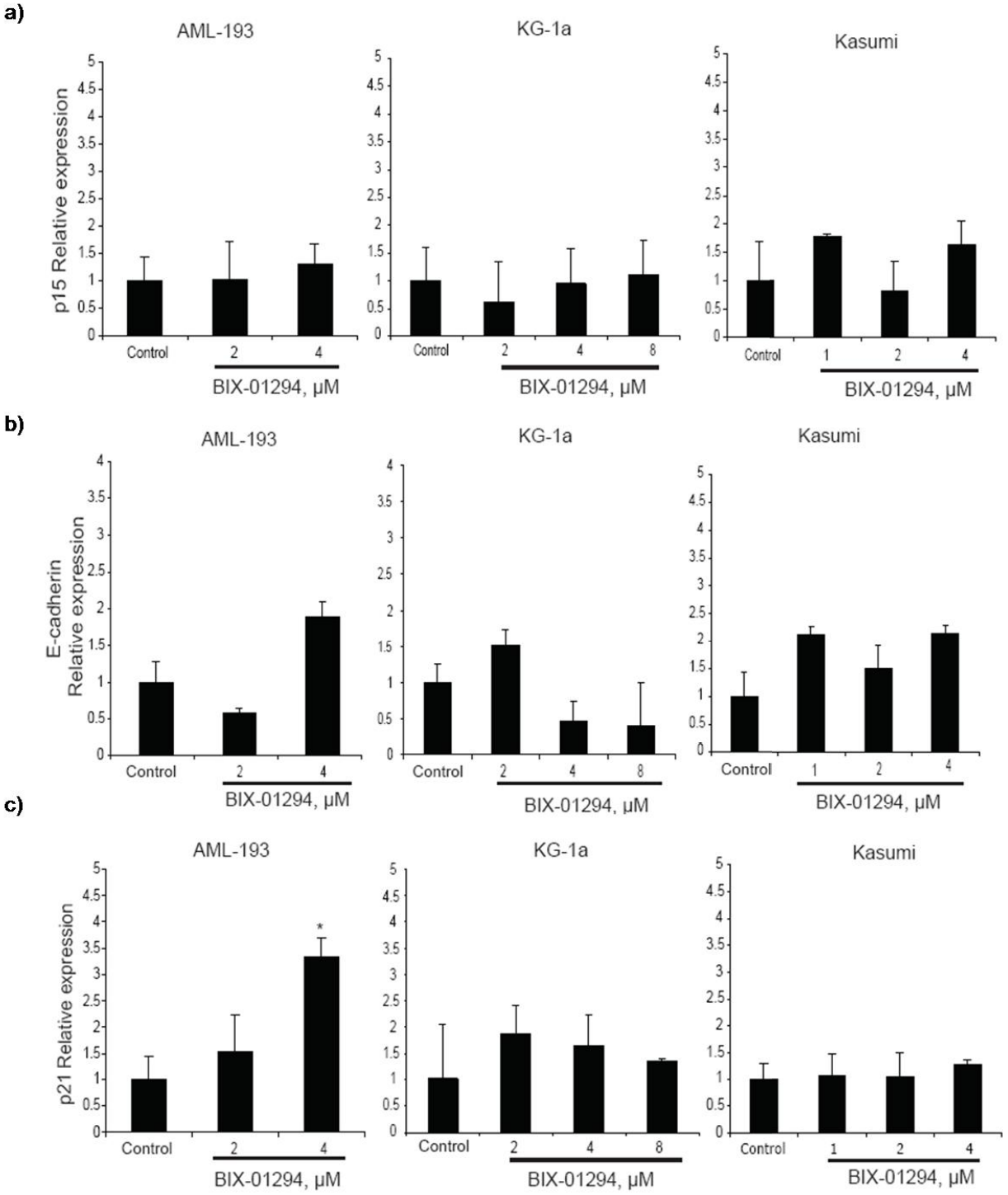

Figure 5.18. Real time PCR analysis of p15, p21, and E-cadherin expression in AML cell lines. AML-193, KG-1a, and Kasumi cell lines were treated with different doses of BIX for 72 hours. p15 (a), E-cadherin (b), and p21(c) gene expression was analyzed using HPRT as endogenous control expression. Error bars represents standard deviation of three independent experiments and (*) represents P-value < 0.05 between treated and untreated cells. Control represents the untreated cells.

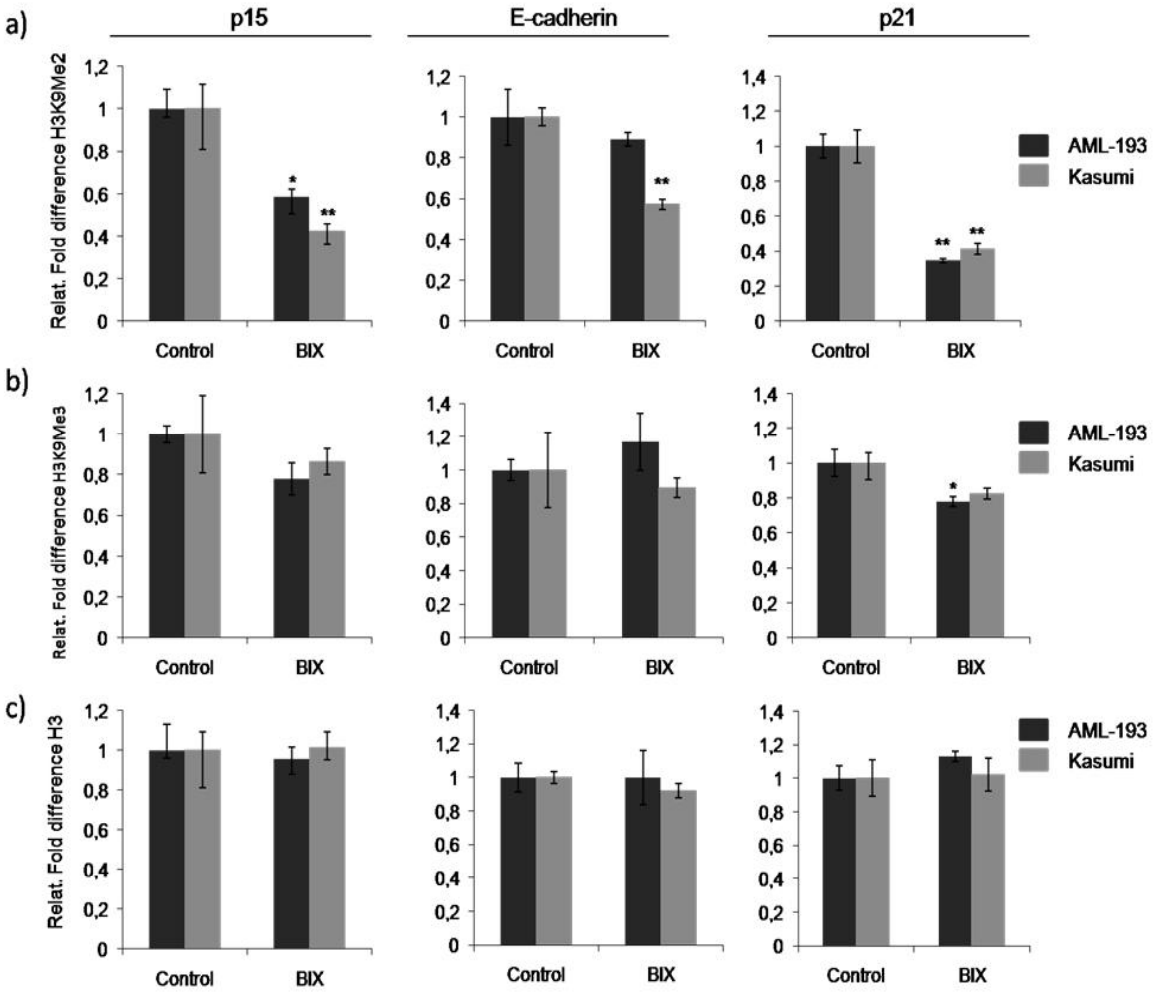

Figure 5.19. Chromatin immunoprecipitation analysis of the effect of BIX on H3K9 di- and tri-methylation and H3 associated with the p15, E-cadherin, and p21 promoter in AML cell lines. (a) ChIP assay of dimethyl-H3K9 (H3K9Me2) antibodies. (b) ChIP assay of trimethyl-H3K9 (H3K9Me3) antibodies. (c) ChIP assay of H3 (H3) antibodies. AML-193 and Kasumi cells were treated with BIX (4 μM) or untreated for 72 hours. Histograms show the relative fold expression of PCR products (immunoprecipitated DNA) quantified using real time PCR. Error bars represent standard deviation of three independent experiments. ** Represents P-values < 0.05 and (**) represent P-value <0.01 between treated and untreated cells. Control represents the untreated cells.

a) Control
% Methylation: 90.3; SD: 13.7

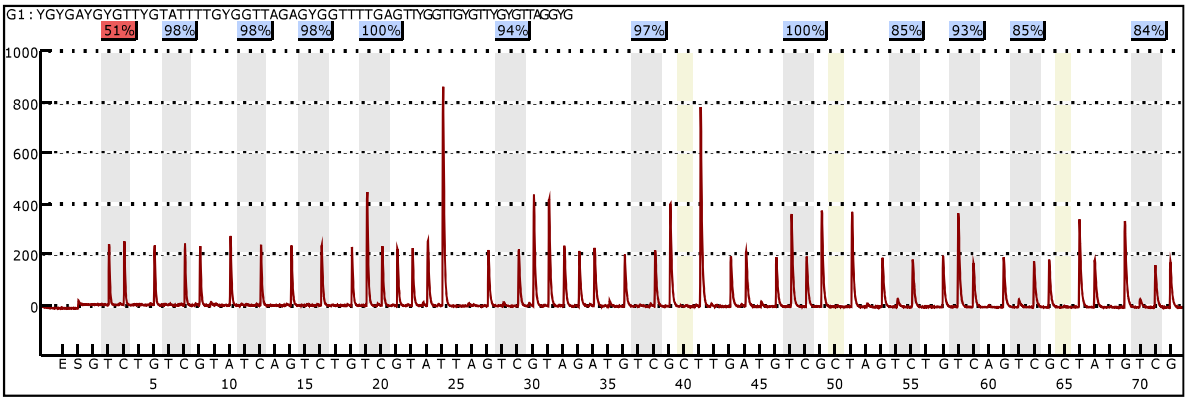

b) 4 µM BIX
% Methylation: 89.8; SD: 13.6

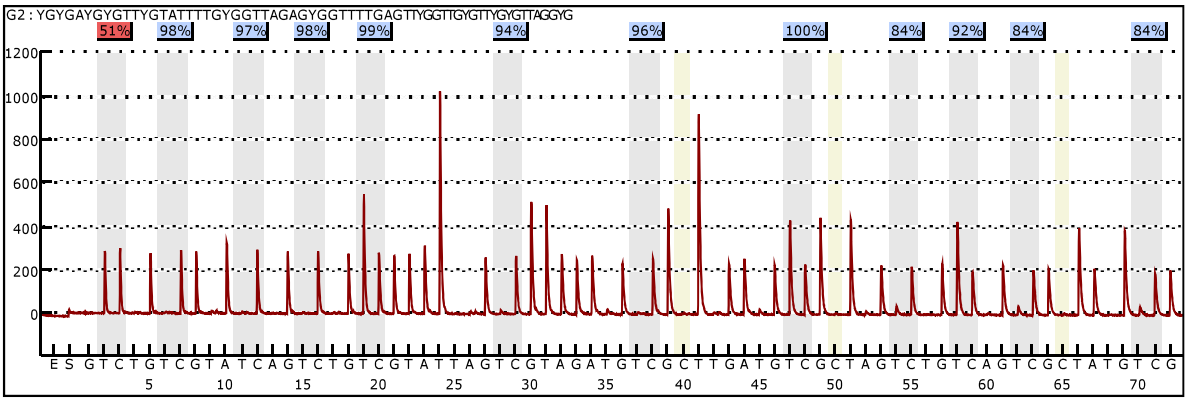

Figure 5.20. Effect of BIX on p15 promoter methylation in AML-193 cell lines. AML-193 cells were untreated (a) or treated (b) for 72 hours with 4µM BIX. Percentage methylation is the mean methylation of CpGs in the p15 promoter. SD, represent the standard deviation of the percentage mean methylation. The sequence analyzed is shown above each pyrogram, where Y represents the location of the cytosine in the CpG. In the pyrogram, the Y-axis represents the signal intensity (arbitrary units), which is proportional to the number of nucleotides incorporated (as peaks heights) and the X-axis is the dispensation order. The gray bars indicate the CpG positions, where the degree of methylation is assessed from the ratio of the peaks heights of C and T. Blue, yellow and red colours represent the confidence of the sequence pattern matches: greater than 90 percent, 70-89 percent and less than 70 percent, respectively.

a) Control
% Methylation: 88.5; SD: 13.7

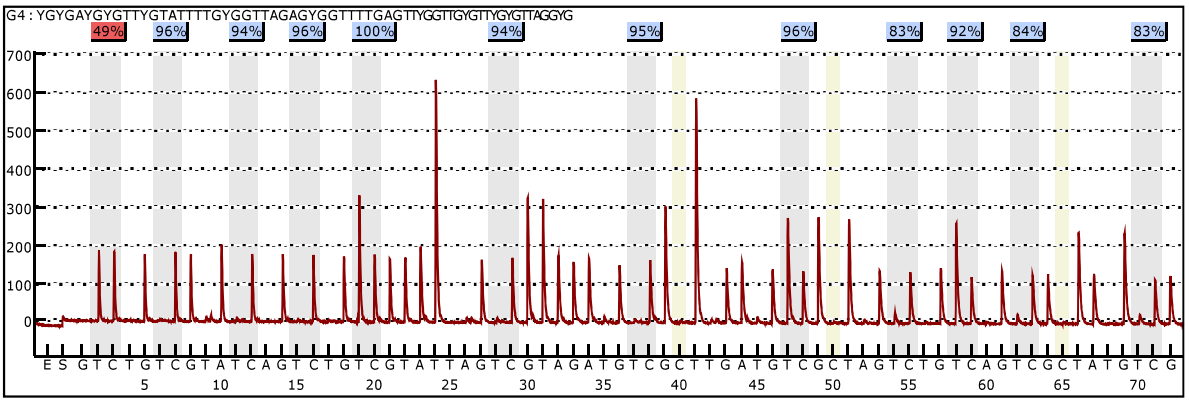

b) 4 µM BIX
% Methylation: 88.8; SD: 13.7

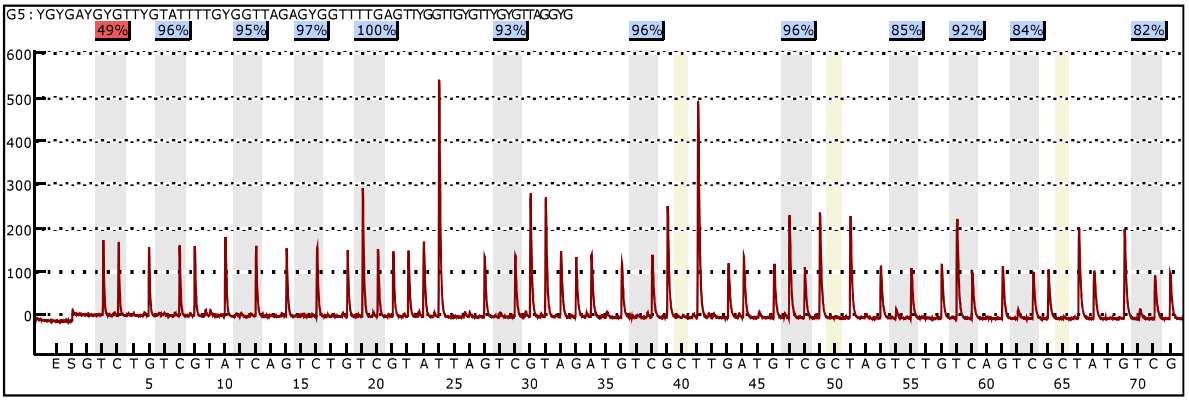

Figure 5.21. Effect of BIX on p15 promoter methylation in the Kasumi cell line. Kasumi cells were untreated (a) or treated (b) for 72 hours with 4 µM BIX. Percentage methylation is the mean methylation of CpGs in the p15 promoter. SD, represent the standard deviation of the percentage mean methylation. The sequence analyzed is shown above each pyrogram, where Y represents the location of the cytosine in the CpG. In the pyrogram, the Y-axis represents the signal intensity (arbitrary units), which is proportional to the number of nucleotides incorporated (as peaks heights) and the X-axis is the dispensation order. The gray bars indicate the CpG positions, where the degree of methylation is assessed from the ratio of the peaks heights of C and T. Blue, yellow and red colours represent the confidence of the sequence pattern matches: greater than 90 percent, 70-89 percent and less than 70 percent, respectively.

a) Control
%Methylation: 96.9; SD: 3.4

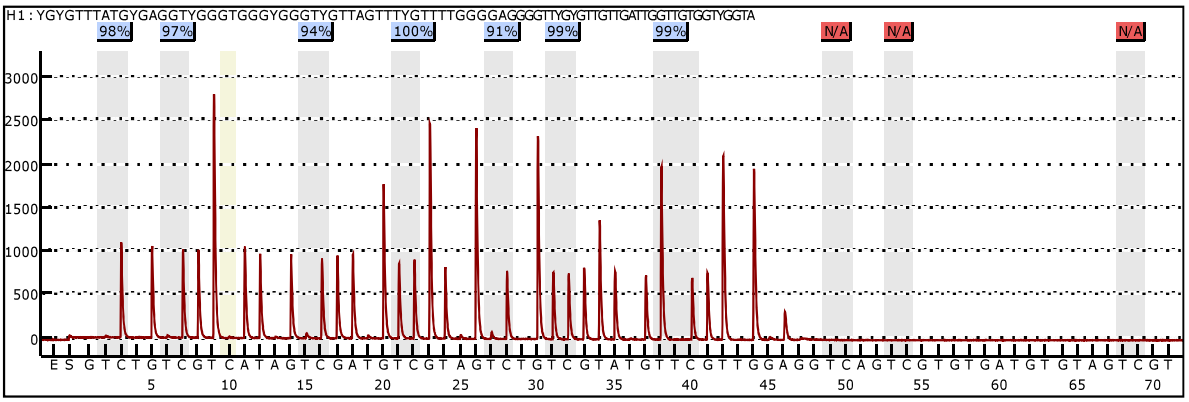

b) 4 µM BIX
% Methylation: 96.4; Sd: 3.3

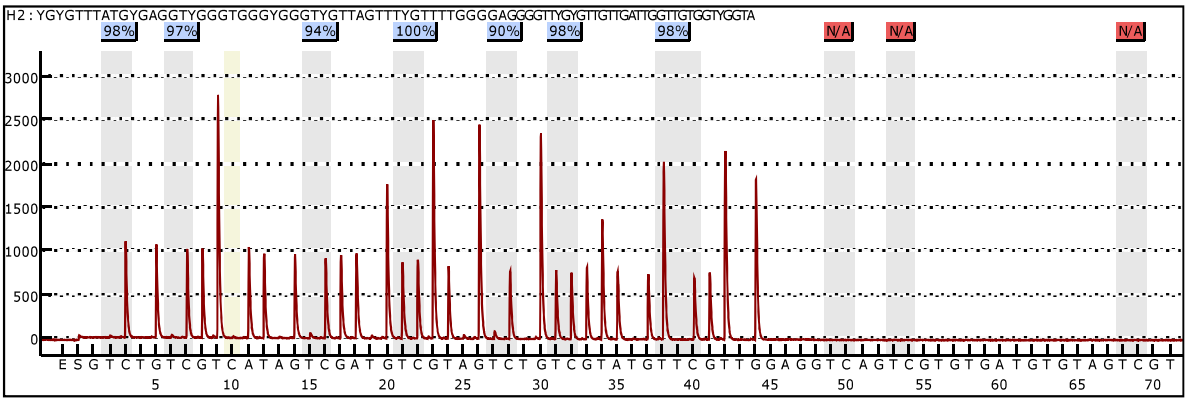

Figure 5.22. Effect of BIX on E-cadherin promoter methylation in the AML-193 cell line. AML-193 cells were untreated (a) or treated (b) for 72 hours with 4µM BIX. Percentage methylation is the mean methylation of CpGs in the E-cadherin promoter. SD, represents the standard deviation of the percentage mean methylation. The sequence analyzed is shown above each pyrogram, where Y represents the location of the cytosine in the CpG. In the pyrogram, the Y-axis represents the signal intensity (arbitrary units), which is proportional to the number of nucleotides incorporated (as peaks heights) and the X-axis is the dispensation order. The gray bars indicate the CpG positions, where the degree of methylation is assessed from the ratio of the peaks heights of C and T. Blue, yellow and red colours represent the confidence of the sequence pattern matches: greater than 90 percent, 70-89 percent and less than 70 percent, respectively.

a) Control
% Methylation : 96.5; SD: 3.3

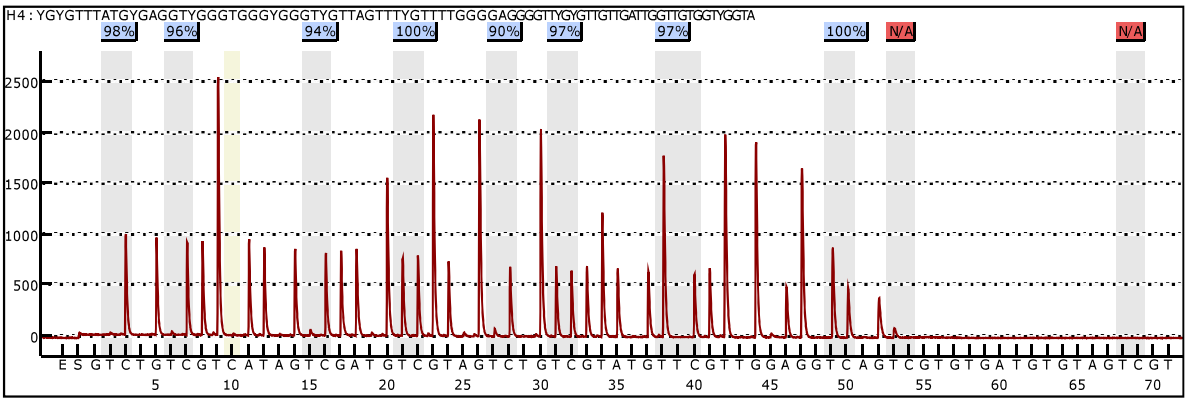

b) 4 µM BIX
% Methylation: 96.4; SD: 3.3

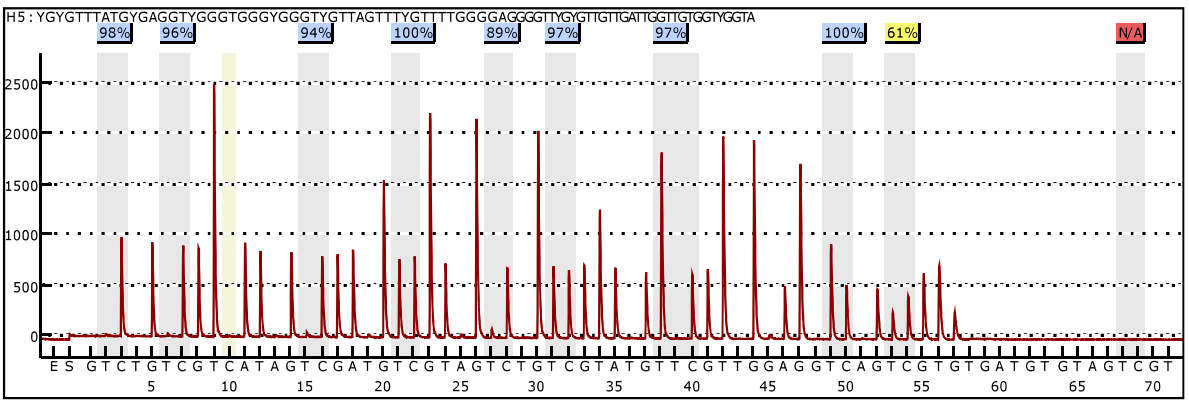

Figure 5.23. Effect of BIX on E-cadherin promoter methylation in the Kasumi cell line. Kasumi cells were untreated (a) or treated (b) for 72 hours with 4µM BIX. Percentage methylation is the mean methylation of CpGs in the E-cadherin promoter. SD, represents the standard deviation of the percentage mean methylation. The sequence analyzed is shown above each pyrogram, where Y represents the location of the cytosine in the CpG. In the pyrogram, the Y-axis represents the signal intensity (arbitrary units), which is proportional to the number of nucleotides incorporated (as peaks heights) and the X-axis is the dispensation order. The gray bars indicate the CpG positions, where the degree of methylation is assessed from the ratio of the peaks heights of C and T. Blue, yellow and red colors represent the confidence of the sequence pattern matches: greater than 90 percent, 70-89 percent and less than 70 percent, respectively.

5.5. Effect of chaetocin on p15, p21, and E-cadherin expression

5.5.1. Chaetocin-induced re-expression of p15, p21, and E-cadherin

Histone methylation is an important transcription mark for regulation of gene expression; however alterations in histone methylation patterns lead to the permanent silencing of relevant-cancer genes (Kouzarides, 2007; Sharma *et al*., 2010). To continue evaluating the effect of histone methylation in the silencing of tumor suppressor genes in AML, we analyzed the effect of chaetocin, an inhibitor of SUV39H1 histone trimethyltransferase, on p15, p21, and E-cadherin gene re-expression in AML cell lines. Treatment of AML-193, KG-1a, and Kasumi cell lines with 50 to 100 nM chaetocin resulted in a significant increase in p15, p21, and E-cadherin gene expression (Figure 5.24). p21 expression increased the most with an ~ 6-fold increase and ~ 8-fold increased following treatment with 100 nM chaetocin in AML-193 and Kasumi cells, respectively (Figure 5.24c). Chaetocin doses up to 100 nM were required to significantly re-express E-cadherin and p15 in AML cell lines (Figure 5.24a and Figure 5.24b).

5.5.2. Chaetocin-mediated expression of p15, p21, and E-cadherin caused changes in H3K9 methylation

To determine if chaetocin induced p15, p21, and E-cadherin gene expression by causing changes in promoter H3K9 methylation, we used ChIP assays. Treatment of AML-193 and Kasumi cells with 100 nM chaetocin significantly decreased levels of trimethyl-H3K9 at p15 and E-cadherin promoters to a greater extent than dimethyl-H3K9 (Figure 5.25a and Figure 5.25b). In contrast to the results observed with DAC, chaetocin decreased H3K9 tri-methylation levels at the p21 promoter of AML-193 and Kasumi cell lines (Figure 5.25b). However, chaetocin was only able to reduce H3K9 di-methylation levels at the p21 promoter in AML-193 cells. In Kasumi cells, this treatment increased levels of dimethyl-H3K9, which was similar to results found with DAC treatment (Figure 5.25a and Figure 5.17a). We did not observed changes in core histone H3 levels, indicating that changes in H3K9 methylation were not due to nucleosome depletion (Figure 5.25c).

5.5.3. Chaetocin enhanced p15 and E-cadherin expression without promoter demethylation

The ability of chaetocin to enhance expression of hypermethylated silenced genes, prompted us to determine whether chaetocin treatment produced changes in the methylation status of p15 and E-cadherin promoters. Treatment of AML-193 and Kasumi cell lines with chaetocin did not change the methylation state across the analyzed CpG islands in the p15 and E-cadherin promoter as indicated by DNA pyrosequencing analysis (Figure 5.26, Figure 27, Figure 28 and Figure 29).

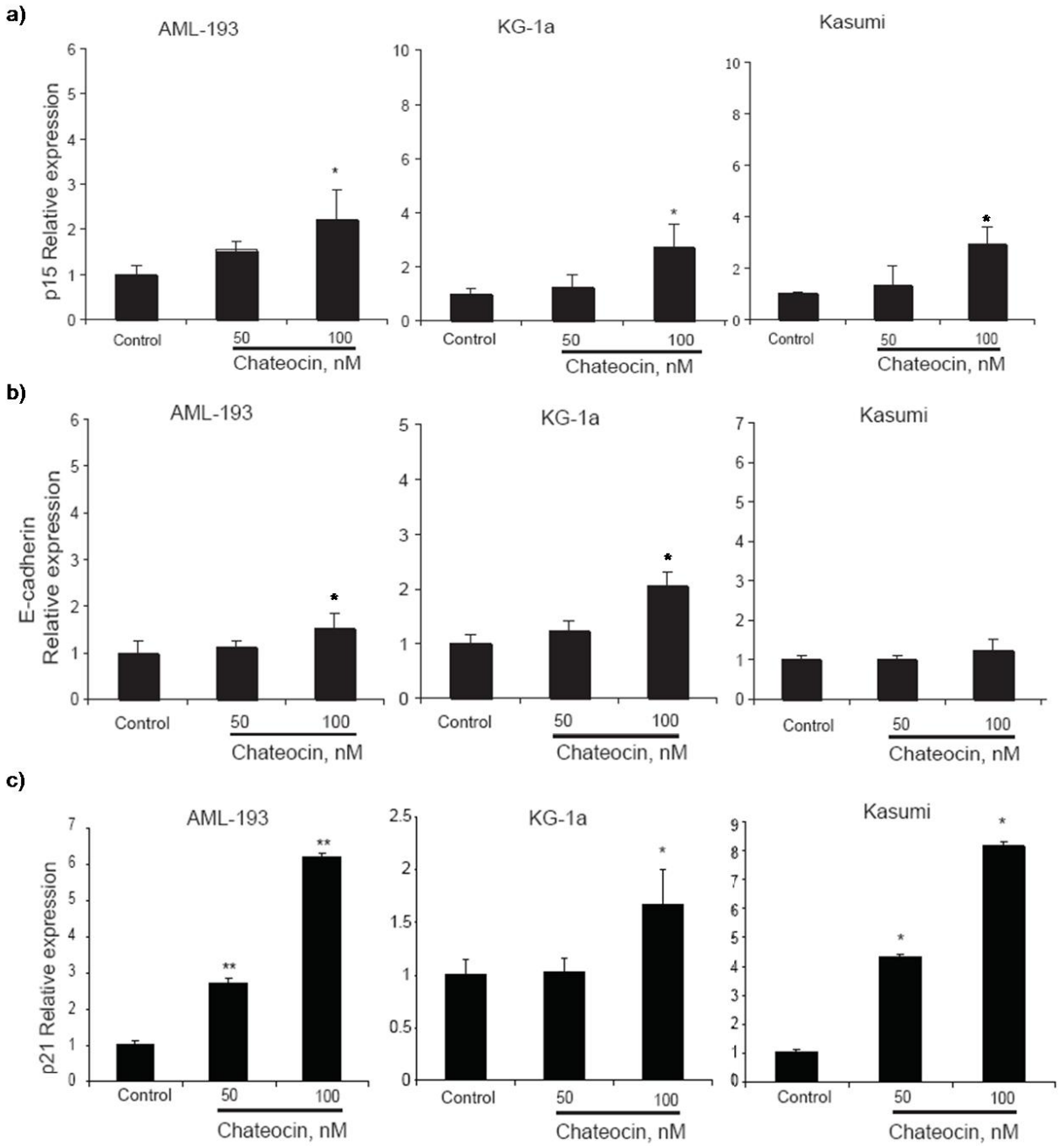

Figure 5.24. Real time PCR analysis of p15, p21, and E-cadherin expression in AML cell lines. AML-193, KG-1a, and Kasumi cell lines were treated with different doses of chaetocin for 72 hours. P15 (a), E-cadherin (b), and p21 (c) gene expression was analyzed using HPRT as endogenous control expression. Error bars represents standard deviation of three independent experiments and (*) represents P-value < 0.05 and (**) represent P-value <0.01 between treated and untreated cells. Control represents the untreated cells.

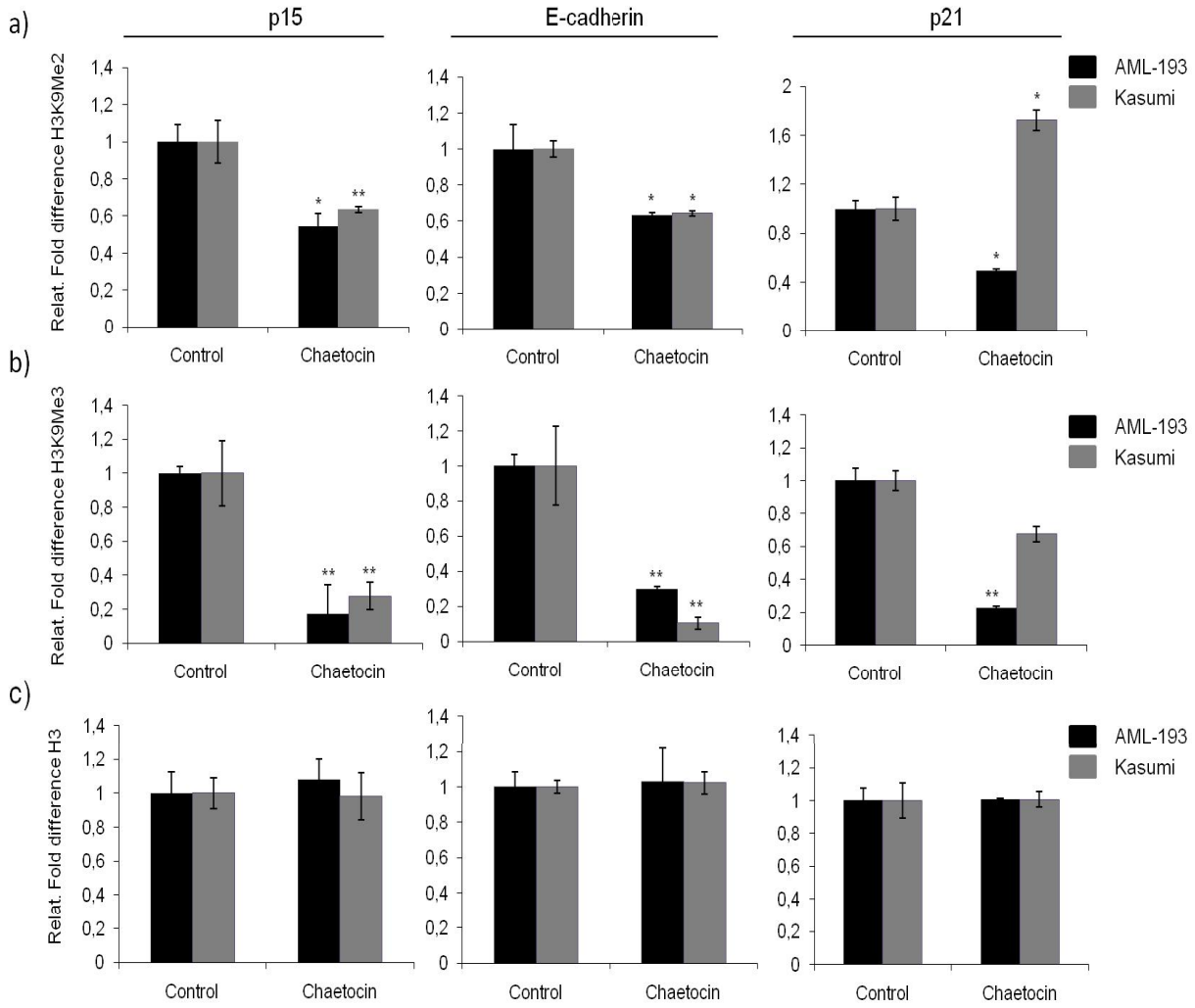

Figure 5.25. Chromatin immunoprecipitation analysis of the effect of chaetocin on H3K9 di- and tri-methylation and H3 associated with the p15, E-cadherin, and p21 promoter in AML cell lines. (a) ChIP assay of dimethyl-H3K9 (H3K9Me2) antibodies. (b) ChIP assay of trimethyl-H3K9 (H3K9Me3) antibodies. (c) ChIP assay of H3 (H3) antibodies. AML-193 and Kasumi cells were treated with Chaetocin (100 nM) or untreated for 72 hours. Histograms show the relative fold expression of PCR products (immunoprecipitated DNA) quantified using real time PCR. Error bars represent standard deviation of three independent experiments. ** Represents P-values < 0.05 and (**) represent P-value <0.01 between treated and untreated cells. Control represents the untreated cells.

AML-193 p15
a) Control
% Methylation: 95.1; SD: 8.0

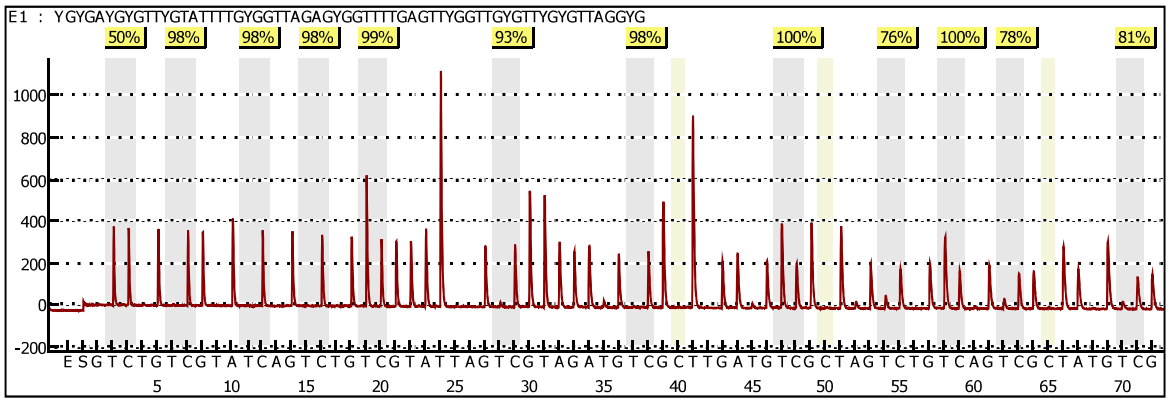

b) 100 nM Chaetocin
% Methylation: 95.2; SD: 7.4

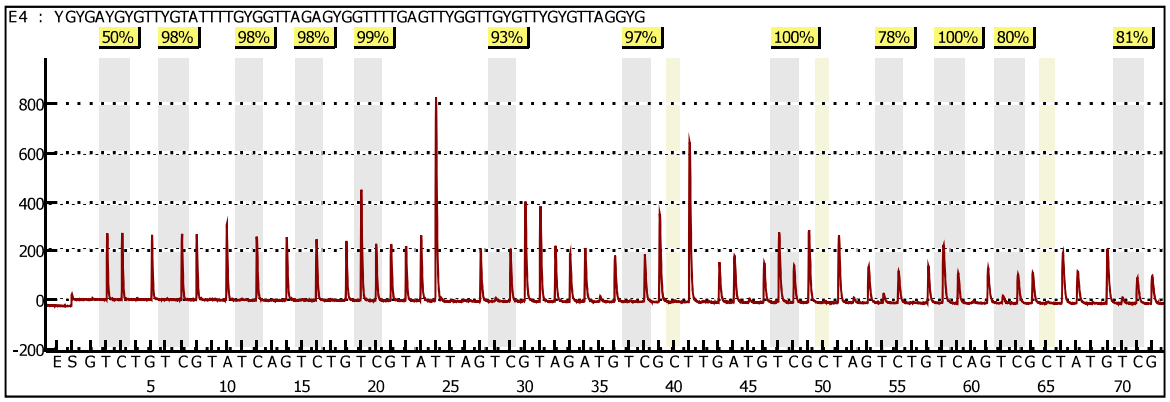

Figure 5.26. Effect of chaetocin on p15 promoter methylation in AML-193 cell line. AML-193 cells were untreated (a) or treated (b) for 72 hours with 100 nM chaetocin. Percentage methylation is the mean methylation of CpGs in the p15 promoter. SD, represents the standard deviation of the percentage mean methylation. The sequence analyzed is shown above each pyrogram, where Y represents the location of the cytosine in the CpG. In the pyrogram, the Y-axis represents the signal intensity (arbitrary units), which is proportional to the number of nucleotides incorporated (as peaks heights) and the X-axis is the dispensation order. The gray bars indicate the CpG positions, where the degree of methylation is assessed from the ratio of the peaks heights of C and T. Yellow color represents that the sequences pattern matches with a confidence between 70-89 percent.

a) Control
% Methylation: 95.0; SD: 7.4

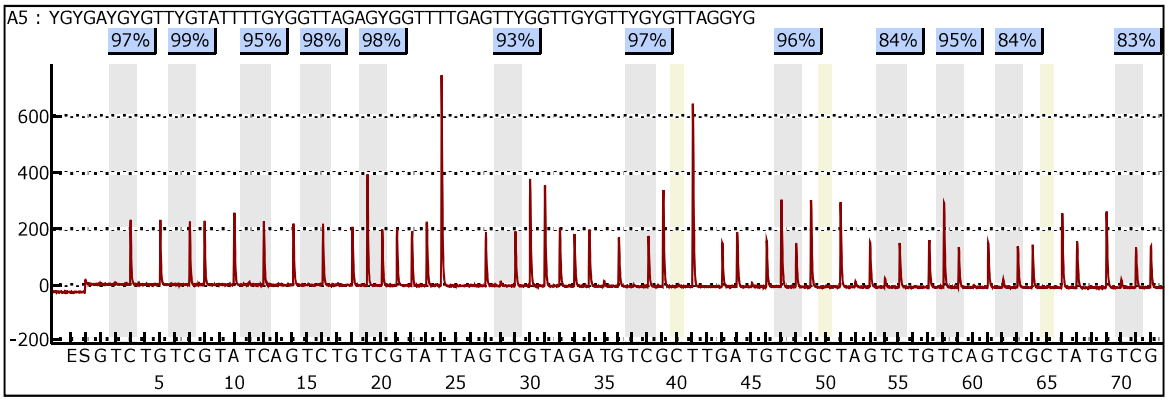

b) 100 nM Chaetocin% Methylation: 95.7; SD: 5.4

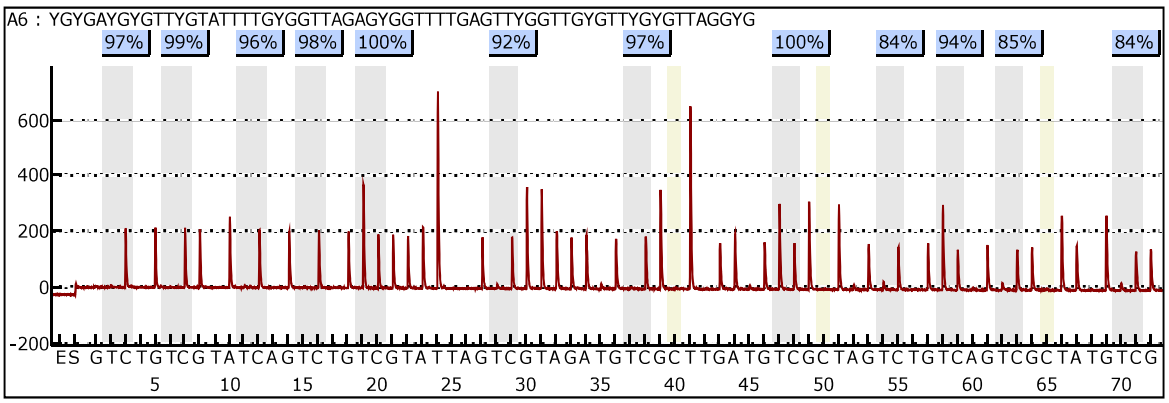

Figure 5.27. Effect of chaetocin on p15 promoter methylation in Kasumi cell line. Kasumi cells were untreated (a) or treated (b) for 72 hours with 100 nM chaetocin. Percentage methylation is the mean methylation of CpGs in the p15 promoter. SD, represents the standard deviation of the percentage mean methylation. The sequence analyzed is shown above each pyrogram, where Y represents the location of the cytosine in the CpG. In the pyrogram, the Y-axis represents the signal intensity (arbitrary units), which is proportional to the number of nucleotides incorporated (as peaks heights) and the X-axis is the dispensation order. The gray bars indicate the CpG positions, where the degree of methylation is assessed from the ratio of the peaks heights of C and T. Blue color represents that the sequence pattern matches with a confidence greater than 90 percent.

a) Control
% Methylation: 95.5; SD: 4.7

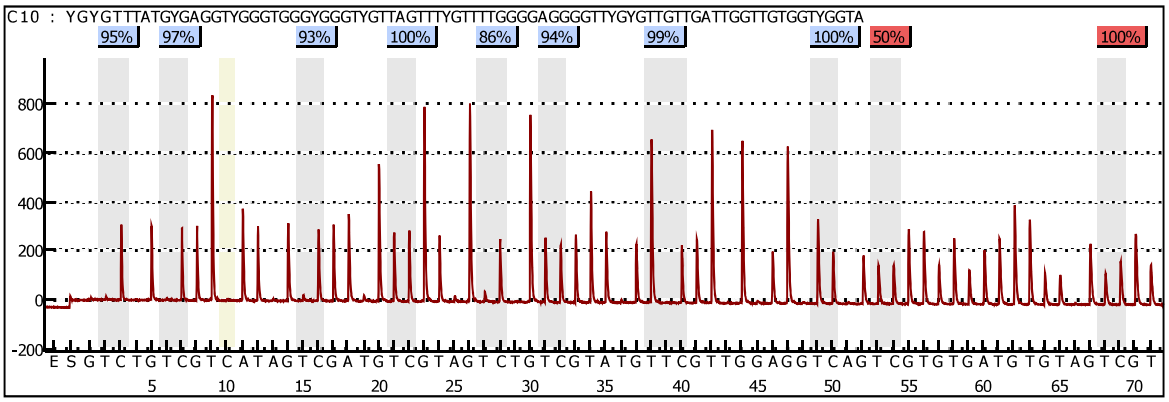

b) 100 nM Chaetocin
% Methylation: 90.6; SD: 10

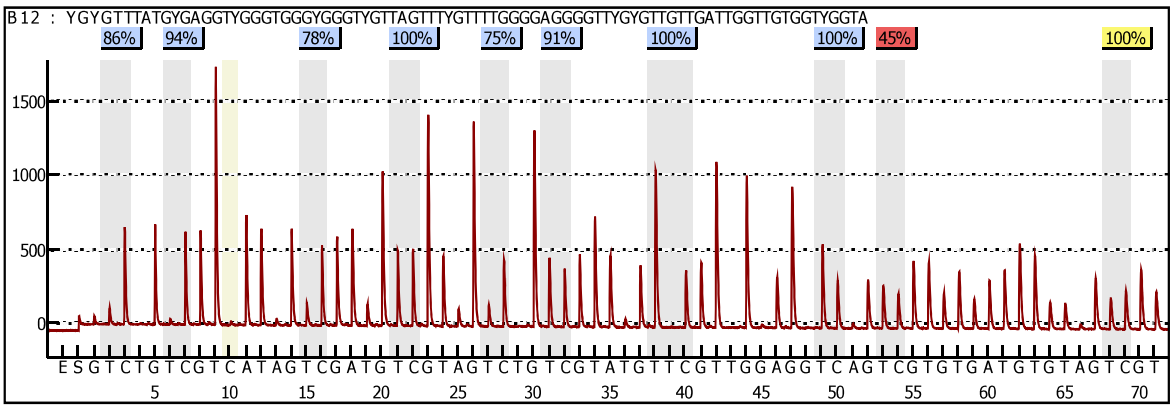

Figure 5.28. Effect of chaetocin on E-cadherin promoter methylation in AML-193 cell line. AML-193 cells were untreated (a) or treated (b) for 72 hours with 4μM BIX. Percentage methylation is the mean methylation of CpGs in the E-cadherin promoters. SD, represents the standard deviation of the percentage mean methylation. The sequence analyzed is shown above each pyrogram, where Y represents the location of the cytosine in the CpG. In the pyrogram, the Y-axis represents the signal intensity (arbitrary units), which is proportional to the number of nucleotides incorporated (as peaks heights) and the X-axis is the dispensation order. The gray bars indicate the CpG positions, where the degree of methylation is assessed from the ratio of the peaks heights of C and T. Blue, yellow and red colors represent the confidence of the sequence pattern matches: greater than 90 percent, 70-89 percent and less than 70 percent, respectively.

a) Control
% Methylation: 90.1; SD: 9.0

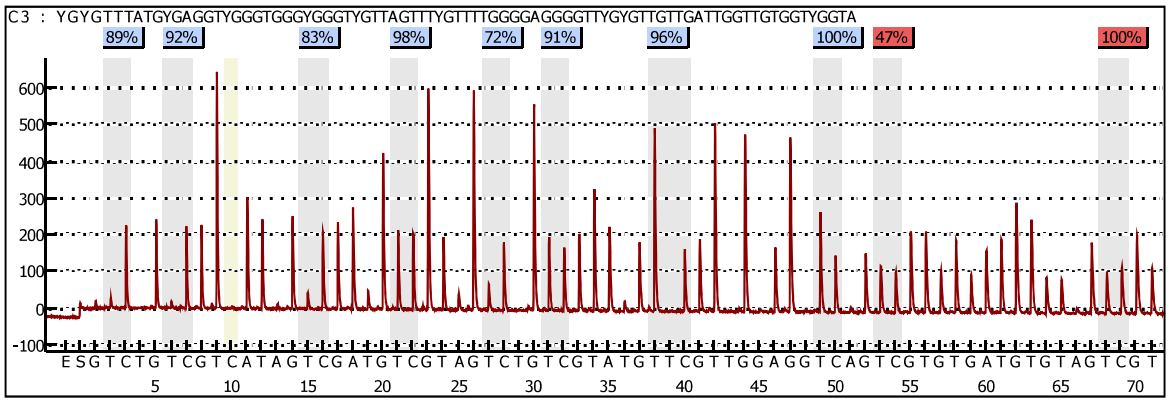

b) 100 nM Chaetocin
% Methylation: 84.9; SD: 11.1

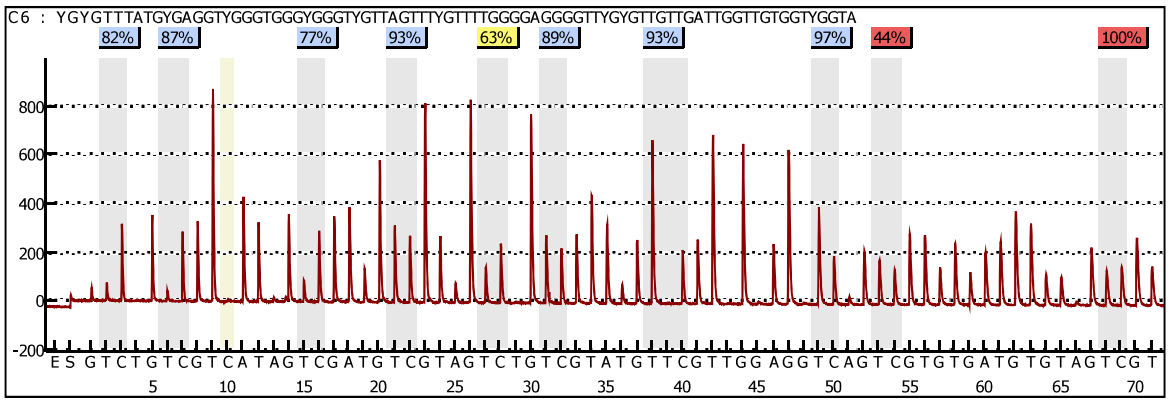

Figure 5.29. Effect of chaetocin on E-cadherin promoter methylation in AML-193 cell line. AML-193 cells were untreated (a) or treated (b) for 72 hours with 4μM BIX. Percentage methylation is the mean methylation of CpGs in the E-cadherin promoters. SD, represents the standard deviation of the percentage mean methylation. The sequence analyzed is shown above each pyrogram, where Y represents the location of the cytosine in the CpG. In the pyrogram, the Y-axis represents the signal intensity (arbitrary units), which is proportional to the number of nucleotides incorporated (as peaks heights) and the X-axis is the dispensation order. The gray bars indicate the CpG positions, where the degree of methylation is assessed from the ratio of the peaks heights of C and T. Blue, yellow and red colours represent the confidence of the sequence pattern matches: greater than 90 percent, 70-89 percent and less than 70 percent, respectively.

5.6. The effect of combinatorial treatments of DAC, BIX, and chaetocin on AML cell proliferation

Previous studies in our lab showed that DAC has little effect on AML cell proliferation. However, we found that DAC potentiated the anti-proliferative cell response to BIX and chaetocin treatment in AML cell lines. Based on this result and the fact that combinations of DNMT and HDAC inhibitors work in synergy to induce greater expression of silenced tumor suppressor genes in cancer cell lines (Zhu and Otterson, 2003; McGarvey *et al*., 2006), we evaluated the effect of combinatorial treatments of DAC, BIX, and chaetocin on the proliferation of AML cells and in the re-activation of tumor suppressor genes in AML cell lines. Initially, we determined median effect doses of BIX and chaetocin in the presence and absence of DAC on AML-193, KG-1a, and Kasumi cell proliferation using MTT assays. Median doses (Dm) were determined based on the MTT assay using CalcuSyn software in accordance with equation 1:

$$\text{Log}\,(Fa/Fu) = m \log (D) - m \log (Dm) \qquad \textbf{(Eq.1)}$$

In equation 1, Fa is the fraction affected for a given dose (D), Fu is the fraction unaffected (1-Fa), D is the dose of drug, Dm is the median dose of the drug and m is the slope. The fraction affected calculated from MTT data was determined by equation 2:

$$Fa = \frac{\text{(Proliferation with drug)}}{\text{(Proliferation without drug)}} \qquad \textbf{(Eq. 2)}$$

We found that chaetocin induced 50% inhibition of AML cell proliferation at lower doses than BIX. However, median-effect doses vary between cell lines due to their sensitivity to drugs. Kasumi was the most sensitive cell line in response to BIX, showing a Dm of 828±481 nM and 10.33±2.92 nM for chaetocin (Table 5.2 and Figure 5.32). Conversely, KG-1a was more sensitive to chaetocin and BIX with a Dms of 7.65±0.36 nM and 1380±269 nM, respectively (Table 5.2 and Figure 5.31). AML-193 was the most resistant cell line to chaetocin and BIX with a Dms of 2590±163 nM and 17±1.74 nM, respectively (Table 5.2 and Figure 5.30).

In all AML cell lines tested, median doses were reduced for chaetocin and BIX in the presence of DAC, confirming that DAC potentiates the effect of these drugs on the proliferation of AML cells (Table 5.2). Chaetocin Dms were reduced in the order of 3 to 5 times in all AML cell lines studied (Table 5.2). In AML-193, the Dm for BIX was as well reduced 3 times. However, in Kasumi and KG-1a the Dm for BIX was slightly reduced (Table 5.2). The ability of DAC to potentiate the activity of BIX and chaetocin may be explained by the correlation between decreased DNA and histone methylation and gene re-activation. This hypothesis can be supported by previous studies carried out in the Geyer lab, where re-activation of hypermethylated tumor suppressor gene RIZ1 takes place when AML cells are treated with chaetocin and DAC (Geyer, *unpublished*).

Table 5.2. Median doses of chaetocin and BIX in AML cell lines

Cell line	+/- DAC	Drugs	Median dose (nM)*
AML-193	-	BIX	2590 ± 163
AML-193	+	BIX	770 ± 290
AML-193	-	Chaetocin	17 ± 1.74
AML-193	+	Chaetocin	3.30 ± 1.56
KG-1a	-	BIX	1380 ± 269
KG-1a	+	BIX	1160 ± 307
KG-1a	-	Chaetocin	7.65 ± 0.36
KG-1a	+	Chaetocin	2.53 ± 0.53
Kasumi	-	BIX	828 ± 481
Kasumi	+	BIX	793 ± 189
Kasumi	-	Chaetocin	10.33 ± 2.92
Kasumi	+	Chaetocin	1.96 ± 0.43

Cells were treated for 72 hours with BIX and chaetocin in combination in presence and absence of DAC (+/-). * Errors represents 95% confidential interval.

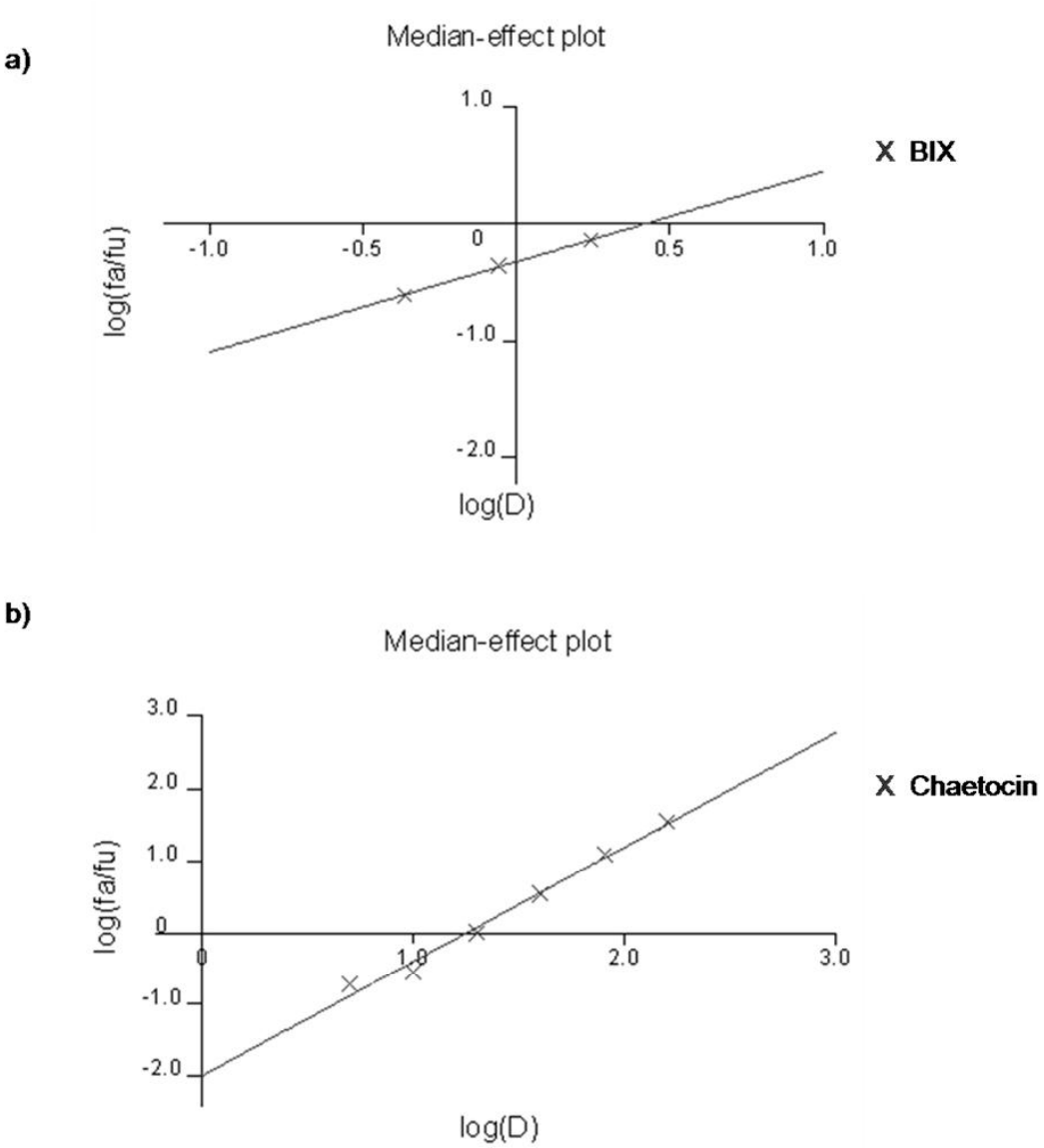

Figure 5.30. Median effect plots of BIX and chaetocin in AML-193 cell line. AML-193 cells were treated for 72 hours with BIX (a) or chaetocin (b). Fa indicates fraction affected for each drug, Fu indicates fraction unaffected (vehicle control), and D represents doses for each drug. DMSO was used as a vehicle control for both drugs. The median doses (Dm) are found from the graphs by taking the antilog of the X intercept.

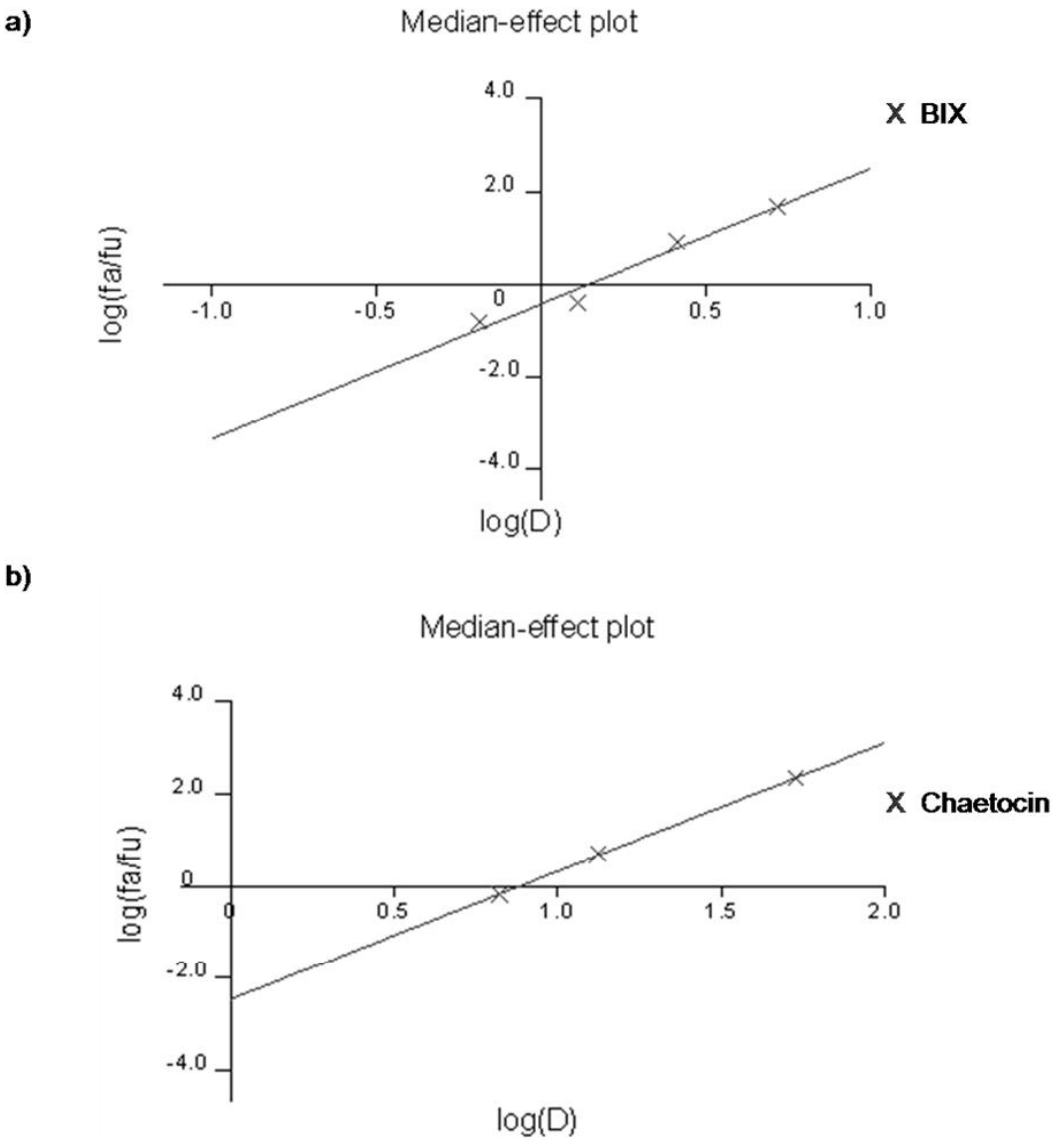

Figure 5.31. Median effect plots of BIX and chaetocin in KG-1a cell line. KG-1a cells were treated for 72 hours with BIX (a) or chaetocin (b). Fa indicates fraction affected for each drug, Fu indicates fraction unaffected (vehicle control), and D represents doses for each drug. DMSO was used as a vehicle control for both drugs. The median doses (Dm) are found from the graphs by taking the antilog of the X intercept.

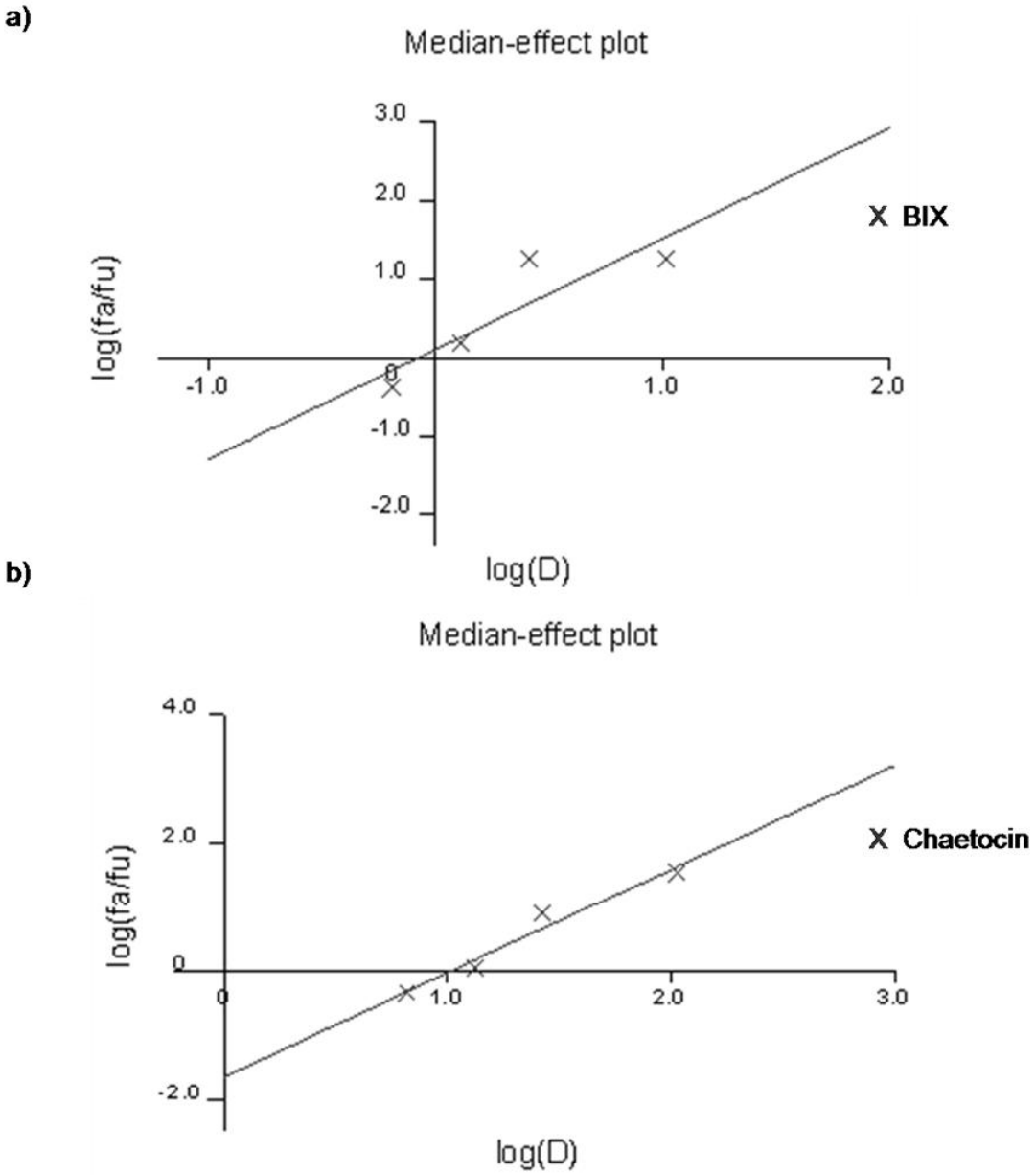

Figure 5.32. Median effect plots of BIX and chaetocin in Kasumi cell line. Kasumi cells were treated for 72 hours with BIX (a) or chaetocin (b). Fa indicates fraction affected for each drug, Fu indicates fraction unaffected (vehicle control), and D represents doses for each drug. DMSO was used as a vehicle control for both drugs. The median doses (Dm) are found from the graphs by taking the antilog of the X intercept.

Based on the ability of DAC to potentiate anti-proliferative response of chaetocin and BIX in AML cell lines, we assessed the synergism or antagonism effects of BIX and chaetocin in presence and absence of DAC. Interaction between drugs was tested using the median effect plot analysis method developed by Chou and Talaly (1977). This method evaluates the nature of interaction of two drugs using the combination index (CI) value, which provides the qualitative information of drug interaction nature and is represented by equation 3:

$$CI = (D_{A,X}/ D_{X,A}) + (D_{B,X}/ D_{X,B}) \qquad \textbf{(Eq. 3)}$$

In equation 3, $D_{A,X}$ and $D_{B,X}$ are concentrations of drugs A and B used in combination to achieve X% drug effect. $D_{X,A}$ and $D_{X,B}$ are the concentrations of each drug (A and B) that alone cause that X% effect. CI is the combination index value. Combination index values can be represented by CI and isobologram plots. Isobolograms are defined as a measure of effectiveness of drug interaction, where two drugs, A and B, are required to produce a defined single agent effect (e,g., IC_{50}/Dm). D_A and D_B used as single agents are placed on the *x* and *y* axes in a two-coordinate plot. The line connecting these points (drug A, D_A, and drug B, D_B, at X% effect "Dx") is the line of additivity and represents a CI value equal to 1, where there is no drug potentiation (based on the concept of "dose equivalence"). A drug combination that causes an effect above the line indicates that drug A and B at *x* and *y* doses synergistically act to cause an effect greater than that caused by the drugs alone. Conversely, when a combination results in a reduced effect (less than "D_x"), then greater quantities of drug A and B are needed to get the "D_x" effect. The point representing the combination will appear above the additive line indicating a CI value more than 1, showing antagonism. Synergism will be described as the opposite of antagonism, where CI value is less than 1. In summary, if the CI is equal to 1, the drug combination is additive, CI is greater than 1, then drugs display antagonism, and if the CI is less than 1, drugs display synergism (Zhao *et al.*, 2004; Tallarida, 2006; Chou, 2006).

Drug combination studies were used to measure drug interactions and potentiation of anti-proliferative response in AML cell lines. CI values were calculated at different effect levels, denoted ED_X (x= 50, 75, and 90) using CalcuSyn software (Table 5.3). In AML-193, BIX and chaetocin treatment displayed antagonistic activity under the drug doses used in study (Figure 5.33). The mean combination index values +/- SD in AML-193 cell lines for different effect levels were ED_{50}: 1.49 +/- 0.38, ED_{75}: 1.48 +/- 0.32, and ED_{90}: 1.48 +/- 0.28 (Table 5.3). In the presence of DAC, antagonism became significant, but it was slightly reduced as the effect-

levels increased. CI values for ED_{50}, ED_{75}, and ED_{90} were 2.73 +/- 0.66, 2.18 +/- 0.42, and 1.74 +/- 0.28, respectively (Table 5.3, Figure 5.33a and Figure 5.33c).

In the case of KG-1a and Kasumi cell lines, a synergistic anti-proliferative effect between BIX and chaetocin was observed in the absence of DAC. In KG-1a, mean CI values +/- SD for effect levels were ED_{50}: 0.77 +/- 0.12, ED_{75}: 0.70 +/- 0.09, and ED_{90}: 0.64 +/- 0.08 (Table 5.3 and Figure 5.34). In Kasumi cells, CI values were ED_{50}: 0.94 +/- 0.23, ED_{75}: 0.93 +/- 0.18, and ED_{90}: 0.92 +/- 0.22 (Table 5.3 and Figure 5.35). In the presence of DAC, BIX, and chaetocin treatment presented an antagonistic interaction at the 50% effect level in KG-1a (ED_{50}: 1.34±0.42) and Kasumi (ED_{50}: 1.52±0.66) cell lines (Table 5.3, Figure 5.34 and Figure 5.35). However, as the effect level increased at 90% BIX and chaetocin treatment displayed synergistic activity in KG-1a (ED_{90}: 0.86±0.21) and Kasumi (ED_{90}: 0.58±0.20) cells (Table 5.3, Figure 5.34 and Figure 5.35).

Table 5.3. CI values for combination of BIX with chaetocin in AML cell lines.

		CI values at inhibition of		
Cell line	**+/- DAC**	**50%**	**75%**	**90%**
AML-193	-	1.49±0.38	1.48±0.32	1.48±0.28
AML-193	+	2.73±0.66	2.18±0.42	1.74±0.28
KG-1a	-	0.77±0.12	0.70±0.09	0.64±0.08
KG-1a	+	1.34±0.42	1.08±0.28	0.86±0.21
Kasumi	-	0.94±0.23	0.93±0.18	0.92±0.22
Kasumi	+	1.52±0.66	0.92±0.36	0.58±0.20

Cells were treated for 72 with BIX and chaetocin in combination in presence of absence of DAC (+/-). CI values = 1 indicates additive effect, <1synergism, >1 antagonism.
*Data represents ± the mean S.D.

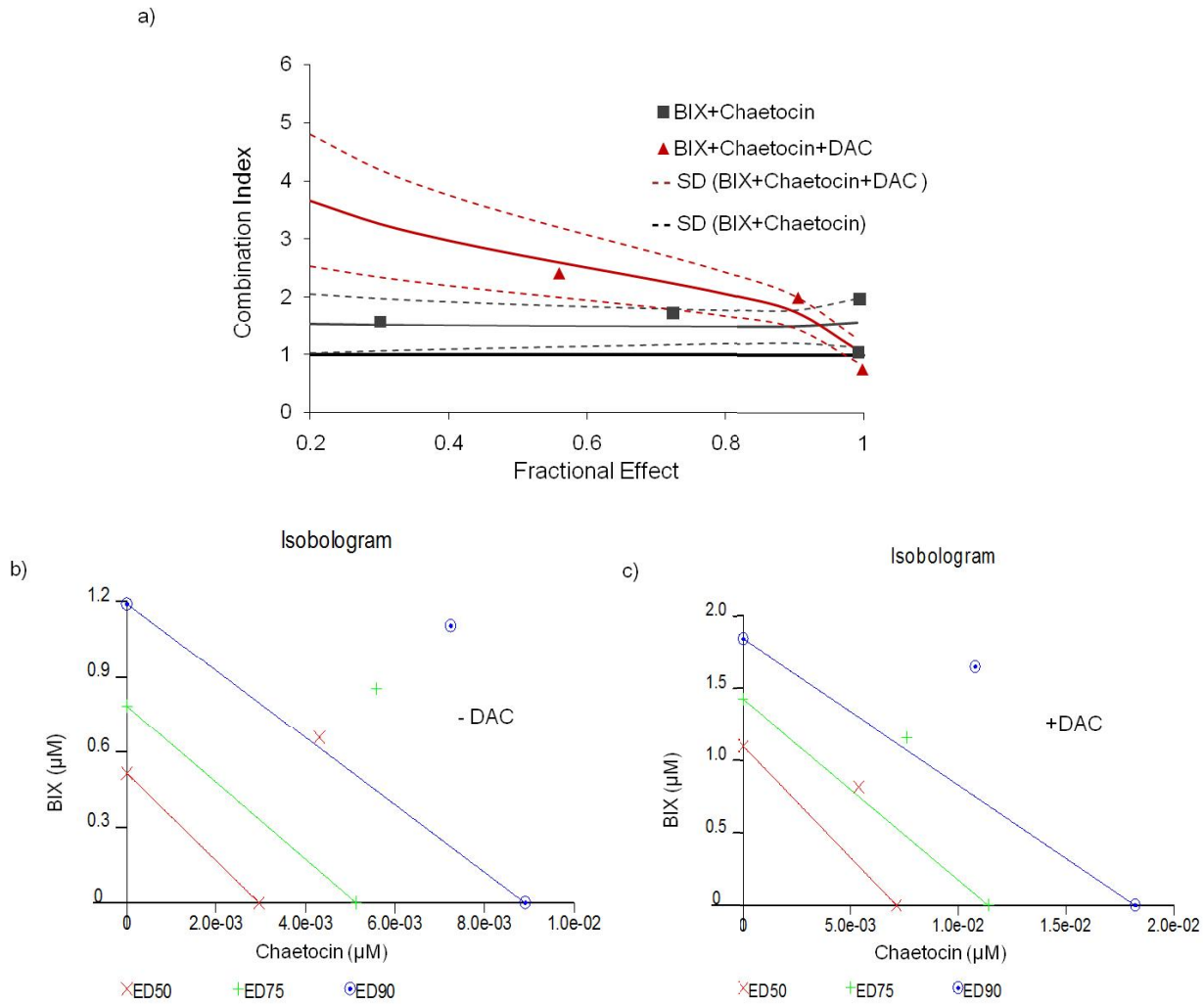

Figure 5.33. Drug combination effect of BIX and chaetocin in the AML-193 cell line. (a) CI plots of BIX and chaetocin in presence or absence of DAC. Isobolograms for different effect doses (ED50, ED75, and ED 90) of BIX and chaetocin in the absence or the presence of DAC are shown in figure (b) and (c), respectively. AML-193 cells were co-treated for 72 hours with BIX and chaetocin in presence and absence of 1 μM DAC. Effect of combinations were assessed by MTT assays and estimated using the CalcuSyn software after cells were incubated with co-treatment of BIX and chaetocin + and – DAC. In CI plots, the horizontal line has a value equal to 1 and represents the line of additivity. CI < 1 indicates synergy, CI= 1 additive effect, and CI >1 indicates antagonism. In isobolograms, the diagonal line is the line of additivity. Experimental data points, represented by symbols show the different effect levels. Symbols located below, on, or above the line indicate synergy, additive or antagonism, respectively.

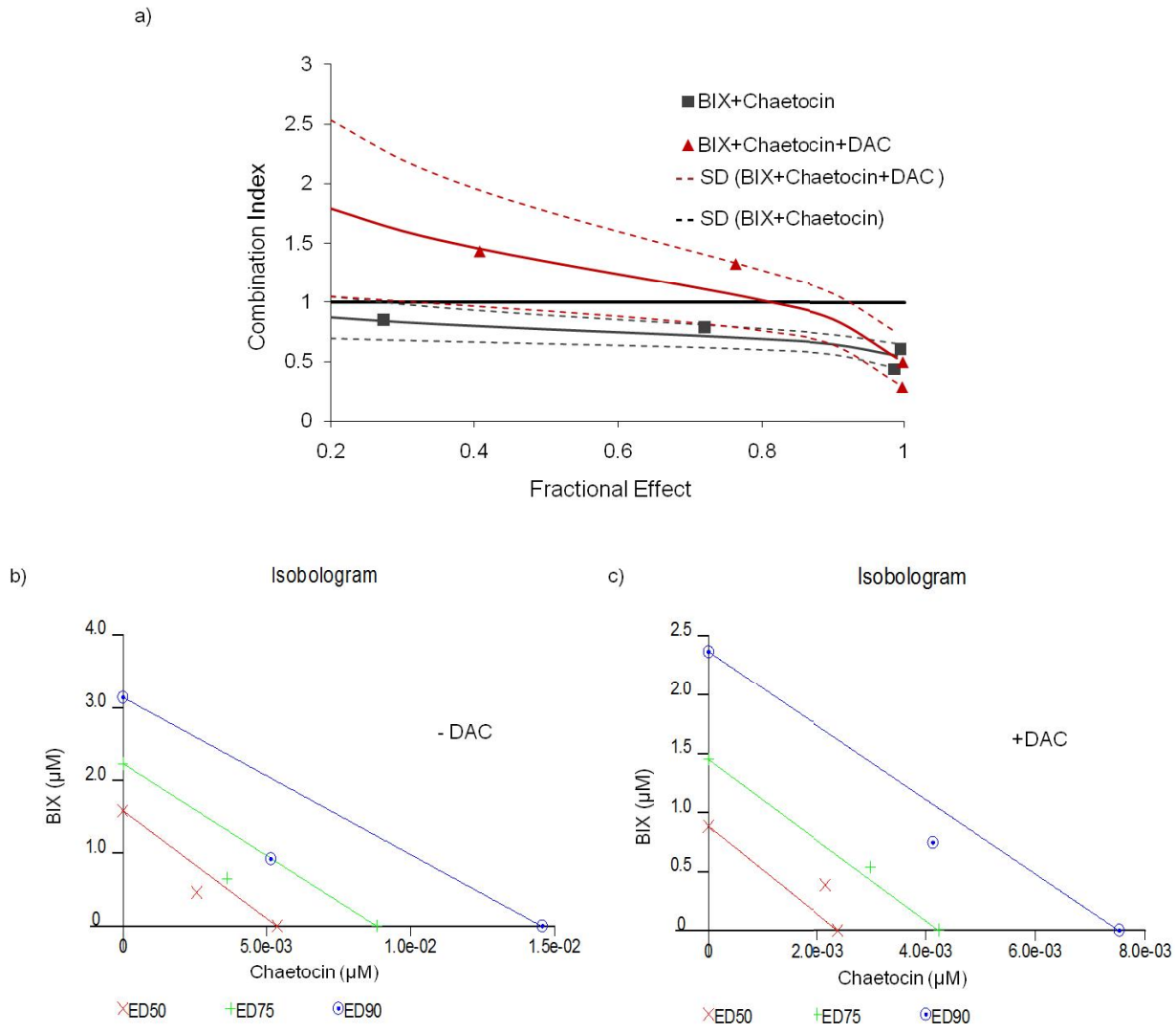

Figure 5.34. Drug combination effect of BIX and chaetocin in the KG-1a cell line. (a) CI plots of BIX and chaetocin in presence or absence of DAC. Isobolograms for different effect doses (ED50, ED75, and ED 90) of BIX and chaetocin in the absence or the presence of DAC are shown in figure (b) and (c), respectively. KG-1a cells were co-treated for 72 hours with BIX and chaetocin in presence and absence of 1 μM DAC. Effect of combinations were assessed by MTT assays and estimated using the CalcuSyn software after cells were incubated with co-treatment of BIX and chaetocin + and – DAC. In CI plots, the horizontal line has a value equal to 1 and represents the line of additivity. CI < 1 indicates synergy, CI= 1 additive effect, and CI >1 indicates antagonism. In isobolograms, the diagonal line is the line of additivity. Experimental data points, represented by symbols show the different effect levels. Symbols located below, on, or above the line indicate synergy, additive or antagonism, respectively.

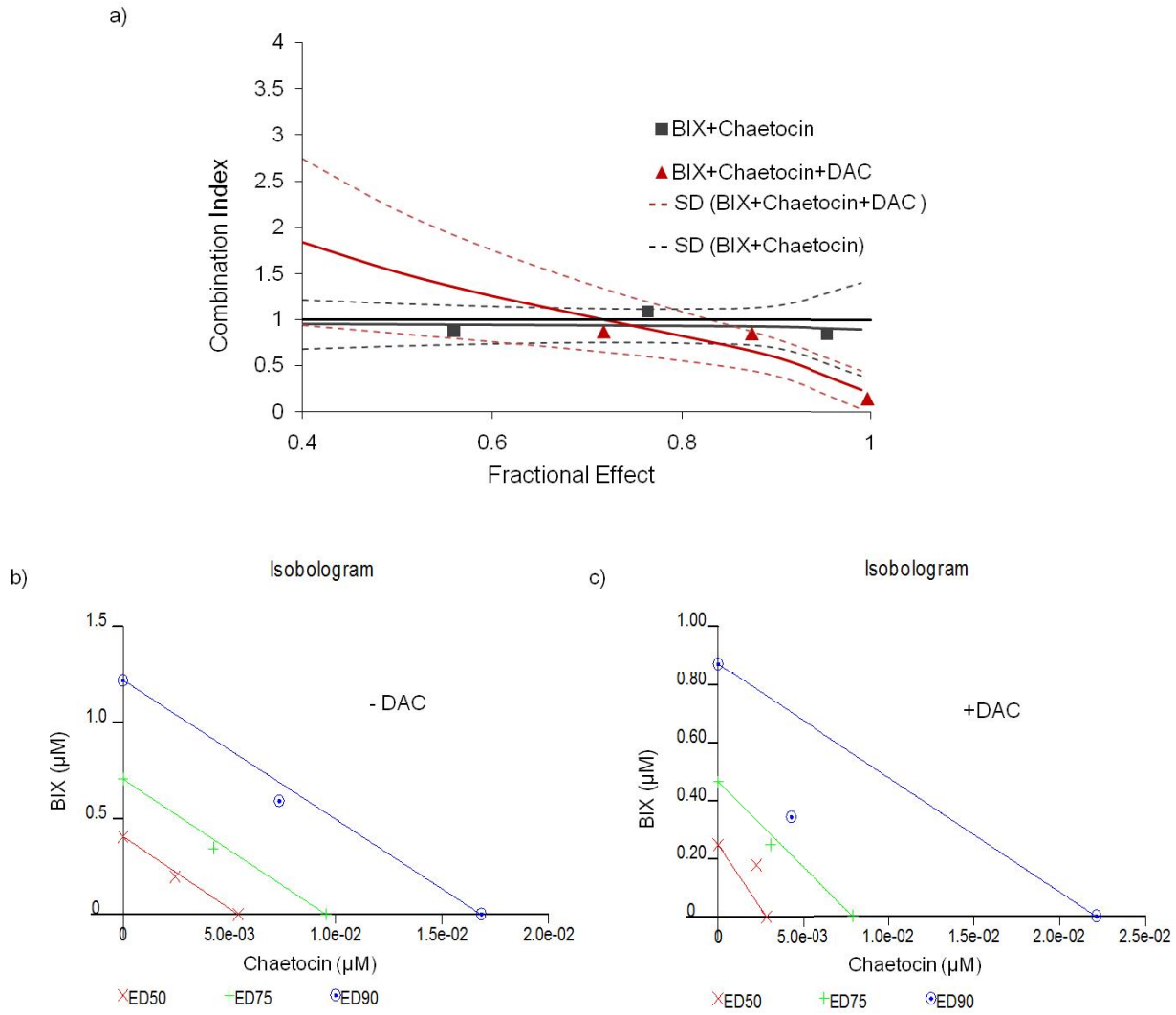

Figure 5.35. Drug combination effect of BIX and chaetocin in the Kasumi cell line. (a) CI plots of BIX and chaetocin in presence or absence of DAC. Isobolograms for different effect doses (ED50, ED75, and ED 90) of BIX and chaetocin in the absence or the presence of DAC are shown in figure (b) and (c), respectively. Kasumi cells were co-treated for 72 hours with BIX and chaetocin in presence and absence of 1 µM DAC. Effect of combinations were assessed by MTT assays and estimated using the CalcuSyn software after cells were incubated with co-treatment of BIX and chaetocin + and – DAC. In CI plots, the horizontal line has a value equal to 1 and represents the line of additivity. CI < 1 indicates synergy, CI= 1 additive effect, and CI >1 indicates antagonism. In isobolograms, the diagonal line is the line of additivity. Experimental data points, represented by symbols show the different effect levels. Symbols located below, on, or above the line indicate synergy, additive or antagonism, respectively.

5.7. Combinatorial treatments of DAC, BIX, and chaetocin influenced gene activation in AML cells

While silencing of p15, p21, and E-cadherin genes occurs in AML, little is known about the repressor components that effect epigenetic silencing of these genes. Previously, we found that p15 and E-cadherin gene promoters were hypermethylated in AML cell lines, while the p21 promoter was completely unmethylated. Moreover, it was found that treatment with DAC and chaetocin as single agents induced expression of the hypermethylated genes p15 and E-cadherin and also the non-hypermethylated p21 gene. To study the relationship between epigenetic events that lead to reactivation of epigenetically silenced genes, we established combinations of DAC, BIX, and chaetocin that lead to re-activation of p15, p21, and E-cadherin genes in the AML cell lines studied. For these assays, we chose concentrations of DAC, BIX, and chaetocin, where AML cell lines showed an enhancement of p15, p21, and E-cadherin expression. We used 1 μM DAC for experiments that involved p15 and p21 genes and 8 μM DAC for E-cadherin gene in AML-193. In KG-1a and Kasumi cell lines 4 μM DAC were used for all three genes. Four micromolar (4 μM) BIX and 100 nM chaetocin were used for p15, p21 and E-cadherin genes in all AML cell lines tested.

5.7.1. Chaetocin and DAC in combination reactivated expression of p15 and E-cadherin genes by reducing levels of promoter methylation and H3K9 tri-methylation

Co-treatment of AML cell lines with DAC and chaetocin induced re-expression of p15 and E-cadherin genes with a greater effect than treatment with DAC or chaetocin alone (Figure 5.36a and Figure 5.36b). Moreover, this enhanced p15 and E-cadherin expression in AML-193 and Kasumi cell lines was accompanied by promoter demethylation and a reduction of H3K9 tri-methylation levels as analyzed by DNA pyrosequencing and ChIP assays, respectively (Figure 5.36a, Figure 5.36b, Figure 5.37, Figure 5.38, Figure 5.39, Figure 5.40, Figure 5.41a and Figure 5.41b). No changes were observed in histone H3 levels, indicating that changes in H3K9 methylation were not due to nucleosome depletion (Figure 5.41c).

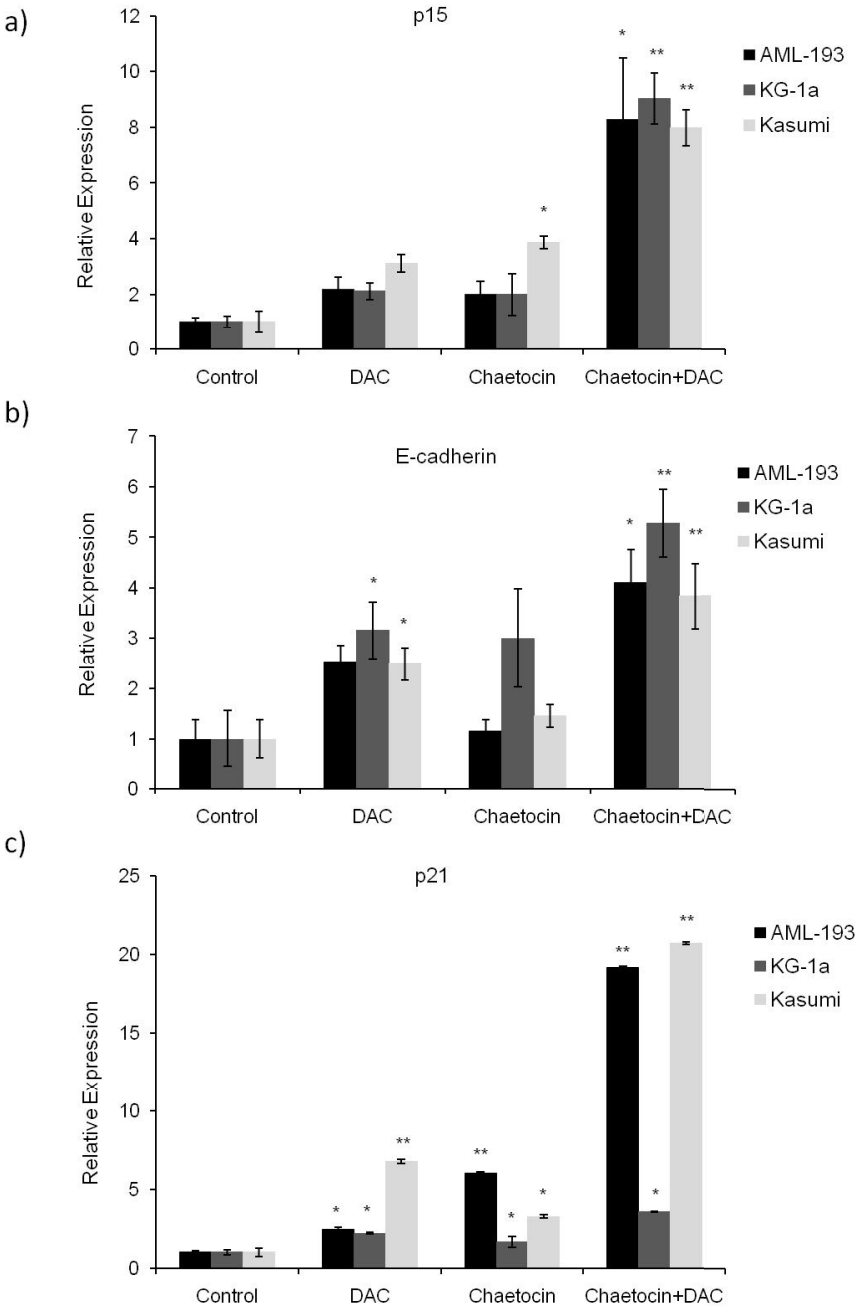

Figure 5.36. Real time PCR analysis of p15, p21, and E-cadherin expression upon treatment with chaetocin and DAC in combination in AML cell lines. AML-193, KG-1a, and Kasumi cell lines were treated with chaetocin (100 nM) and following concentrations of DAC: AML-193: p15 and p21 (1 µM), E-cadherin (8 µM); Kasumi: p15, E-cadherin, and p21 (4 µM). Histograms show the relative fold expression of p15 (a), E-cadherin (b), and p21 (c) gene expression in AML-193, KG-1a, and Kasumi cell lines. HPRT was used as endogenous control expression. Error bars represents standard deviation of three independent experiments and (*) represents P-value < 0.05 and (**) represent P-value <0.01 between treated and untreated cells. Control, represents the untreated cells.

a) Control
% Methylation: 95.1; SD: 8.0

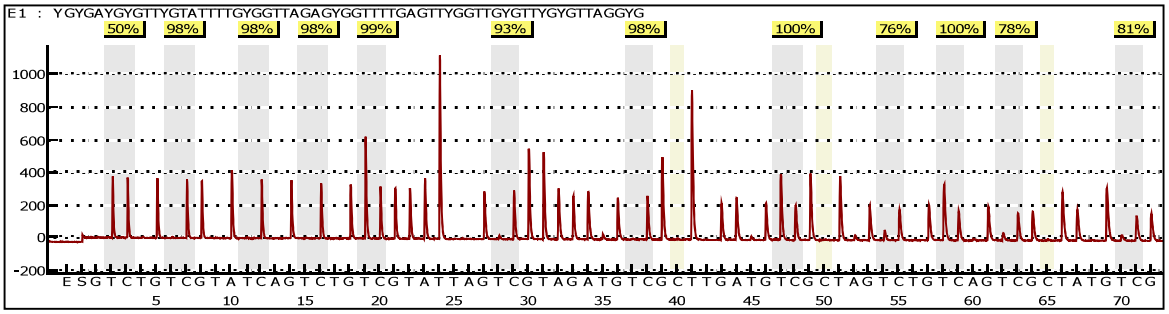

b) 1 µM DAC
% Methylation: 57.7%; SD: 6.2

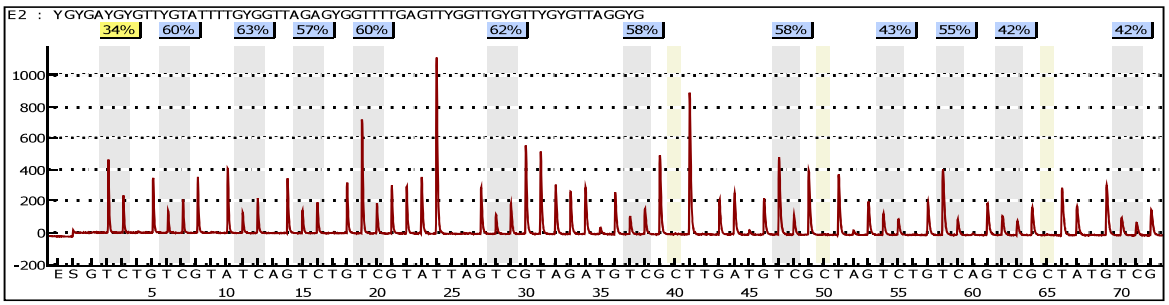

c) 100 nM Chaetocin + 1 µM DAC
% Methylation: 67; SD: 12

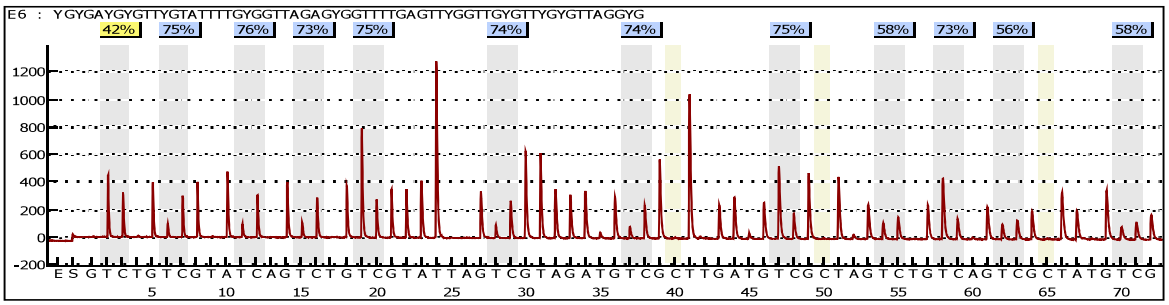

Figure 5.37. Effects of chaetocin and DAC combinatorial treatment on p15 promoter methylation in AML-193 cell line. AML-193 cells were co-treated for 72 hours with 100 nM chaetocin and 1 µM DAC. Percentage methylation is the mean methylation of CpGs in the p15 promoter. SD, represents the standard deviation of the percentage mean methylation. The sequence analyzed is shown above each pyrogram, where Y represents the location of the cytosine in the CpG. In the pyrogram, the Y-axis represents the signal intensity (arbitrary units), which is proportional to the number of nucleotides incorporated (as peaks heights) and the X-axis is the dispensation order. The gray bars indicate the CpG positions, where the degree of methylation is assessed from the ratio of the peaks heights of C and T. Blue and yellow colors represent the confidence of the sequence pattern matches: greater than 90 percent and between 70-89 percent, respectively.

a) Control
% Methylation: 95%; SD: 4.9

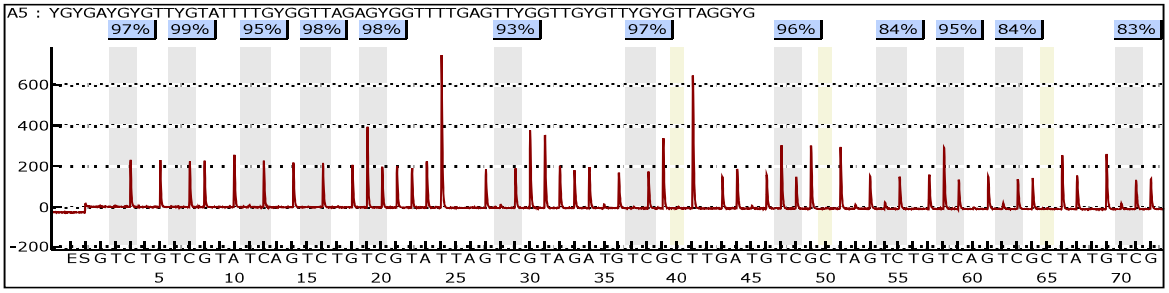

b) 4 µM DAC
% Methylation: 57.7%; SD: 6.2

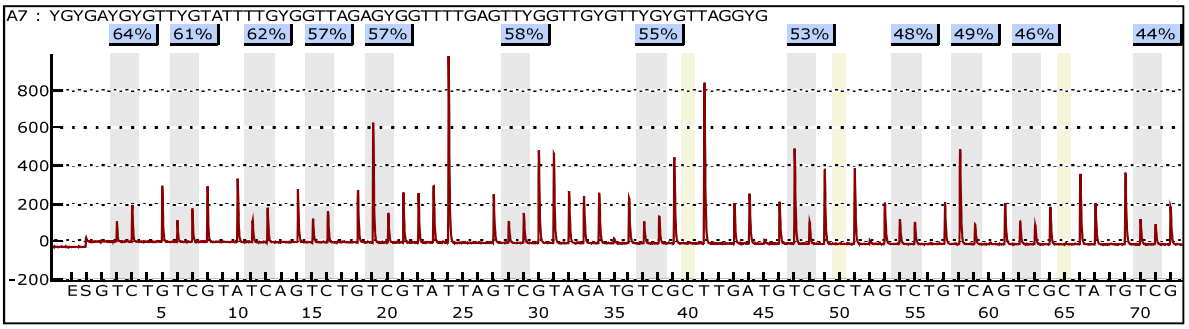

c) 100 nM chaetocin + 4 µM DAC
% Methylation: 68%; SD: 12.1

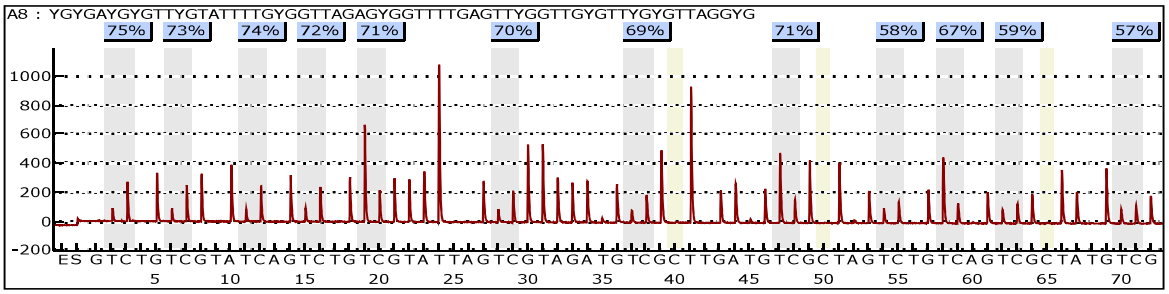

Figure 5.38. Effects of chaetocin and DAC in combinatorial treatment on p15 promoter methylation in Kasumi cell line. Kasumi cells were co-treated for 72 hours with 100 nM chaetocin and 1 µM DAC. Percentage methylation is the mean methylation of CpGs in the p15 promoter. SD, represents the standard deviation of the percentage mean methylation. The sequence analyzed is shown above each pyrogram, where Y represents the location of the cytosine in the CpG. In the pyrogram, the Y-axis represents the signal intensity (arbitrary units), which is proportional to the number of nucleotides incorporated (as peaks heights) and the X-axis is the dispensation order. The gray bars indicate the CpG positions, where the degree of methylation is assessed from the ratio of the peaks heights of C and T. Blue and yellow colors represent the confidence of the sequence pattern matches: greater than 90 percent and between 70-89 percent, respectively.

a) Control
% Methylation: 95.5; SD:4.7

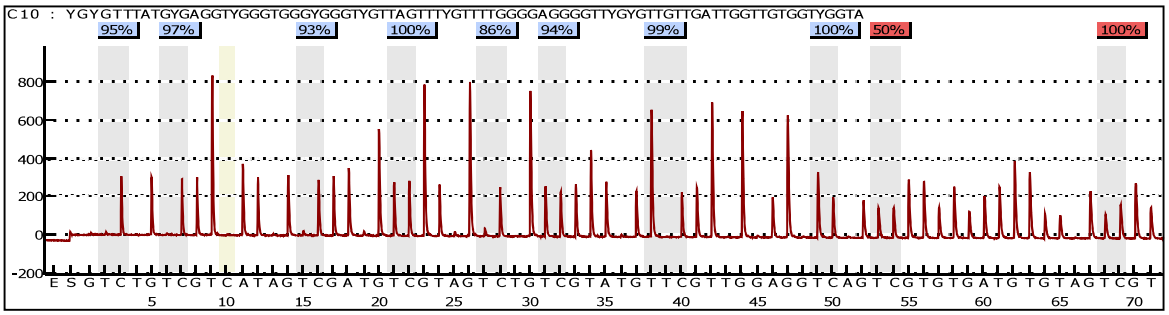

b) 8 µM DAC
% Methylation: 66.8; SD: 7.0

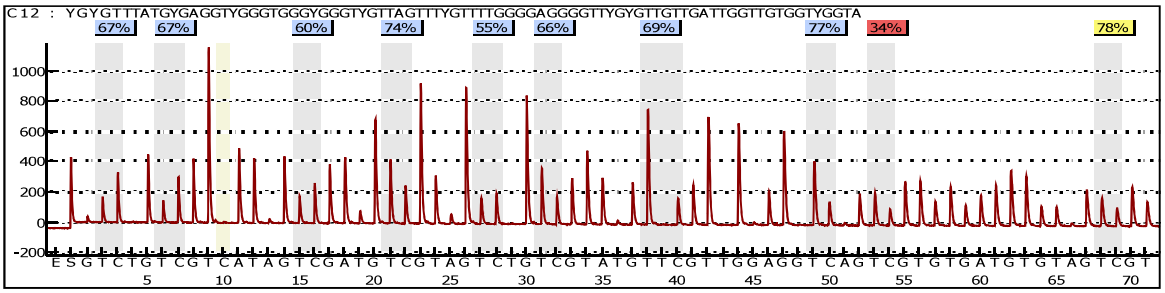

b) 100 nM chaetocin + 8 µM DAC
% Methylation: 88; SD: 4.2

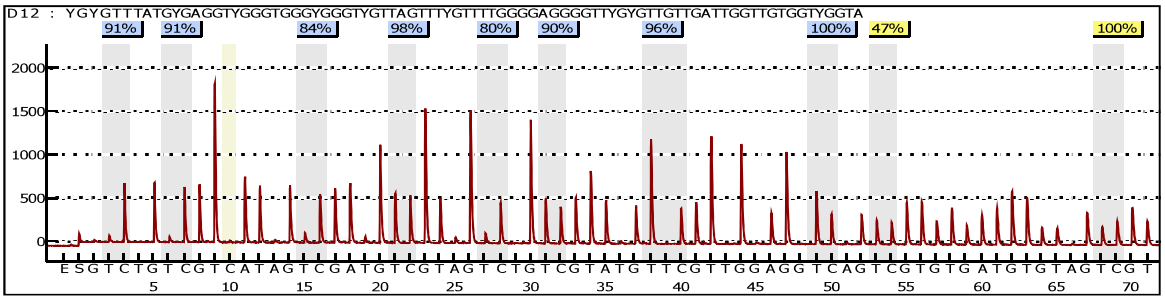

Figure 5.39. Effects of chaetocin and DAC in combinatorial treatment on E-cadherin promoter methylation in AML-193 cell line. AML-193 cells were co-treated for 72 hours with 100 nM chaetocin and 8 µM DAC. Percentage methylation is the mean methylation of CpGs in the E-cadherin promoter. SD, represents the standard deviation of the percentage mean methylation. The sequence analyzed is shown above each pyrogram, where Y represents the location of the cytosine in the CpG. In the pyrogram, the Y-axis represents the signal intensity (arbitrary units), which is proportional to the number of nucleotides incorporated (as peaks heights) and the X-axis is the dispensation order. The gray bars indicate the CpG positions, where the degree of methylation is assessed from the ratio of the peaks heights of C and T. Blue, yellow and red colors represent the confidence of the sequence pattern matches: greater than 90 percent, 70-89 percent and less than 70 percent, respectively.

a) Control
% Methylation: 90.1; SD: 9.0

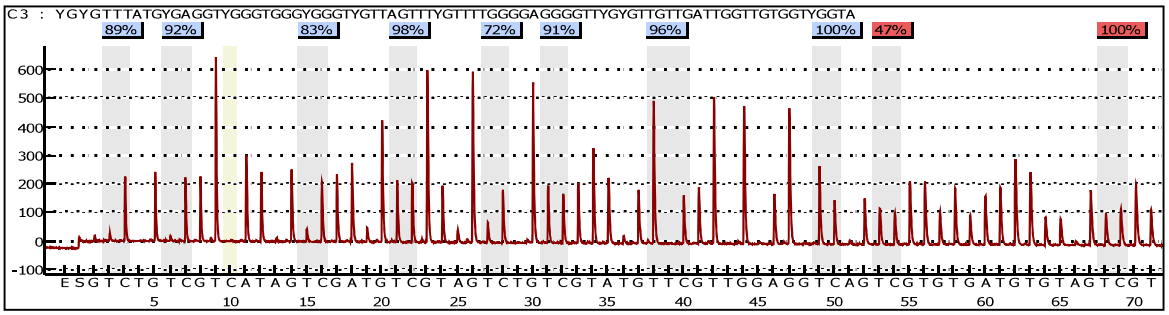

b) 4 µM DAC
% Methylation: 55.8; SD: 9.2

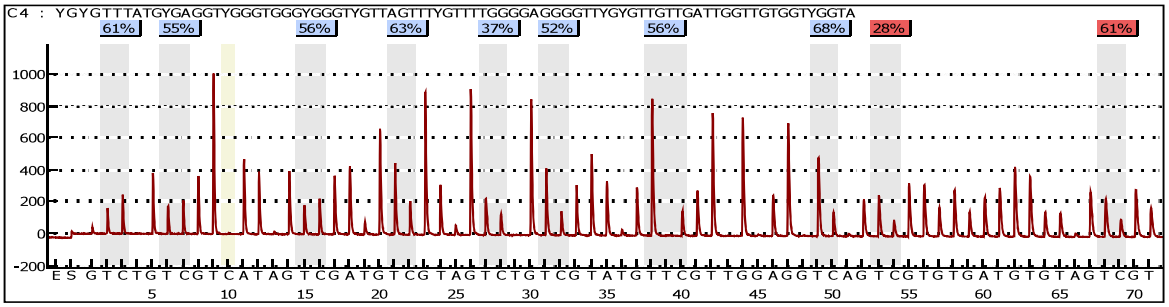

c) 100 nM chaetocin + 4 µM DAC
% Methylation: 59; SD: 5.3

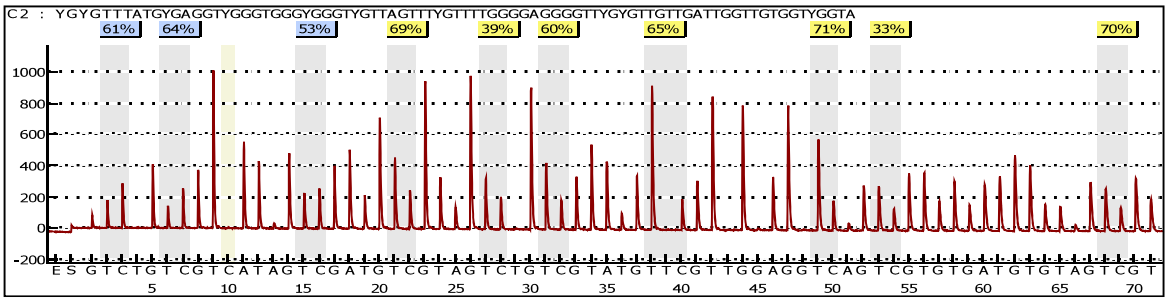

Figure 5.40. Effect of chaetocin and DAC combinatorial treatment on E-cadherin promoter methylation in Kasumi cell line. Kasumi cells were co-treated for 72 hours with 100 nM chaetocin and 4 µM DAC. Percentage methylation is the mean methylation of CpGs in the E-cadherin promoter. SD, represents the standard deviation of the percentage mean methylation. The sequence analyzed is shown above each pyrogram, where Y represents the location of the cytosine in the CpG. In the pyrogram, the Y-axis represents the signal intensity (arbitrary units), which is proportional to the number of nucleotides incorporated (as peaks heights) and the X-axis is the dispensation order. The gray bars indicate the CpG positions, where the degree of methylation is assessed from the ratio of the peaks heights of C and T. Blue, yellow and red colors represent the confidence of the sequence pattern matches: greater than 90 percent, 70-89 percent and less than 70 percent, respectively.

5.7.2. Chaetocin and DAC in combination reactivated expression of p21 gene by causing changes on H3K9 di-methylation

p21 gene was not silenced by promoter hypermethylation in AML cell lines; however treatment of DAC led to re-expression of p21 and caused changes in H3K9 promoter methylation levels. To determine whether the combination of chaetocin and DAC potentiates re-expression of p21 gene by causing changes in H3K9 methylation levels, we used real time PCR to measure the expression level of p21 and ChIP assays to determine changes in promoter H3K9 methylation in the AML cell lines studied. Co-treatment of AML-193, KG-1a, and Kasumi cell lines with DAC and chaetocin caused a higher level of p21 expression than observed with treatments with either DAC or chaetocin alone (Figure 5.36c). In contrast to the results observed with DAC and chaetocin treatments alone, the combination of DAC and chaetocin significantly reduced H3K9 di-methylation levels at p21 promoter as analyzed by ChIP assays (Figure 5.41c). However, this treatment did not reduce trimethyl H3K9 levels as was observed with chaetocin treatment alone. In contrast, H3K9 tri-methylation at p21 promoter was increased in AML-193 and Kasumi cell lines in response to DAC and chaetocin co-treatment (Figure 5.41c).

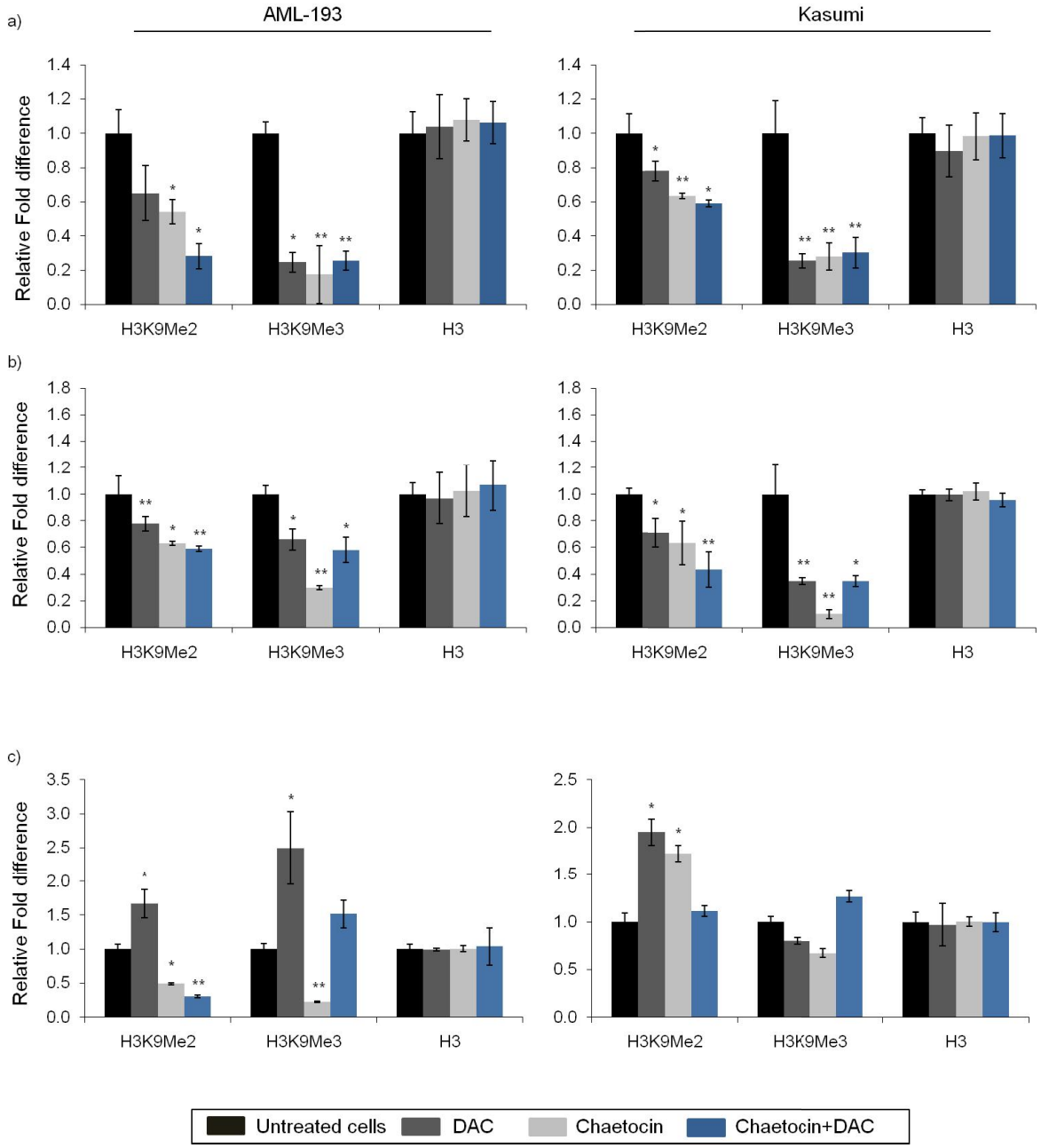

Figure 5.41. Chromatin immunoprecipitation analysis of the effect of DAC and chaetocin in combination on H3K9 di- and tri-methylation and H3 associated with the p15, E-cadherin and p21 promoter in AML cell lines. AML-193 and Kasumi cells were treated for 72 hours with chaetocin (100 nM) and DAC as followed: AML-193: p15 and p21 (1 µM), E-cadherin (8 µM); Kasumi: p15, E-cadherin and p21 (4 µM). Cross-linked protein/DNA was immunoprecipitated with dimethyl-H3K9 (H3K9Me2) antibody or trimethyl-H3K9 (H3K9Me3) antibody or of H3 (H3). Histograms show the relative fold expression of PCR products (immunoprecipitated DNA) of p15 (a), E-cadherin (b), and p21 (c) genes quantified using real time PCR. Error bars represent standard deviation. ** Represents P-values < 0.05 and (**) represent P-value < 0.01 between treated and untreated cells. Control, represents the untreated cells.

5.7.3. Co-treatment of BIX and DAC caused differential expression of p15, p21 and E-cadherin genes in AML cell lines

We showed that DAC potentiated the effect of BIX on AML cells proliferation, induced p15, p21 and E-cadherin expression, and caused changes in promoter DNA methylation and histone H3K9 methylation in AML cell lines. To study the relationship between DNA methylation and histone H3K9 di-methylation at the p15, p21, and E-cadherin promoters, we measured the effect of combinations of DAC and BIX on gene expression, DNA methylation, and H3K9 methylation in AML cell lines. Co-treatment of AML-193, KG-1a, and Kasumi cells with BIX and DAC was able to induce p21 expression (Figure 5.42c). However, significant expression in p15 and E-cadherin genes were only evident in KG-1a and Kasumi cells, but not in AML-193 cells where this treatment did not cause p15 and E-cadherin re-expression (Figure 5.42a and Figure 5.42b). Treatment with BIX and DAC in combination induced p15, p21, and E-cadherin expression to a greater extent than that of each drug alone. Surprisingly, this treatment had little effect on reversing p15 and E-cadherin promoter methylation than treatment with DAC alone (Figure 5.43, Figure 5.44, Figure 5.45 and Figure 5.46).

We also observed significant changes in H3K9 di- and tri-methylation levels at p15 and E-cadherin promoters following BIX and DAC co-treatment as analyzed by ChIP assays (Figure 5.47a and Figure 5.47b). However, we only observed that at p21 promoter, combination of BIX and DAC preferentially caused reduction of H3K9 di-methylation in Kasumi cells, but not as much as that caused by treatment of BIX alone (Figure 5.47c). We did not observed changes in histone H3 levels in any of the analyzed genes, indicating that changes in H3K9 methylation were not due to nucleosome depletion (Figure 5.47).

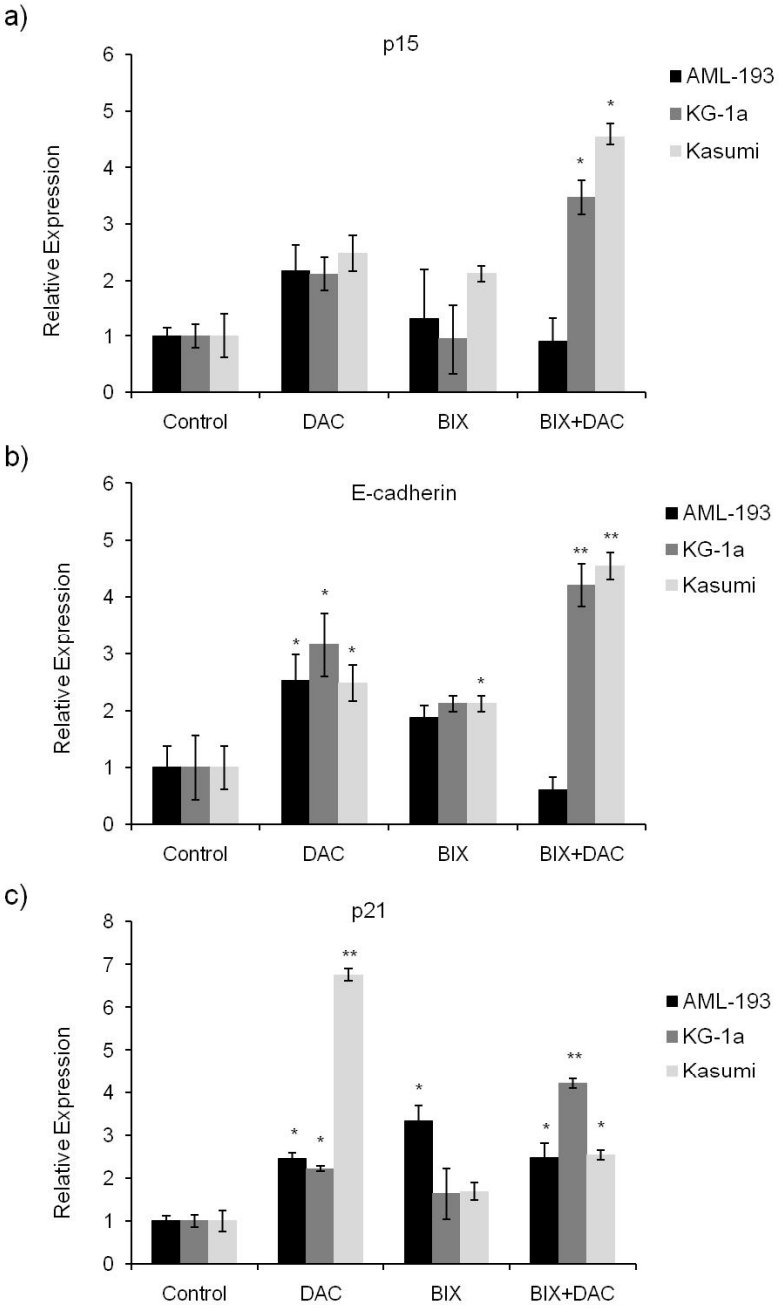

Figure 5.42. Real time PCR analysis of p15, p21 and E-cadherin expression upon treatment with BIX and DAC in combination in AML cell lines. AML-193, KG-1a, and Kasumi cell lines were treated with BIX (4 μM) and following concentrations of DAC: AMl-193: p15 and p21 (1 μM), E-cadherin (8 μM); Kasumi: p15, E-cadherin and p21 (4 μM). Histograms show the relative fold expression of p15 (a), E-cadherin (b) and p21(c) gene expression in AML-193, KG-1a and Kasumi cell lines. HPRT was used as endogenous control expression. Error bars represents standard deviation of three independent experiments and (*) represents P-value < 0.05 and (**) represent P-value <0.01 between treated and untreated cells. Control, represents the untreated cells.

a) Control
% Methylation: 95.1; SD: 8.0

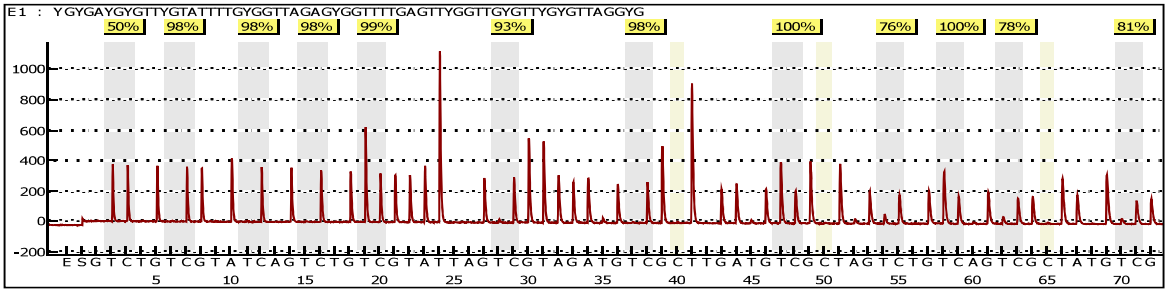

b) 1 µM DAC
% Methylation: 57.7%; SD: 6.2

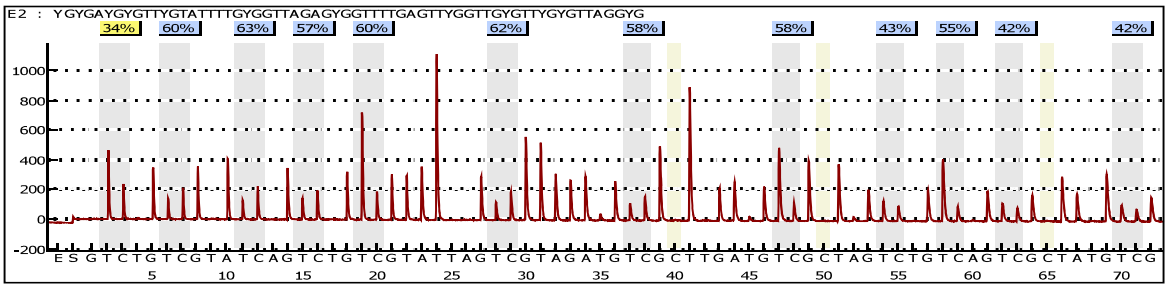

c) 4 µM BIX + 1 µM DAC
% Methylation: 67; SD: 12

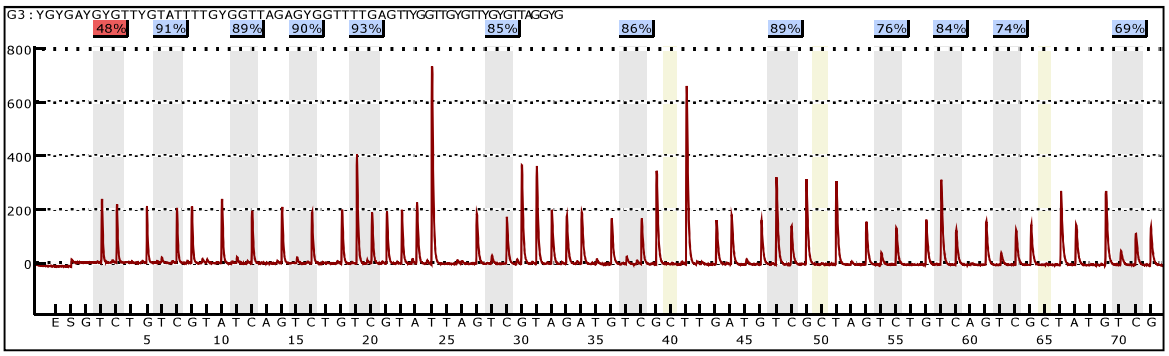

Figure 5.43. Effects of BIX and DAC combinatorial treatment on p15 promoter methylation in AML-193 cell line. AML-193 cells were co-treated for 72 hours with 4 µM BIX and 1 µM DAC. Percentage methylation is the mean methylation of CpGs in the E-cadherin promoter. SD, represents the standard deviation of the percentage mean methylation. The sequence analyzed is shown above each pyrogram, where Y represents the location of the cytosine in the CpG. In the pyrogram, the Y-axis represents the signal intensity (arbitrary units), which is proportional to the number of nucleotides incorporated (as peaks heights) and the X-axis is the dispensation order. The gray bars indicate the CpG positions, where the degree of methylation is assessed from the ratio of the peaks heights of C and T. Blue, yellow and red colors represent the confidence of the sequence pattern matches: greater than 90 percent, 70-89 percent and less than 70 percent, respectively.

a) Control
% Methylation: 95%; SD: 4.9

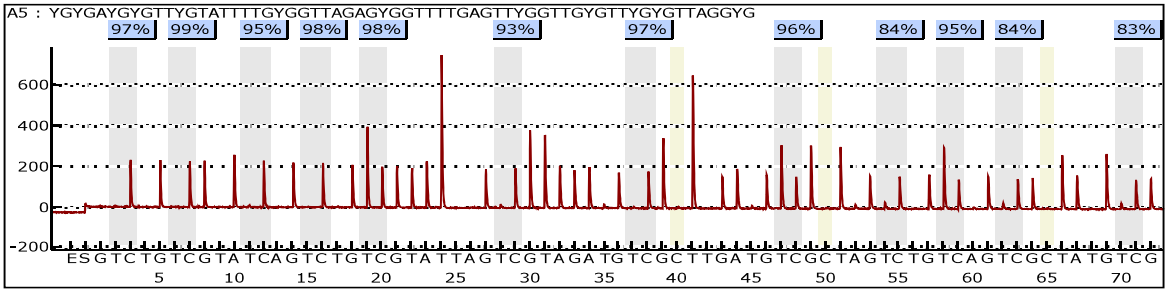

b) 4 µM DAC
% Methylation: 57.7%; SD: 6.2

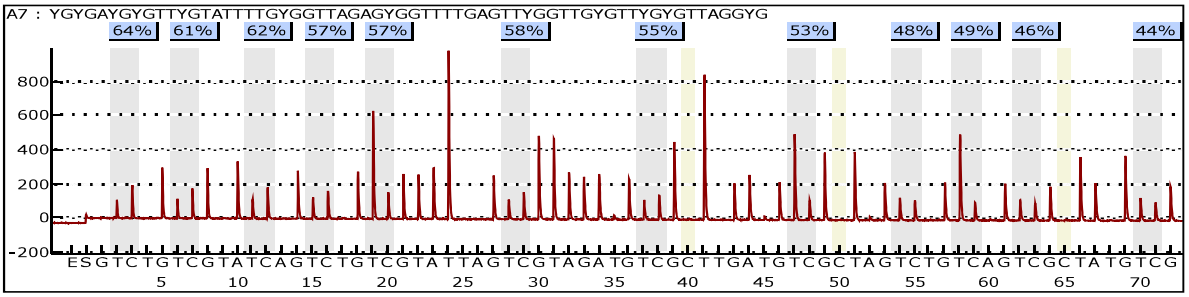

c) 4 µM BIX + 4 µM DAC
% Methylation: 63%; SD: 11.7

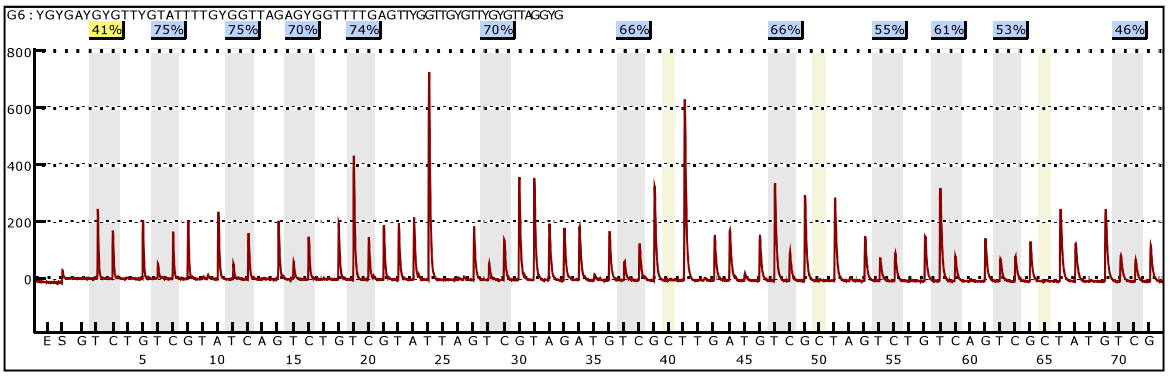

Figure 5.44. Effect of BIX and DAC combinatorial treatment on p15 promoter methylation in Kasumi cell line. Kasumi cells were co-treated for 72 hours with 4 µM BIX and 4 µM DAC. Percentage methylation is the mean methylation of CpGs in the E-cadherin promoter. SD, represents the standard deviation of the percentage mean methylation. The sequence analyzed is shown above each pyrogram, where Y represents the location of the cytosine in the CpG. In the pyrogram, the Y-axis represents the signal intensity (arbitrary units), which is proportional to the number of nucleotides incorporated (as peaks heights) and the X-axis is the dispensation order. The gray bars indicate the CpG positions, where the degree of methylation is assessed from the ratio of the peaks heights of C and T. Blue color represents that the sequence pattern matches with a confidence greater than 90 percent.

a) Control
% Methylation: 95.5; SD:4.7

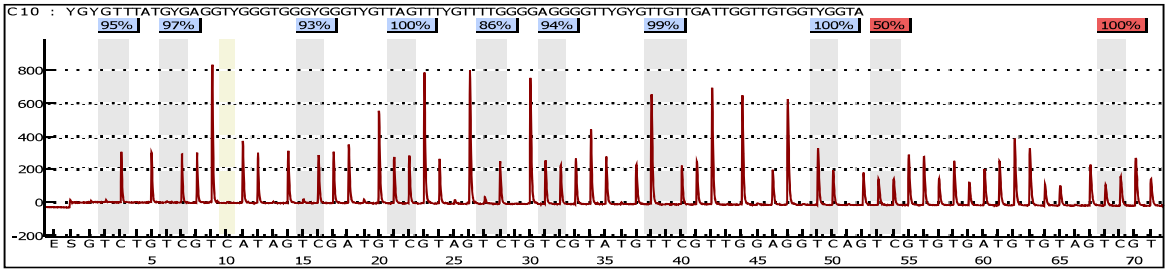

b) 8 µM DAC
% Methylation: 66.8; SD: 7.0

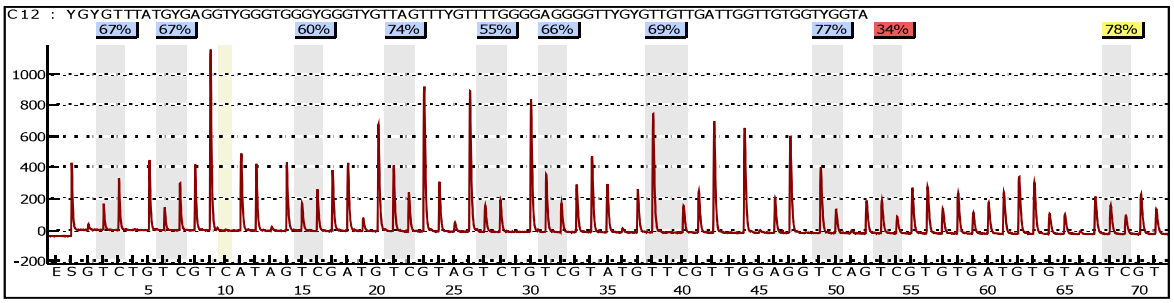

b) 4 µM BIX + 8 µM DAC
% Methylation: 84%; SD: 5.1

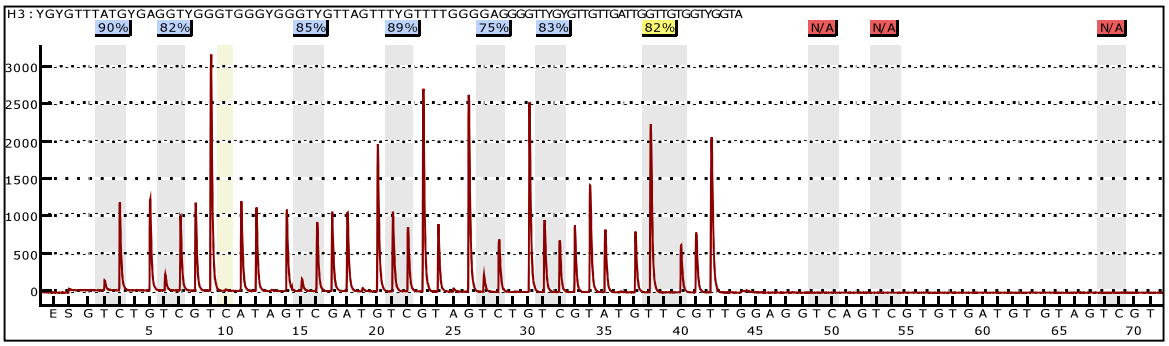

Figure 5.45. Effect of BIX and DAC combinatorial treatment on E-cadherin promoter methylation in AML-193 cell line. AML-193 cells were co-treated for 72 hours with 4 µM BIX and 8 µM DAC. Percentage methylation is the mean methylation of CpGs in the E-cadherin promoter. SD, represents the standard deviation of the percentage mean methylation. The sequence analyzed is shown above each pyrogram, where Y represents the location of the cytosine in the CpG. In the pyrogram, the Y-axis represents the signal intensity (arbitrary units), which is proportional to the number of nucleotides incorporated (as peaks heights) and the X-axis is the dispensation order. The gray bars indicate the CpG positions, where the degree of methylation is assessed from the ratio of the peaks heights of C and T. Blue, yellow and red colors represent the confidence of the sequence pattern matches: greater than 90 percent, 70-89 percent and less than 70 percent, respectively.

a) Control
% Methylation: 90.1; SD: 9.0

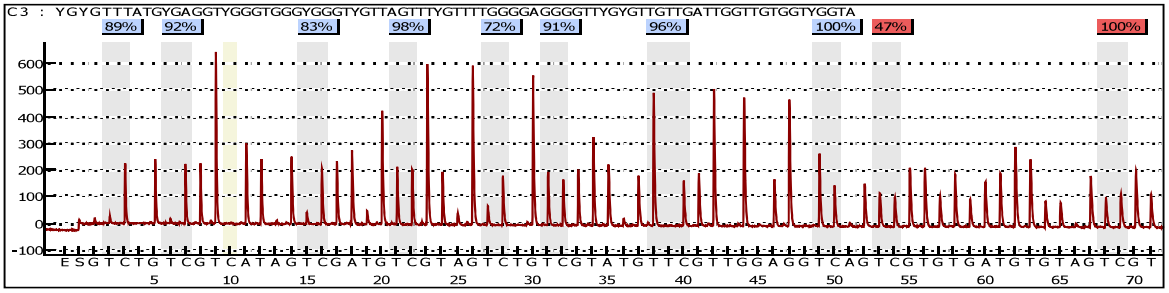

b) 4 µM DAC
% Methylation: 55.8; SD: 9.2

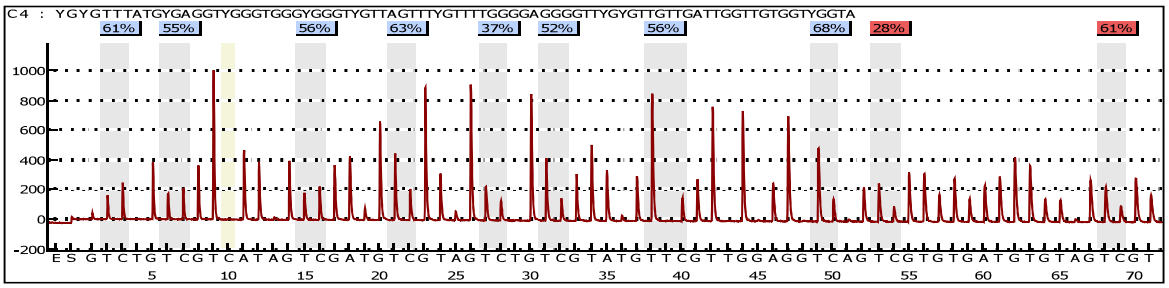

b) 4 µM BIX + 4 µM DAC
% Methylation: 80; SD: 4.8

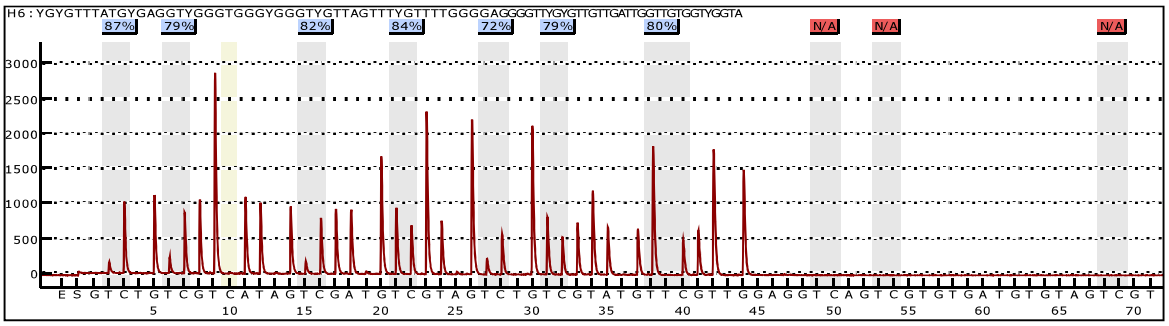

Figure 5.46. Effect of BIX and DAC combinatorial treatment on E-cadherin promoter methylation in Kasumi cell line. Kasumi cells were co-treated for 72 hours with 4 µM BIX and 4 µM DAC. Percentage methylation is the mean methylation of CpGs in the E-cadherin promoter. SD, represents the standard deviation of the percentage mean methylation. The sequence analyzed is shown above each pyrogram, where Y represents the location of the cytosine in the CpG. In the pyrogram, the Y-axis represents the signal intensity (arbitrary units), which is proportional to the number of nucleotides incorporated (as peaks heights) and the X-axis is the dispensation order. The gray bars indicate the CpG positions, where the degree of methylation is assessed from the ratio of the peaks heights of C and T. Blue and red colors represent the confidence of the sequence pattern matches: greater than 90 percent and less than 70 percent, respectively.

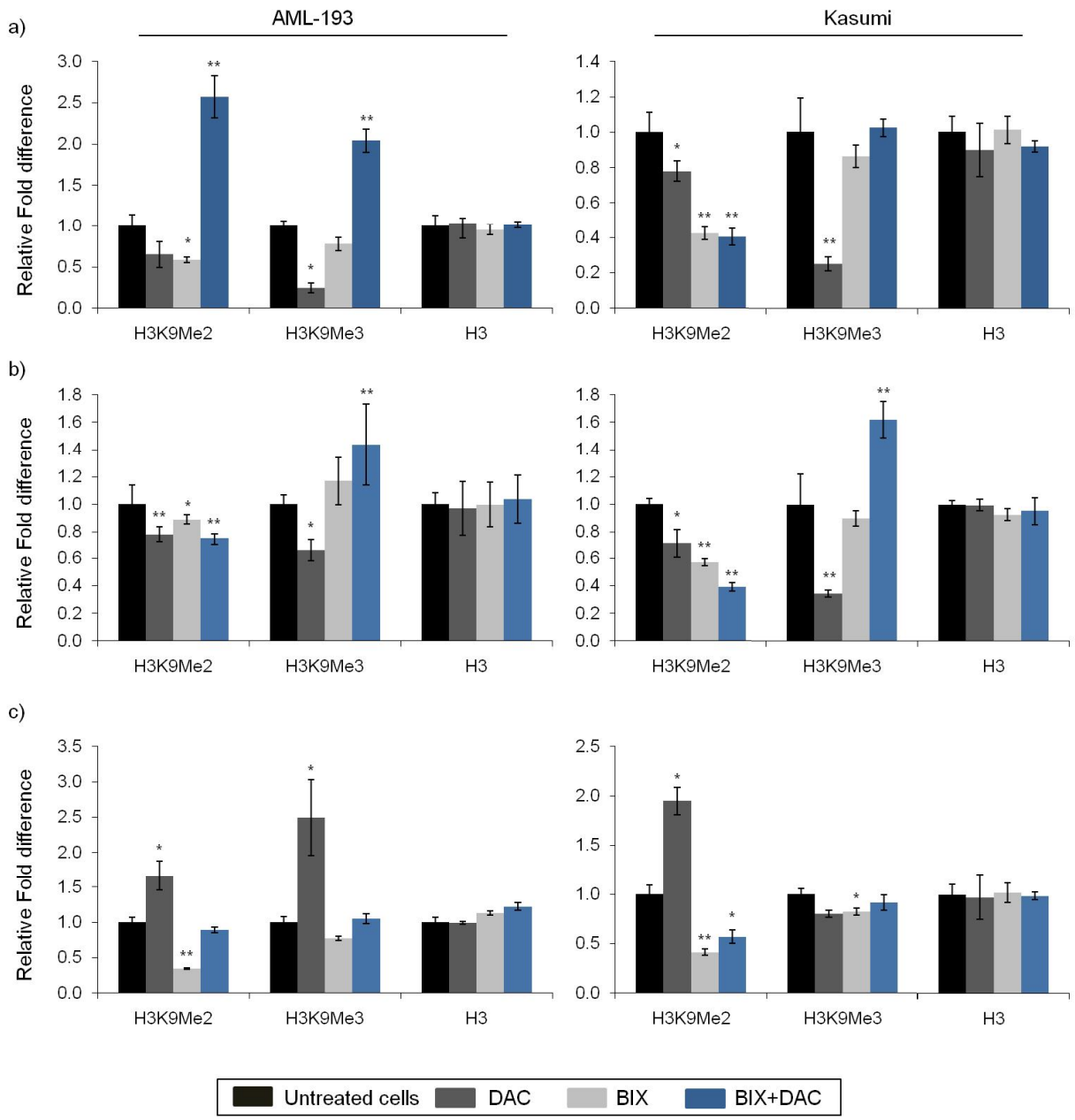

Figure 5.47. Chromatin immunoprecipitation analysis of the effect of DAC and BIX in combination on H3K9 di- and tri-methylation and H3 associated with the p15, E-cadherin, and p21 promoters in AML cell lines. AML-193 and Kasumi cells were treated for 72 hours with BIX (4 µM) and DAC as followed: AML-193: p15 and p21 (1 µM), E-cadherin (8 µM); Kasumi: p15, E-cadherin and p21 (4 µM). Cross-linked protein/DNA was immunoprecipitated with dimethyl-H3K9 (H3K9Me2) antibody or trimethyl-H3K9 (H3K9Me3) antibody or of H3 (H3). Histograms show the relative fold expression of PCR products (immunoprecipitated DNA) of p15 (a), E-cadherin (b), and p21 (c) genes quantified using real time PCR. Error bars represent standard deviation of three independent experiments. ** Represents P-values < 0.05 and (**) represent P-value <0.01 between treated and untreated cells. Control, represents the untreated cells.

5.7.4. The combination of BIX and chaetocin induced differential p15 and E-cadherin expression and increased H3K9 tri-methylation levels

To evaluate whether coordinated changes in promoter H3K9 di- and tri-methylation influence re-expression of silenced tumor suppressor genes in AML, we measured the effect of the combination of BIX and chaetocin on p15 and E-cadherin gene expression and promoter H3K9 methylation using real time PCR and ChIP assays, respectively. Combinatorial treatment of BIX and chaetocin in KG-1a and Kasumi cells enhanced p15 and E-cadherin expression similar to those levels observed with combinations of DAC with BIX and DAC with chaetocin, and to a greater extent than p15 and E-cadherin expression caused by single drug treatments (Figure 5.48a and Figure 5.48b). These results suggested that p15 and E-cadherin genes in Kasumi and KG-1a cells required changes on DNA methylation and H3K9 di- and tri-methylation in order to be re-activated in AML cell lines. In contrast, we found that co-treatment of AML-193 cells with BIX and chaetocin did not induce p15 and E-cadherin expression (Figure 5.48a and Figure 5.48b). These correlated with results observed in drug combination studies, where co-treatment of BIX and chaetocin displayed an antagonistic activity in AML-193 cell proliferation indicating that combination of these epigenetic inhibitors results in a negative interaction that interfere with drug activity.

In order to determine whether p15 and E-cadherin re-expression can be achieved by combining changes on H3K9 di- and tri-methylation, ChIP assays were performed. Co-treatment of Kasumi cells with BIX and chaetocin did not reduce H3K9 methylation levels at p15 and E-cadherin promoters (Figure 5.49a and Figure 5.49b). Surprisingly, we observed that treatment of AML-193 with combination of BIX and chaetocin significantly increased trimethyl-H3K9 levels at p15 and E-cadherin promoters (Figure 5.49a and Figure 5.49b); which supports our previous results that showed that this combination did not cause re-expression of p15 and E-cadherin genes (Figure 5.49a and Figure 5.49b).

5.7.5. BIX and chaetocin in combination induced expression of p21 gene and increased promoter H3K9 di- and tri-methylation

We measured the effect of combining BIX and chaetocin in the re-activation of p21 gene in AML cell lines. p21 expression following co-treatment with BIX and chaetocin was significantly induced to levels greater than that observed with either drug alone (Figure 5.31c).

Using ChIP assays, we showed that co-treatment of AML cell lines with BIX and chaetocin did not reduce H3K9 di- and tri-methyl levels at p21 promoter, but instead levels of di- and tri-methyl H3K9 significantly increased (Figure 5.49c). These results suggested that H3K9 methylation itself might be a positive regulatory event in the expression of p21 gene or changes in H3K9 methylation leads to interaction with other epigenetic events for regulation of p21 gene. No changes were observed in histone H3 levels in any of the analyzed genes, indicating that changes in H3K9 methylation were not due to nucleosome depletion (Figure 5.49).

In summary, a decrease in DNA methylation and H3K9 tri-methylation seems to be the major epigenetic events by which hypermethylated genes, such as p15 and E-cadherin can be re-expressed in AML cell lines. In contrast, for p21 gene, which contains a non-hypermethylated promoter, regulation of H3K9 di- and tri-methylation levels appears to be a main event for its activation.

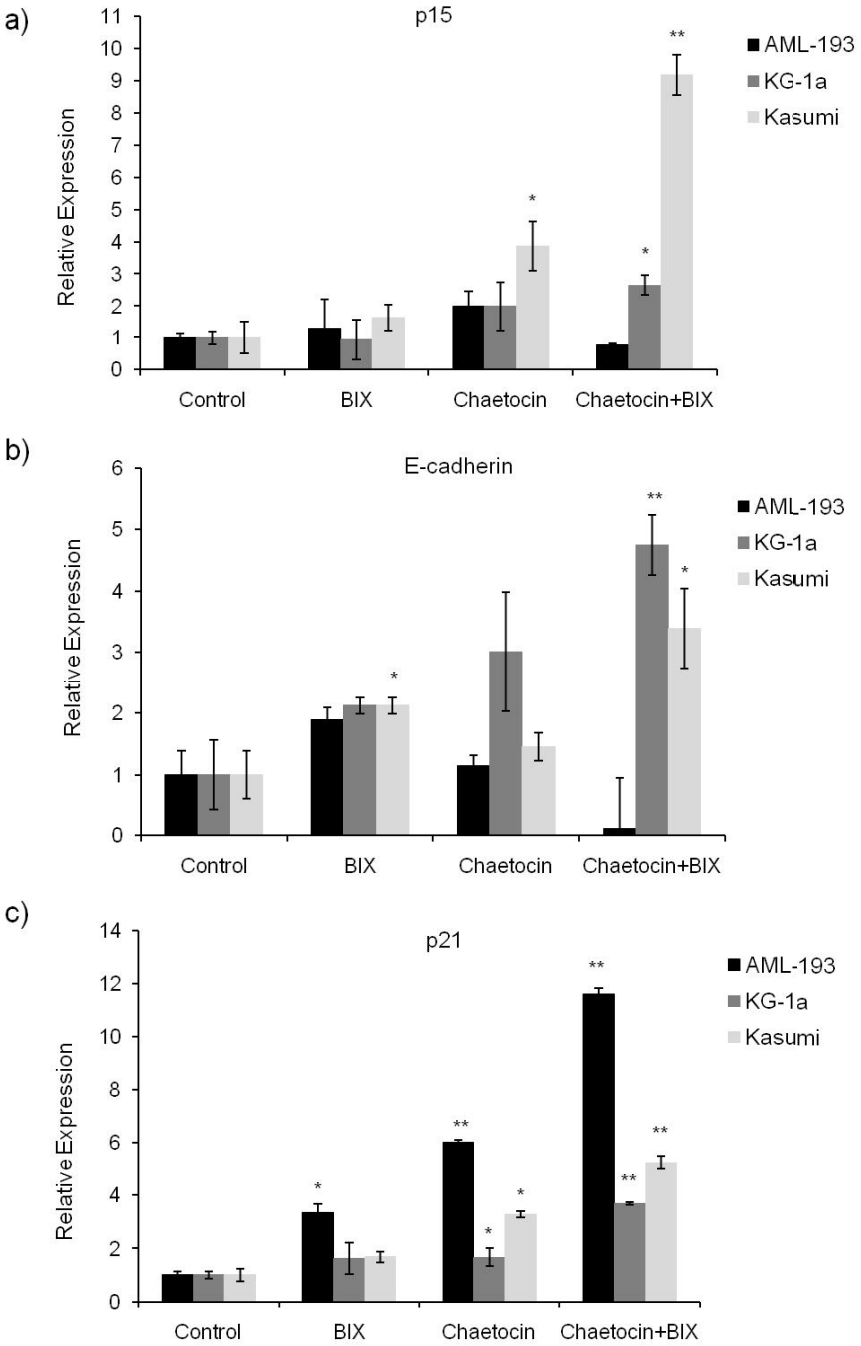

Figure 5.48. Real time PCR analysis of p15, p21, and E-cadherin expression upon treatment with chaetocin and BIX in combination in AML cell lines. AML-193, KG-1a and Kasumi cell lines were co-treated with chaetocin (100 nM) and BIX (4 μM) for 72 hours. Histograms show the relative fold expression of P15 (a), E-cadherin (b), and p21(c) gene expression in AML-193, KG-1a, and Kasumi cell lines. HPRT was used as endogenous control expression. Error bars represents standard deviation of three independent experiments and (*) represents P-value < 0.05 and (**) represent P-value <0.01 between treated and untreated cells. Control, represents the untreated cells.

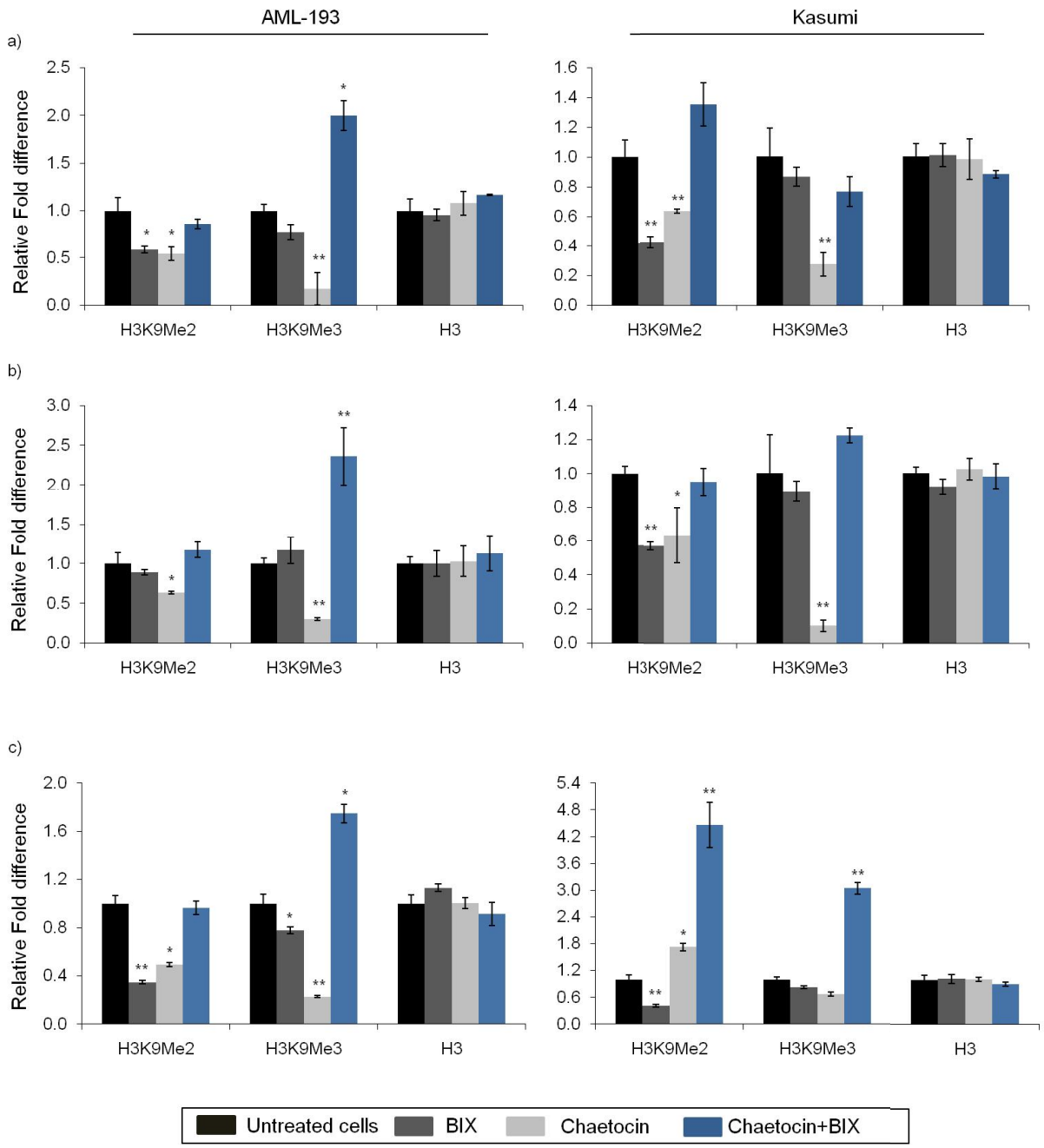

Figure 5.49. Chromatin immunoprecipitation analysis of the effect of chaetocin and BIX in combination on H3K9 di- and tri-methylation and H3 associated with the p15, E-cadherin and p21 promoter in AML cell lines. AML-193 and Kasumi cells were co-treated with BIX (4 µM) and chaetocin (100 nM) for 72 hours. Cross-linked protein/DNA was immunoprecipitated with dimethyl-H3K9 (H3K9Me2) antibody or trimethyl-H3K9 (H3K9Me3) antibody or of H3 (H3). Histograms show the relative fold expression of PCR products (immunoprecipitated DNA) of p15 (a), E-cadherin (b), and p21 (c) genes quantified using real time PCR. Error bars represent standard deviation of three independent experiments. ** Represents P-values < 0.05 and (**) represent P-value <0.01 between treated and untreated cells. Control, represents the untreated cells.

6. DISCUSSION

Epigenetic silencing of tumor suppressor genes involved in cell cycle control and suppression of metastasis, such as p15, p21, and E-cadherin, are associated with AML development (Corn *et al*., 2000; Melki *et al*., 1999, 2000; Boultwood, 2007). Emerging interest in using epigenetic inhibitors that reverse the aberrant silencing of tumor suppressor genes in cancer, prompted us to evaluate strategies to re-express p15, p21, and E-cadherin genes in AML cell lines. Table 6.1, Table 6.2 and Table 6.3, show a summary of the epigenetic regulatory events that occur at p15, E-cadherin and p21 genes upon treatment with epigenetic drugs.

Table 6.1. Epigenetic regulation of p15 gene upon treatment with epigenetic inhibitors, DAC, BIX and chaetocin

			Drug treatment					
		cell line	DAC	BIX	Chaetocin	BIX+DAC	Chaetocin+DAC	BIX+Chaetocin
p15	Gene expression	AML-193						
		Kasumi						
	Promoter Methylation	AML-193						Not analyzed
		Kasumi						Not analyzed
	H3K9Me2	AML-193						
		Kasumi						
	H3K9Me3	AML-193						
		Kasumi						

Gene expression: > 4 fold; > 2 fold; no change

Promoter methylation and H3K9 di and tri-methylation: increase > 30% methylation; decrease > 30% methylation; no change

Table 6.2. Epigenetic regulation of E-cadherin gene upon treatment with epigenetic inhibitors, DAC, BIX and chaetocin

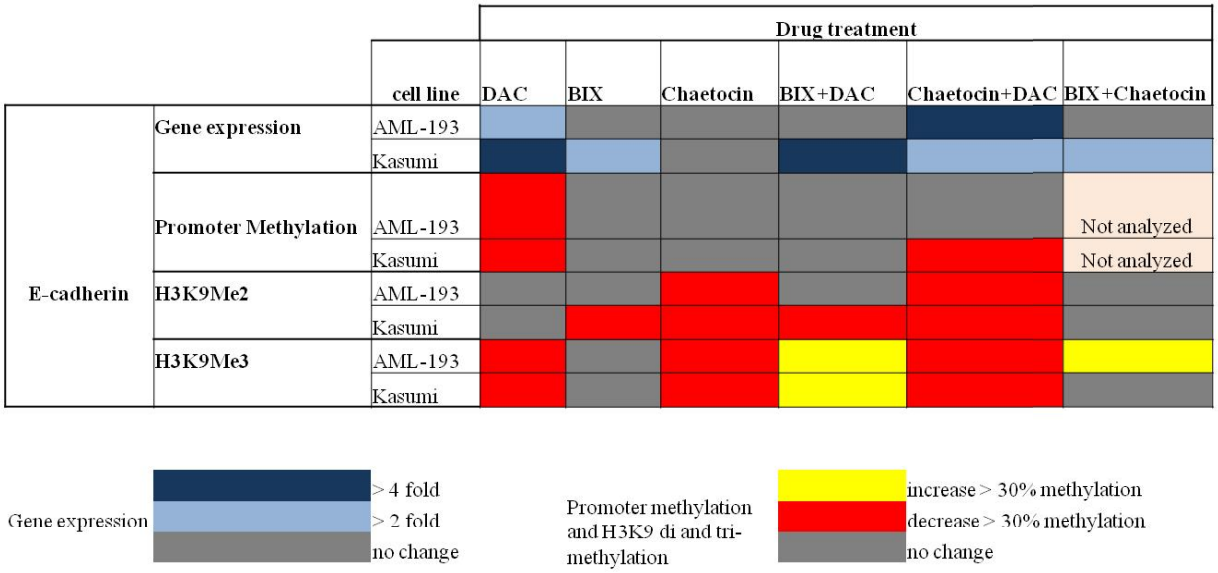

Table 6.3. Epigenetic regulation of p21gene upon treatment with epigenetic inhibitors, DAC, BIX and chaetocin

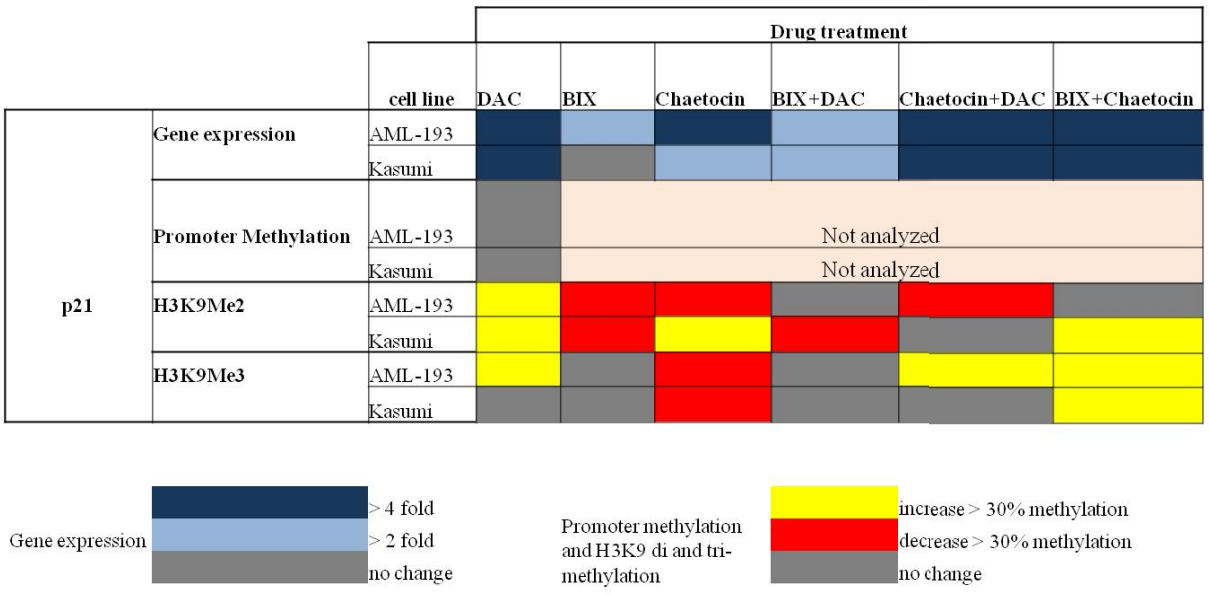

6.1. Epigenetic regulation of p15, p21, and E-cadherin genes upon treatment with DAC, BIX and chaetocin

In this study, the observed silencing of p15 and E-cadherin genes in AML-193 and Kasumi cell lines correlated with increased promoter hypermethylation. p21 was also silenced in the AML cell lines tested, but in contrast to p15 and E-cadherin, we did not observe hypermethylation at p21 promoter. Instead, we found that the CpGs analyzed at the p21 promoter were completed unmethylated. This observation suggests that methylation independent epigenetic mechanisms contribute to p21 silencing in AML-193 and Kasumi cell lines.

To efficiently evaluate re-activation of p15, p21, and E-cadherin genes in AML cell lines using the epigenetic inhibitors, DAC, BIX-01294, and chaetocin, we first determined the effect of these drugs on AML cell proliferation and optimized concentration of drugs that caused an enhancement of gene expression. Treatment with BIX and chaetocin inhibited viability and proliferation of AML-193, KG-1a, and Kasumi cell lines, whereas DAC had no effect on cell viability and proliferation as previously reported (Geyer *et al*., unpublished). DAC however, potentiated the anti-proliferative activity of BIX and chaetocin in AML cell lines. Loss of cell proliferation was correlated with changes in cell cycle profile, where a decrease in cell population in the S dividing phase and arrest in G1 and subG1 was observed following treatment with BIX and chaetocin.

In AML cell lines, treatment with DAC enhanced p15 and E-cadherin expression and decreased promoter and H3K9 methylation. Interestingly, we found that DAC treatment also caused re-expression of the unmethylated p21 gene, but instead of decreasing promoter H3K9 methylation, it increased H3K9 di-methylation levels at p21 promoter of AML-193 and Kasumi cell lines and H3K9 tri-methylation at the p21 promoter of AML-193 cells. The ability of DAC to enhance expression and induce chromatin remodelling of unmethylated genes (Nguyen *et* al., 2002; Coombes *et al*., 2003; Wu *et al*., 2005; Scott *et al*., 2006) suggested that it may have effect on other epigenetic changes that are independent of DNA demethylation. Importantly, the finding that enhanced p21 expression was accompanied with an increase in H3K9 di- and tri-methylation was in disagreement with the well recognized H3K9 tri-methylation gene-silencing mark and its association to heterochromatin regions (Heard *et al*., 2001; Peters *et al*., 2003; Rice *et al*., 2003). Our findings concur with previous studies where Vakoc and colleagues (2005)

presented a surprising finding that trimethyl-H3K9 mark is present in transcribed regions of genes (Vakoc, *et al*., 2005). More importantly, Wiencke (2008) recently showed that unmethylated genes that have been expressed in acute leukemic cell lines present in their promoter increased levels of H3K9 di and tri-methylation as well as H3K9 acetylation marks (Wiencke *et al*., 2008). A possible explanation for this observation is that H3K9 di- and tri-methylation are dynamic intermediates of different methylated states that regulate different functional chromatin rearrangements and therefore effect expression of genes in a specific-gene manner.

While H3K9 di-methylation levels mostly decreased at the p15, p21 and E-cadherin gene-promoters upon treatment with BIX, major changes on gene expression were not observed, except in AML-193 and Kasumi cell lines where E-cadherin and p21 genes were expressed upon treatment with highest doses of chaetocin, respectively. Thus, it appears that H3K9 di-methylation *per se* is not a dominant event in transcriptional silencing of p15, p21, and E-cadherin genes in AML. Further, we showed that chaetocin treatment significantly enhanced p15 expression and decreased H3K9 methylation levels at p15 and E-cadherin promoter without inducing promoter demethylation. Interestingly, these results demonstrated that H3K9 demethylation was a dominant event over promoter demethylation in re-expressing genes silenced by promoter hypermethylation in AML. Moreover, these results agree with previous observations found in the Geyer lab, which demonstrated that blocking the activity of the SUV39H1 enzyme with shRNA lead to the re-expression of the hypermethylated genes, p15 and E-cadherin, without effecting promoter methylation (Lakshmikuttyamma, *et al*., 2010). Similar observations of gene reactivation in the absence of promoter demethylation have been reported in studies that involved decreasing the H3K27 methyltransferase, EZH2 and H3K9 deacetylase, SIRT1 activities (McGarvey *et al*., 2007; Cao *et al*., 2008; Kondo *et al*., 2008). In addition, we also observed that chaetocin re-expressed p21 gene in AML-193 cell line, but in contrast to those results found with DAC, promoter H3K9 tri-methylation levels were reduced upon chaetocin treatment. Thus, due to the controversy between this result and the results observed with DAC treatment, we cannot conclude whether H3K9-trimethylation is a positive transcriptional mark in the active p21 gene-promoter. However, we could hypothesize that up- or down-regulation of H3K9-trimethylation levels at the p21 promoter might be associated as a secondary step activated by another dominant epigenetic event.

6.2. Epigenetic regulation of p15, p21, and E-cadherin genes upon treatment with combinations of epigenetic inhibitors

A large body of evidence has shown that epigenetic interaction between DNA methylation and histone modifications leads to transcriptional gene silencing. Several studies have established that SUV39H1-mediated H3K9 methylation may initiate promoter methylation by providing a binding site for chromodomain transcriptional repressor HP1 proteins, which in turn recruit other transcriptional repression machinery, such as DNA methyltransferases and histone deacetylases (HDACs) to achieve promoter gene silencing (Wang *et al.*, 2000; Nguyen *et al*., 2002; Fuks *et al*., 2003; Lehnertz *et al*., 2003; Fuks, 2005). Moreover, DNMTs have been also shown to directly interact with histone methyltransferase G9a in directing *de novo* DNA methylation and establishing coordinated mechanism of DNA and histone methylation leading to gene repression (Esteve *et al*., 2006; Epztejn-Litman *et al*., 2008; Dong *et al*., 2008). Thus, to further explore in more molecular detail the role of epigenetic changes in p15, p21, and E-cadherin gene silencing, we focused on assessing the effect of combinatorial treatments of epigenetic inhibitors on gene reactivation.

Previous studies have indicated that combinations of DNMT and HDAC inhibitors work in synergy to induce greater expression of silenced tumor suppressor genes in cancer cell lines (Zhu and Otterson, 2003; McGarvey *et al*., 2006). However, whether there is or not synergy between combinations of DNMT and HMT inhibitors and between HMT inhibitors targeting different lysine methylating enzymes on reactivation of epigenetically silenced p15, p21, and E-cadherin genes in AML, was unknown.

Previously, we established that DAC potentiated anti-proliferative response of BIX and chaetocin in AML cell lines, but because DAC did not affect AML cell proliferation we could only determine whether the presence of DAC affected BIX and chaetocin drug interaction. We evaluated the effectiveness of combining BIX and chaetocin by determining CI values. CI measures the degree of synergism or antagonism in drug interaction. Combinations of BIX and chaetocin displayed synergistic activity at high effect levels in KG-1a and Kasumi cells, as CI values were less than 1 (Table 5.3). The addition of DAC to BIX and chaetocin co-treatment caused the CI values to increase to values more than 1 (Table 5.3). This result indicated that DAC reduced the effectiveness of BIX and chaetocin interaction, thus affecting synergy. Combination of DAC and chaetocin strongly stimulated p15 and E-cadherin expression to

greater levels than those caused by individual drug treatments in AML cell lines and also decreased promoter DNA and H3K9 methylation. However, changes in promoter demethylation were not as significant as that caused by DAC treatment alone suggesting that promoter demethylation was principally caused by the presence of the demethylated agent DAC. These results were also consistent with our previous findings, suggesting that H3K9 demethylation was the dominant epigenetic event necessary for p15 and E-cadherin re-activation. In the case of p21, we found p21 re-expression upon treatment with combination of DAC and chaetocin and showed that p21 re-expression was associated with increased H3K9 tri-methylation levels.

Treatment with BIX and chaetocin were also able to induce p15 and E-cadherin re-expression only in AML-193 cell line and p21 expression in both AML-193 and Kasumi cell line. Thus, the mode of action of this treatment varied between cell lines and genes. p15 and E-cadherin re-expression was accompanied by promoter demethylation but without significant changes in H3K9 methylation. Surprisingly, treatment of AML-193 cells with combination of BIX and chaetocin caused re-silencing of hypermethylated genes p15 and E-cadherin and more importantly we observed that p15 and E-cadherin inactive-promoters were associated with increased H3K9 di- and tri-methylation levels. This result suggested that increased promoter H3K9 methylation may represent a repressive epigenetic mark that is associated with silenced promoter hypermethylation.

Using combinations of histone methyltransferase inhibitors, BIX and chaetocin, we evaluated whether co-ordinated changes in promoter H3K9 di- and tri-methylation are required for influencing p15, p21, and E-cadherin re-activation. Interestingly, similar to the result observed with a combination of BIX and DAC in AML-193, p15, and E-cadherin genes were also re-silenced upon co-treatment with BIX and chaetocin. This silencing was accompanied by increased promoter H3K9 tri-methylation, which supported our previous findings and indicated that H3K9 tri-methylation may act as repressive epigenetic mark when it is associated with silenced hypermethylated promoters. p21 gene in contrast to p15 and E-cadherin was re-activated with co-treatment of BIX and chaetocin and this re-activation was associated with significant increased in promoter H3K9 di- and tri-methylation.

Further, our results showed that H3K9 demethylation was the dominant epigenetic event in re-expressing tumor suppressor genes that were silenced by promoter hypermethylation and that loss of DNA methylation indirectly leads to gene reactivation by reducing repressive histone

modifications. Hence, these findings corroborate that high levels of tri-methyl H3K9 mark found at promoters of hypermethylated silenced genes function as dominant repressive silent mark, as previously proposed (Bird, 2002; Rice *et al*., 2003; Kondo *et al*., 2004). We also found that increased H3K9 tri-methylation can be linked to transcriptional activation of tumor suppressor genes with unmethylated promoters. Moreover, we determined that treatment of AML cell lines with combination of DNMTs and HMT inhibitors have a greater effect on p15, p21, and E-cadherin gene re-expression than treatment with individual drugs. This result strongly indicates the effectiveness of combinatorial strategies using epigenetic inhibitors in treatment of acute myeloid malignancies.

Taken together, our results allow us to propose strategies for re-expressing genes silenced by promoter hypermethylation. The first strategy highlights the importance of combining DNMT and HMT inhibitors. Treatment with DAC induces dissociation of DNMT1, SUV39H1, and G9a from promoter hypermethylation. This enzyme dissociation and inhibition of SUV39H1 and G9a activities by treatment with chaetocin and BIX results in decreased promoter H3K9 di- and tri-methylation, which would lead to transcription factors and other regulatory machinery such as HAT enzymes to induce activation of gene-promoter and thus gene transcription can progress. The second strategy involves inhibition of SUV39H1 and G9a activities. G9a and SUV-39H1 inhibition results in promoter H3K9 demethylation, which allow free lysine residues to undergo other epigenetic modification such as lysine acetylation leading to other transcriptional signals to be activated.

Reactivation of unmethylated tumor suppressor genes in AML does not fit with the strategies presented above, since we showed that p21 re-activation was associated with increased promoter H3K9 tri-methylation. However, treatment with chaetocin also induced p21 expression, but in this case p21 re-activation was accompanied by promoter H3K9 demethylation. Discrepancies between these results only allow us to speculate whether inhibition of SUV39H1 activity itself is the important event for p21 re-activation rather than changes in H3K9 methylation levels. However, our studies cannot provide further insights on this point as we did not evaluate SUV39H1 activity nor its interactions.

Finally, our findings have strong relevance in using combinatorial treatment of epigenetic inhibitors in cancer therapy. Combination of drugs that affect the epigenetic machinery such as DNMT and HDAC inhibitors are emerging as cancer therapeutics, particularly in leukemias. In

this study, we demonstrated that combining SUV39H1 and G9a inhibitors with DNMT inhibitors enhanced DNMT activity in re-expressing hypermethylated and unmethylated silenced genes and showed greater effectiveness in epigenetic drug therapies in AML. Since re-expression of p15, p21, and E-cadherin in AML cell lines requires changes in promoter H3K9 methylation without undergoing promoter demethylation, it is possible that HMTs inhibitors may be more effective than DNMT inhibitors in epigenetic therapies and that may be chemotherapeutic toxicity will be reduced. Our study highlights the relevance in determining the dominance of epigenetic event in gene re-activation and the need for clinical testing of histone methyltransferase inhibitors. Moreover, detailed drug interaction studies are needed in order to identify synergy between drug combinations, which would lead to optimal cancer epigenetic therapies.

7. Future Directions

In order to continue evaluating the epigenetic mechanism involved in silencing of tumor suppressor genes in AML, it will be necessary to determine the association of histone lysine methylating enzymes SUV39-H1 and G9a and HDAC enzymes with p15, p21 and E-cadherin gene promoters. Further, it will be interesting to determine the interaction between these enzymes and other repressor proteins using co-immunoprecipitation assays. The experiments performed in this study could also be done evaluating patient material to confirm the results that were seen in AML cell lines.

8. References

Aagaard, L., Laible, G., Selenko, P., Schmid, M., Dorn, R., Schotta, G., Kuhfittig, S., Wolf, A., Lebersorger, A., Singh, P. B., et al. (1999). Functional mammalian homologues of the Drosophila PEV-modifier Su(var)3-9 encode centromere associated proteins which complex with the heterochromatin component M31. EMBO J. *18*, 1923-1938.

Abbas, T., and Dutta, A. (2009). p21 in cancer: intricate networks and multiple activities. Nat. Rev. *9*, 400-413.

Albert, M., and Helin, K. (2010). Histone methyltransferases in cancer. Sem. Cell Dev. Biol. *21*, 209-220.

Aniello, F., Collela, G., Muscariello, G., Lanza, A., Ferrara, D., Branno, M., and Minucci, S. (2006). Expression of four lysine-methyltransferases in parotid gland tumors. Anticancer Res. *26*, 2063-2067.

Bachman, K. E., Park, B., Rhee, I., Rajagopalan, H., Herman, J. G., and Baylin, S. (2003). Histone modifications and silencing prior to DNA methylation of a tumor suppressor genes. Cancer Cell 3, 89-95.

Bachmann, I. M., Halvorsen, O. J., Collett, K., Stefansson, I. M., Straume, O., Haukaas, S. A., Salvesen, H. B., Otte, A. P., and Akslen, L. A. (2006). EZH2 expression is associated with high proliferation rate and aggressive tumor subgroups in cutaneous melanoma and cancers of the endometrium, prostate, and breast. J. Clin. Oncol. *24*, 268-273.

Baylin, S. B. (2005). DNA methylation and gene silencing in cancer. Nat. Clin. Prac. Oncol. *2*, S4-S11.

Bellacosa, A. (2003). Genetic hits and mutation rate in colorectal tumorigenesis: versatility of Knudson's theory and implications for cancer prevention. Genes Chromosome Canc. *38*, 382-388.

Bernstein, B., Meissner, A., and Lander, E. (2007). The mammalian epigenome. Cell *128*, 669-681.

Bryant, R. J., Cross, N. A., Eaton, C. L., Hamdy, F. C., and Cunliffe, V. T. (2007). EZH2 promotes proliferation and invasiveness of prostate cancer cells. Prostate *67*, 547-556.

Cameron, E., Bachman, K., Myohanen, S., Herman, J. G., and Baylin, S. B. (1999). Synergy of demethylation and histone deacetylase inhibition in the re-expression of genes silenced in cancer. Nat. Genet. *21*, 103-107.

Carmichael, J., DeGraff, W. G., Gazdar, A. F., Minna, J. D. and Mitchell, J. B. (1987). Evaluation of a tetrazolium-based semiautomated colorimetric assay: assessment of radiosensitivity. Cancer Res. *47,* 943-946.

Cedar, H., and Bergman, Y. (2009). Linking DNA methylathion and Histone modification: Patterns and paradigms. Nat. Rev. Genet. *10*, 295-304.

Chang, Y., Zhang, X., Horton, J. R., Upadhyay, A. K., Spannhoff, A., Liu, J., Snyder J. P, Bedford, M. T., and Cheng, X. (2009). Structural basis for G9a-like protein lysine methyltransferase inhibition by BIX-01294. Nat. Struct. Mol. Biol. *16*, 312-317.

Chen, J., Jackson, P., Kirschner, M., and Dutta, A. (1995). Separate domains of p21 involved in the inhibition of p21 involved in the inhibition of cdk kinase and PCNA. Nature *374*, 386-388.

Cheng, J., Yoo, C., Weisenberger, J., Chuang, C., Wozniak, G., Liang, V.,Marquez, S., Greer, T. F., and Jones, P. A. (2004). Preferential responses of cancer cells to Zebularine. Cancer Cell *6*, 151-158.

Chen, J., Odenike, O., and Rowley, J. D. (2010). Leukaemogenesis: more than mutant genes. Nat. Rev. Cancer *10*, 23-36.

Chen, T., Hevi, S., Gay, F., Tsujimoto, N., He, T., Zhang, B., Ueda, Y., and Li, E. (2007). Complete inactivation of DNMT1 leads to mitotic catastrophe in human cancer cells. Nat. Genet. *39*, 391-396.

Cheng, T., Rodrigues, N., Shen, H., Yang, Y., Dombkowski, D., Sykes, M., and Scadden, D. T. (2000). Hematopoietic stem cell quiescence maintained by p21cip1/waf1. Science *287*, 1804-1808.

Cherrier, T., Suzanne, S., Redel, L., Calao, M., Marban, C., Samah, B., Mukerjee, R., Schwartz, C., Gras, G., and Sawaya, B. E. (2009). p21(WAF1) gene promoter is epigenetically silenced by CTIP2 and SUV39H1. Oncogene *28*, 3380-3389.

Chim, C. S., Tam, C. Y., Liang, R., and Kwong, Y. L. (2001). Methylation of p15 and p16 genes in adult acute leukemia: lack of prognostic significance. Cancer *91*, 2222-2229.

Christiansen, D. H., Andersen, M. K., and Pedersen-Bjergaard, J. (2003). Methylation of p15INK4B is common, is associated with deletion of genes on chromosome arm 7q and predicts a poor prognosis in therapy-related myelodysplasia and acute myeloid leukemia. Leukemia *17*, 1813-1819.

Coombes, M. M., Briggs, K. L., Bone, J. R., Clayman, G. L., El-Naggar, A. K., and Dent, S. Y. (2003). Resetting the histone code at CDKN2A in HNSCC by inhibition of DNA methylation. Oncogene *22*, 8902-8911.

Cooper, C. S., Campbell, C., and Jhavar, S. (2007). Mechanisms of Disease: biomarkers and molecular targets from microarray gene expression studies in prostate cancer. Nat. Clin. Pract. Urol. *4*, 677-687.

Corn, P., Smith, B. D., Ruckdeschel, D. D., Baylin, S. B., and Herman, J. (2000). E-cadherin expression is silenced by 5' CpG island methylation in Acute leukemia. Clin. Cancer Res. *6*, 4243-4248.

Cosgrove, M. S., and Wolberger, C. (2005). How does the histone code work? Biochem. Cell. Biol. *83*, 468-476.

Daskalakis, M., Nguyen, T. T., Nguyen, C., Guldberg, P., Kohler, G., Wijermans, P., Jones, P. A. and Lubbert, M. (2002). Demethylation of a hypermethylated P15/INK4B gene in patients with myelodysplastic syndrome by 5-Aza-2'-deoxycytidine (decitabine) treatment. Blood *100,* 2957-2964.

Deschler, B., and Lubbert, M. (2006). Acute myeloid leukemia: epidemiology and etiology. Cancer *107*, 2099-2107.

Ding, L., Erdmann, C., Chinnaiyan, A. M., Merajver, S. D., and Kleer, C. G. (2006). Identification of EZH2 as a molecular marker for a precancerous state in morphologically normal breast tissues. Cancer Res. 66, 4095-4099.

Dong, K. B., Maksakova, I. A., Mohn, F., Leung, D., Appanah, R., Lee, S., Yang, H. W., Lam, L. L., Mager, D. L., Schübeler D., et al. (2008). DNA methylation in ES cells requires the lysine methyltransferase G9a but not its catalytic activity. EMBO J. *27*, 2691-2701.

Egger, G., Aparicio, A. M., Escobar, S. G., and Jones, P. A. (2007). Inhibition of histone deacetylation does not block resilencing of p16 after 5-Aza-2'-deoxycytidine treatment. Cancer Res. *67*, 346-353.

Ekmekci, C., Gutierrez M., Siraj, A. K., Ozbek, U., and Bhatia, K. (2004). Aberrant methylation of multiple tumor suppressor genes in acute myeloid leukemia. Am. J. Hematol. *77*, 233-240.

Epsztejn-Litman, S., Feldman, N., Abu-Remaileh, M., Shufaro, Y., Gerson, A., Ueda, J., Deplus, R., Fuks, F., Shinkai, Y., Cedar, H., and Bergman, Y. (2008). De novo DNA methylation promoted by G9a prevents reprogramming of embryonically silenced genes. Nat. Struct. Mol. Biol. *15*, 1176- 1183.

Espada, J., and Esteller, M. (2010). DNA methylation and the functional organization of the nuclear compartment. Semin. Cell Dev. Biol. *21*, 238-246.

Esteller, M. (2007). Cancer epigenomics: DNA methylomes and Histone-modification maps. Nat. Rev. Genet. *8*, 286-298.

Esteve, P. O., Chin, H. G., Smallwood, A., Feehery, G. R., Gangisetty, O., Karpf, A. R., Carey, M. F., and Pradhan, S. (2006). Direct interaction between DNMT1 and G9a coordinates DNA and histone methylation during replication. Genes Dev. *20*, 3089-3103.

Estey, E., and Dohner, H. (2006). Acute myeloid leukemia. Lancet *368*, 1894-1907.

Evan, G. I., and Vousden, K. H. (2001). Proliferation, cell cycle and apoptosis in cáncer. Nature *411*, 342-348.

Ewald, B., Sampath, D., and Plunkett, W. (2008). Nucleosides analogs: molecular mechanisms signaling cell death. Oncogene *27*, 6522-6537.

Fearon, E. R., and Vogelstein, B. (1990). A genetic model for colorectal tumorigenesis. Cell *61*, 759-767.

Feinberg, A. (2007). Phenotypic plasticity and the epigenetic of human disease. Nat. Insight Rev. 433-440.

Fraga, M., Ballestar, E., Villar-Garea, A., Boix-Chornet, M., Espada, J., Schotta, G., Bonaldi, T., Haydon, C., Ropero, S., Petrie, K., et al. (2005). Loss of acetylation at Lys16 and trimethylation at Lys 20 of histone H4 is a common hallmark of human cancer. Nat. Genet. *37*, 391-400.

Frankfurt, O., Licht, J. D., and Tallman, M. S. (2007). Molecular characterization of acute myeloid leukemia and its impact on treatment. Curr. Opin. Oncol. *19*, 635-649.

Fritsch, L., Robin, P., Mathieu, J. R., Souidi, M., Hinaux, H., Rougeulle, C., Harel-Bellan, A., Ameyar-Zazoua, M., and Ait-Si-Ali, S. (2010). A subset of the histone 3 lysine 9 methyltransferases Suv39h1, G9a, GLP, SETDB1 participate in a multimeric complex. Mol. Cell *37*, 46-56.

Galmarini, C. M., Mackey, J. R., and Dumontet, C. (2001). Nucleosides analogues: Mechanisms of drug resistance and reversal strategies. Leukemia *15*, 875-890.

Gardiner-Garden, M. and Frommer, M. (1987). CpG islands in vertebrate genomes. J. Mol. Biol. *196*, 261.

Gartel, A., and Tyner, A. (1999). Transcriptional regulation of the p21 WAF1/CIP1 gene. Exp. Cell Res. *246*, 280-289.

Gil, J., and Peters, G. (2006). Regulation of the INK4b-ARF-INK4a tumour suppressor locus: all for one or one for all. Nat. Rev. *7*, 667-677.

Gonzalez-Zulueta, M., Bender, C. M., Yang, A. S., Nguyen, T., Beart, R. W., Van Tornout, J. M., and Jones, P. A. (1995). Methylation of the 5' CpG island of the p16/CDKN2 tumor suppressor gene in normal and transformed human tissues correlates with gene silencing. Cancer Res. *55*, 4531-4535.

Graff, J. R., Herman, J. G., Lapidus, R. G., Chopra, H., Xu, R., Jarrard, D. F., Isaacs, W. B., Pitha, P. M., Davidson, N. E., and Baylin, S. B. (1995). E-cadherin expression is silenced by DNA hypermethylation in human breast and prostate carcinomas. Cancer Res. *55*, 5195-5199.

Greger, V., Passarge, E., Hopping, W., Messmer, E., and Horsthemke, B. (1989). Epigenetic changes may contribute to the formation and spontaneous regression of retinoblastoma. Hum. Genet. *83*, 155-158.

Greiner, D., Bonaldi, T., Eskeland, R., Roemer, E. and Imhof, A. (2005). Identification of a specific inhibitor of the histone methyltransferase SU(VAR)3-9. Nature Chem. Biol. *1*, 143-145.

Hamamoto, R., Furukawa, Y., Morita, M., Iimura, Y., Silva, F. P., Li, M., and Yagyu, R., and Nakamura Y. (2004). SMYD3 encodes a histone methyltransferase involved in the proliferation of cancer cells. Nat. Cell. Biol. *6*, 731-740.

Hamamoto, R., Silva, F. P., Tsuge, M., Nishidate, T., Katagiri, T., Nakamura, Y., and Furukawa Y. (2006). Enhanced SMYD3 expression is essential for the growth of breast cancer cells. Cancer Sci. *97*, 113-118.

Hanahan, D. and Weinberg, R. A. (2000). The hallmarks of cancer. Cell *100*, 57–70

Hannon, G. J., and Beach, D. (1994). p15INK4B is a potential effector of TGF beta-induced cell cycle arrest. Nature *371*, 257-261.

Hayatsu, H. (2008). Discovery bisulfite-mediated cytosine conversion to uracil, the key reaction for DNA methylation analysis- a personal account. Proc. Jpn. Acad, *8*, 321-330.

Heerema-McKenney, A., and Arber, D. (2009). Acute myeloid leukemia. Hematol. Oncol. Clin. North. Am. *23*, 633-654.

Hellebrekers, D. M., Griffioen, A., and Engeland, M. (2007). Dual trageting of epigenetic therapy in cancer. Biochem. Biophys. Acta *1775*, 76-91.

Herman, A., Schmitt S., and Jeltsch A. (2003). The human Dnmt2 has residual DNA-(Cytosine-C5) methyltransferase acytivity. J. Biol. Chem. *278*, 31717-31721.

Herman, J., Civin, C., P, I. J., Collector, M. I., Sharkis, S. J., and Baylin, S. B. (1997). Distintict patterns of inactivation of p15INK4B and p16INK4A characterize the major tyes of hematological malignancies. Cancer Res. *57*, 837-841.

Herman, J. C., and Baylin, S. B. (2003). Gene silencing in cancer in association with promoter hypermethylation. N. Engl. J. Med. *349*, 2042-2054.

Hirosashi, S. (1998). Inactivation of the E-cadherin mediated cell adhesion system in human cancers. Am. J. Pathol. *153*, 333-339.

Huang, J., Sengupta, R., Espejo, A. B., Lee, M. G., Dorsey, J. A., Richter, M., Opravil, S., Shiekhattar, R., Bedford, M. T., Jenuwein T., and Berger, S. L. (2007). p53 is regulated by the lysine demethylase LSD1. Nature, *449*, 105-108.

Hublitz, P., Albert, M., and Peters, A. (2009). Mechanisms of transcriptional repression by histone lysine methylation. Int. J. Dev. Biol. *53*, 335-334.

Ilyas, M., Straub, J., Tomlinson, I. P., and Bodmer, W. F. (1999). Genetic pathways in colorectal and other cancers. Eur. J. Cancer *35*, 335-351.

Isham, C., Tibodeau, J. D., Jin, W., Xu, R., Timm, M., and Bible, K. (2007). Chaetocin: a promising new antimyeloma agent with in vitro and in vivo activity mediated via imposition of oxidative stress. Blood *109*, 2579-2588.

Issa, J. P. (2000). The epigenetics of colorectal cancer. Ann N. Y. Acad. Sci. *910*, 140-153.

Jaffe, E. S., Harris, N. L., Stein, H., and Vardiman, J. W. (2001). World Health Organization Classification of Tumours. Pathology and Genetics of Tumours of Haematopoietic and Lymphoid Tissues (Lyon, IARC Press).

Jones, P. A. and Baylin, S. B. (2002). The fundamental role of epigenetic events in cancer. Nat. Rev. Genet. *3*, 415-428.

Jones, P. and Baylin, S. (2007). The epigenomics of cancer. Cell *128*, 683-692.

Kane, M. F., Loda, M., Gaida, G. M., Lipman, J., Mishra, R., Goldman, H., Jessup,J. M., and Kolodner, R. (1997). Methylation of the hMLH1 promoter correlates with lack of expression of hMLH1 in sporadic colon tumors and mismatch repairdefective human tumor cell lines. Cancer Res. *57*, 808-811.

Kang, M. Y., B., L. B., Kim, Y., Chang, D., Kyu, P., and Chun, H. K. (2007). Association of the SUV39H1 histone methyltransferase with the DNMT1 at mRNA expression level in primary colorectal cancer. Int. J. Cancer *121*, 2192-2197.

Kim, G. D., Ni, J., Kelesoglu, N., Roberts, R. J., and Pradhan, S. (2002). Co-operation and communication between the human maintenance and de novo DNA (cytosine-5) methyltransferases. EMBO J. *21*, 4183- 4195.

Kim, W., and Sharpless, N. (2006). The regulation of INK4/ARF in cancer and aging. Cell 265-275.

Knudson, A. G. (1996). Hereditary cancer: two hits revisited. J. Cancer Res. Clin. Oncol. *122*, 135-140.

Kondo, Y., Shen, L., Ahmed, S., Boumber, Y., Sekido, Y., Haddad, B. R., and Issa J. P. (2008). Downregulation of histone H3 lysine 9 methyltransferase G9a induces centrosome disruption and chromosome instability in cancer cells. PloS One *3*, e2037.

Kouzarides, T. (2007). Chromatin modifications and their function. Cell *128*, 693-705.

Krug, U., Ganser, A., and Koeffler, H. P. (2002). Tumor suppressor genes in normal and malignant hematopoiesis. Oncogene *21*, 3475-3495.

Kubicek, S., O'Sullivan, R. J., August, E. M., Hickey, E. R., Zhang, Q., Teodoro, M. L., Rea, S., Mechtler, K., Kowalski, J. A., and Homon, C. A . (2007). Reversal of H3K9me2 by a small-molecule inhibitor for the G9a histone methyltransferase. Mol. Cell. *25*, 473-481.

Lakshmikuttyamma, A., Scott, S. A., DeCoteau, J. F., and Geyer, C. R. (2010). Reexpression of epigenetically silenced AML tumor suppressor genes by SUV39H1 inhibition. Oncogene *24*, 76-588.

Lee, P. P., Fitzpatrick, D. R., Beard, C., Jessup, H. K., Lehar, S., Makar, K. W., Perez-Melgosa, M., Sweetser, M. T., Schlissel, M. S., Nguyen, S., Cherry, S. R., Tsai, J. H., Tucker, S. M., Weaver, W. M., Kelso, A., Jaenisch, R. and Wilson, C. B. (2001). A critical role for Dnmt1 and DNA methylation in T cell development, function, and survival. Immunity *15,* 763-774.

Lehnertz, B., Ueda, Y., Derijck, A. A., Braunschweig, U., Perez-Burgos, L., Kubicek, S., Chen, T., Li, E., Jenuwein, T., and Peters, A. H. (2003). Suv39h-mediated histone H3 lysine 9 methylation directs DNA methylation to major satellite repeats at pericentric heterochromatin. Curr. Biol. *13*, 1192-1200.

Leonhardt, H., Page, A. W., Weier, H. U., and Bestor, T. H. (1992). A targeting sequence directs DNA methyltransferase to sites of DNA replication in mammalian nuclei. Cell *71*, 865-873.

Li, E., Beard, C., and Jaenisch, R. (1993). Role for DNA methylation in genomic imprinting. Nature *366*, 362-365.

Li, H., Rauch, T., Chen, Z. X., Szabo, P. E., Riggs, A. D., and Pfeifer, G. P. (2006). The histone methyltransferase SETDB1 and the DNA methyltransferase DNMT3A interact directly and localize to promoters silenced in cancer cells. J. Biol. Chem. *281*, 19489-19500.

Luo, Y., Hurwitz, J., and Massague, J. (1995). Cell-cycle inhibition of cdk kinase and PCNA binding domains in p21 CIP1. Nature *375*, 159-161.

Malumbres, M., and Barbacid, M. (2009). Cell cycle, CDKs and cancer: a changing paradigm. Nature Rev. *9*, 153-166.

Malumbres, M., and Barbacid, M. (2005). Mammalian cyclin dependent kinases. *Trends Biochem. Sci. 30*, 630-641.

Martin-Caballero, J., Flores, J. M., Garcia-Palencia, P., and Serrano, M. (2001). Tumor susceptibility of p21 WAF1/CIP1 deficient mice. Cancer Res. *61*, 6234-6238.

Martin, C., and Zhang, Y. (2005). The diverse functions of histone lysine methylation. Nat. Rev. Mol. Cell Biol. *6*, 838-849.

Massague, J. (2004). G1 cell-cycle control and cancer. Nature *432*, 298-306.

McCormack, E., Bruserud, O., and Gjertsen, B. T. (2008). Review: genetic models of acute leukemia. Oncogene *27*, 3765-3779.

McGarvey, K. M., Fahrner, J. A., Greene, E., Martens, J., Jenuwein, T., and Baylin, S. B. (2006). Silenced tumor suppressor genes reactivated by DNA demethylation do not return to a fully euchromatic chromatin state. Cancer Res. *66*, 3541-3549.

McManus, K. J., Biron, V., Heit, R., Underhill, D., and Hendzel, M. (2006). Dynamic changes in Histone H3 lysine 9 methylations: identification of a mitosis- specific function for dynamic methylation in chromosome congression and segregation. J. Biol. Chem. *281*, 8888-8897.

Melki, J. R., Vicent, P. C., and Clark, S. J. (1999). Concurrent DNA hypermethylation of multiple genes in acute myeloid leukemia. Cancer Res. *59*, 3730-3740.

Melki, J., Vincent, P., Brown, R. D., and Clark, S. J. (2000). Hypermethylation of E-cadherin in leukaemia. Blood *95*, 3028-3213.

Melo, J. V., and Barnes., D.J. (2007). Chronic myeloid leukaemia as a model of disease evolution in human cancer. Nat. Rev. Cancer *7*, 441-453.

Moldovan, G., Pfander, B., and Jentsch, S. (2007). PCNA, the maestro of the replication fork. Cell *129*, 665-679.

Mund, C., Brueckner, B., and Lyko, F. (2006). Reactivation of epigenetically silenced genes by DNA methyltransferase inhibitors: basic concepts and clinical applications. Epigenetics *1*, 7-13.

Nguyen, C. T., Weisenberger, D. J., Velicescu, M., Gonzales, F. A., Lin, J. C., Liang, G. and Jones, P. A. (2002). Histone H3-lysine 9 methylation is associated with aberrant gene silencing in cancer cells and is rapidly reversed by 5-aza-2'-deoxycytidine. Cancer Res. *62*, 6456-6461.

Ohm, J. E., McGarvey, K. M., Yu, X., Cheng, L., Schuebel, K. E., Cope, L., Mohammad, H.P., Chen, W., Daniel, V. C., Yu, W., et al. (2007). A stem cell-like chromatin pattern may predispose tumor suppressor genes to DNA hypermethylation and heritable silencing. Nat. Genet. *39*, 237-242.

Okamoto, A., Demetrick, D. J., Spillare, E. A., Hagiwara, K., Hussain, S. P., Bennett, W. P., Forrester, K., Gerwin, B., Serrano, M., Beach, D. H., et al. (1994). Mutations and altered expression of p16INK4 in human cancer. Proc. Natl. Acad. Sci. USA. *91*, 11045-11049.

Okano, M., Xie S., and Li, E. (1998). Dnmt2 is not required for de novo and maintenance methylation of viral and DNA in embryonic stem cells. Nucleic Acids Res. *26*, 2536-2540.

Okano, M., Bell, D. W., Haber, D. A. and Li, E. (1999). DNA methyltransferases Dnmt3a and Dnmt3b are essential for de novo methylation and mammalian development. Cell *99,* 247-257.

Ooi, S. K., Qiu, C., Bernstein, E., Li, K., Jia, D., Yang, Z., Erdjument-Bromage, H., Tempst, P., Lin, S. P., Allis, C. D., Cheng, X., and Bestor, T. H. (2007). DNMT3L connects unmethylated lysine 4 of histone H3 to the novo methylation of DNA. Nature *448*, 714- 717.

Peng, D. F., Kanai, Y., Sawada, M., Ushijima, S., Hiraoka, N., Kosuge, T. and Hirohashi, S. (2005). Increased DNA methyltransferase 1 (DNMT1) protein expression in precancerous conditions and ductal carcinomas of the pancreas. Cancer Sci. *96*, 403-408.

Peters, A. H., O'Carroll, D., Scherthan, H., Mechtler, K., Sauer, S., Schöfer, C., Weipoltshammer, K., Pagani, M., Lachner, M., Kohlmaier, A., et al. (2001). Loss of the Suv39h histone methyltransferase impairs mammalian heterochromatin and genome stability. Cell *107*, 323-337.

Plass, C., Oakes, C., Blum, W., and Marcucci, G. (2008). Epigenetics in acute myeloid leukemia. Semin. Oncol. *35*, 378-387.

Plickmark, E., Katarjian, H., and Issa, J. (2007). Decitabine and its role in the treatment of hematopoetic malignancies. Leuk. Lymph. *48*, 1472-1481.

Poole, A. J., Heap, D., Carroll, R. E., and Tyner, A. L. (2004). Tumor suppressor functions for the Cdk inhibitors p21 in mouse colon. Oncogene *23*, 8128-8134.

Rea, S., Eisenhaber, F., O'Carroll, D., Strahl, B. D., Sun, Z. W., Schmid, M., Opravil, S., Mechtler, K., Ponting, C. P., Allis, C. D., and Jenuwein, T. (2000). Regulation of chromatin structure by site-specific histone H3 methyltransferases. Nature *406*, 593-599.

Rhee, I., Jair, K. W., Yen, R. W., Lengauer, C., Herman, J. G., Kinzler, K. W., Vogelstein, B., Baylin, S. B. and Schuebel, K. E. (2000). CpG methylation is maintained in human cancer cells lacking DNMT1. Nature *404,* 1003-1007.

Rhee, I., Bachman, K. E., Park, B. H., Jair, K. W., Yen, R. W., Schuebel, K. E., Cui, H., Feinberg, A. P., Lengauer, C., Kinzler, K. W., et al. (2002). DNMT1 and DNMT3b cooperate to silence genes in human cancer cells. Nature *416*, 552-556.

Rice, J. C., Briggs, S. D., Ueberheide, B., Barber, C. M., Shabanowitz, J., Hunt, D. F., Shinkai Y., and Allis, C. D. (2003). Histone methyltransferases direct different degrees of methylation to define distinct chromatin domains. Mol. Cell *12*, 1591-1598.

Schlesinger, Y., Straussman, R., Keshet, I., Farkash, S., Hecht, M., Zimmerman, J., Eden, E., Yakhini, Z., Ben-Shushan, E., Reubinoff, B. E., et al. (2007). Polycomb-mediated methylation on Lys27 of histone H3 pre-marks genes for de novo methylation in cancer. Nature Genet. *39*, 232-236.

Scott, S. A, Dong, W. F, Ichinohasama R., Hirsch, C., Sheridan, D., Sanche, S. E., Geyer, C. R., and Decoteau, J. F. (2006). 5-Aza-2'-deoxycytidine (decitabine) can relieve p21WAF1 repression in human acute myeloid leukemia by a mechanism involving release of histone deacetylase 1 (HDAC1) without requiring p21WAF1 promoter demethylation. Leuk Res. *30*, 69-76.

Seoane, J., Pouponnot, C., Staller, P., Schader, M., Eilers, M., and Massague, J. (2001). TGF beta influences Myc, Miz-1 and Smad to control the CDK inhibitor p15INK4b. Nature Cell Biol. *3*, 400-408.

Sharma, S., Kelly, T. K., and Jones, P. (2010). Epigenetics in cancer. Carcinogenesis *31*, 27-36.

Sharpless, N. E. (2005). INK4a/ARF: a multifunctional tumor suppressor locus. Mutat. Res. *576*, 22-38.

Sherr, C. J., and Roberts, J. M. (1995). Inhibitors of mammalian G1 cyclindependent kinases. Genes Dev. *9*, 1149-1163.

Shi, X., Kachirskaia, I., Yamaguchi, H., West, L. E., Wen, H., Wang, E. W., Dutta, S., Appella, E., Gozani, O., et al. (2007). Modulation of p53 function by SET8-mediated methylation at lysine 382. Mol. Cell *27*, 636-646.

Shimamoto, T., Ohyashiki, J. H., and Ohyashiki, K. (2005). Methylation of p15 (INK4b) and E-cadherin genes is independently correlated with poor prognosis in acute myeloid leukemia. Leuk. Res. *29*, 653-659.

Shiohara, M., el-Deiry, W. S., Wada, M., Nakamaki, T., Takeuchi, S., Yang, R., Chen, D. L., Vogelstein, B., Koeffler, H. P., et al. (1994). Absence of WAF1 mutations in a variety of human malignancies. Blood *84*, 3781-3784.

Sjöblom, T., Jones, S., Wood, L. D., Parsons, D. W., Lin, J., Barber, T. D., Mandelker, D., Leary, R. J., Ptak, J., Silliman, N., et al. (2006). The consensus coding sequences of human breast and colorectal cancers. Science *314*, 268-274.

Skawran, B., Steinemann, D., Weigmann, A., Flemming, P., Becker, T., Flik, J., Kreipe, H., Schlegelberger, B., and Wilkens, L. (2008). Gene expression profiling in hepatocellular carcinoma: upregulation of genes in amplified chromosome regions. Mod. Pathol. *21*, 505-516.

Smith, S. S., Kaplan, B. E., Sowers, L. C., and Newman, E. M. (1992). Mechanism of human methyl-directed DNA methyltransferase and the fidelity of cytosine methylation. Proc. Natl. Acad. Sci. USA *89*, 4744-4748.

Spannhoff, A., Sippl, W., and Jung, M. (2009). Cancer treatment of the future: Inhibitors of histone methyltransferases. Intern. J. Biochem. Cell Biol. *41*, 4-11.

Suzuki, H., Gabrielson, E., Chen, W., Anbazhagan, R., van Engeland, M., Weijenberg, M. P., Herman, J. G., and Baylin, S. B. (2002). A genomic screen for genes upregulated by demethylation and histone deacetylase inhibition in human colorectal cancer. Nat. Genet. *31*, 141-149.

Tachibana, M., Sugimoto, K., Nozaki, M., Ueda, J., Ohta, T., Ohki, M., Fukuda, M., Takeda, N., Niida, H., Kato, H., and Shinkai, Y. (2002). G9a histone methyltransferase plays a dominant role in euchromatic histone H3 lysine 9 methylation and is essential for early embryogenesis. Genes Dev. *16*, 1779-1791.

Tachibana, M., Ueda, J., Fukuda, M., Takeda, N., Ohta, T., Iwanari, H., Sakihama, T., Kodama, T., Hamakubo, T., and Shinkai, Y. (2005). Histone methyltransferases G9a and GLP form heteromeric complexes and are both crucial for methylation of euchromatin at H3-K9. Genes Dev. *19*, 815-826.

Vardiman, J. W. (2009). The World Health Organization (WHO) classification of tumors of the hematopoietic and lymphoid tissues: an overview with emphasis on the myeloid neoplasms. Chem. Biol. Interact. *184*,16-20.

Waddington, C. H. (1942). The epigenotype. Endeavour *1*, 18-20.

Warner, B., Blain, S. W., Seoane, J., and Massague, J. (1999). Myc downregulation by transforming growth factor beta required for activation of the p15(Ink4b) G(1) arrest pathway. Mol. Cell Biol. *19*, 5913-5922.

Ying, J., Srivastava, G., Gao, Z., Zhang, X., Murray, P., Ambinder, R., and Tao, Q. (2004). Promoter hypermethylation of the cyclin-dependent kinase inhibitor (CDKI) gene p21WAF1/CIP1/SDI1 is rare in various lymphomas and carcinomas. Blood *103*, 743-746.

Yoshiura, K., Kanai, Y., Ochiai, A., Shimoyama, Y., Sugimura, T., and Hirohashi, S. (1995). Silencing of the E-cadherin invasion-suppressor gene by CpG methylation in human carcinomas. Proc. Natl. Acad. Sci. USA *92*, 7416-7419.

Zhu, W. G., Dai, Z., Ding, H., Srinivasan, K., Hall, J., Duan, W., Villalona-Calero, M. A., Plass, C., and Otterson, G. A. (2001). Increased expression of unmethylated CDKN2D by 5-aza-2'-deoxycytidine in human lung cancer cells. Oncogene *20*, 7787-7796.

Zhu, W. G., and Otterson, G. (2003). The interaction of Histones Deacetylase inhibitors and DNA methyltranferase inhibitors in the treatment of human cancer cells. Curr. Medicinal Chem. *3*, 187-199.